Bone Morphogenetic Proteins as regulators of cortical excitation and inhibition

Inauguraldissertation

zur
Erlangung der Würde eines Doktors der Philosophie
vorgelegt der
Philosophisch-Naturwissenschaftlichen Fakultät
der Universität Basel

von

Zeynep Okur

2024

Genehmigt von der Philosophisch-Naturwissenschaftlichen Fakultät

auf Auftrag von:

Erstbetreuer: Prof. Dr. Peter Scheiffele

Zweitbetreuer: Prof. Dr. Markus Affolter

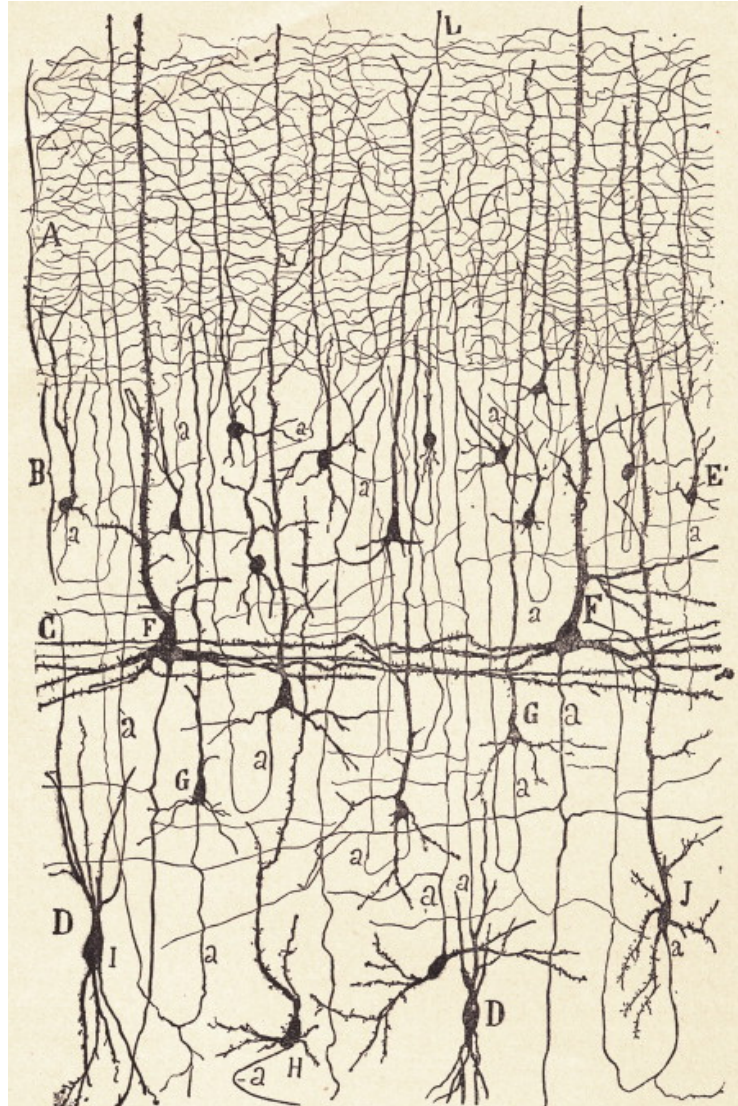Externer Experte: Prof. Dr. Michael Eldon Greenberg

Basel, 20. Juni 2023

<div style="text-align: right">

_____

The Dean of Faculty

Prof. Dr. Marcel Mayor

</div>

"The mysterious butterflies of the soul,

whose beating of wings may one day reveal to us the secrets of the mind."

Santiago Ramón y Cajal (1852-1934)

Table of Contents

Summary

Summary

Plasticity is the underlying mechanism for neuronal circuits to develop and adapt to the environment for organisms to regulate different body states, learn new tasks, form memories and use their cognitive abilities. Over the last century, studies demonstrated that neurons utilize the plethora and variety of their synaptic properties to store and integrate the environmental cues on shorter timescales from milliseconds to hours. However, how neurons, in particular synapses, adapt to longer periods of stimuli which is essential for learning a new task and memory consolidation, remains largely unknown.

Secreted molecules, especially growth factors, are great candidates for such adaptations in the brain areas such as cortex where multiple types of cells constantly work in harmony and exchange information to adapt to sensory stimuli. In this thesis, I investigated whether Bone Morphogenetic Proteins (BMPs), key players of the patterning during embryonic development, are re-utilized as a transcellular signal underlying homeostatic plasticity in the adult somatosensory cortex.

BMPs are ligands of the transforming growth factor family (TGF) which are encoded by more than 20 genes in vertebrates. I first contributed to a collaborative study with the group of Ralf Schneggenburger in EPFL, Lausanne. In this project, we explored if BMP signaling regulates the development of inhibitory long-term potentiation (iLTP) from Parvalbumin interneurons (PV interneurons) onto layer 4 principal cells in the primary auditory cortex (A1) during critical period plasticity. Conditional/genetic deletion of BMP receptor-1a (Bmpr1a) and 1b (Bmpr1b) demonstrated that loss of BMP signaling in PV interneurons results in disruption of iLTP formation onto layer 4 principal neurons.

In my main project, I screened BMP ligands to identify their sites of expression in the mouse neocortex and examined whether neuronal network activity can mobilize the signaling. For the first time, I demonstrated that the BMP pathway is active in mature neurons of the mouse brain and can be recruited by neuronal activity. By advancing a reporter generated from BMP responsive element of the target genes, I showed that BMP2 mobilization from principal cells are responded by Parvalbumin interneurons through SMAD1, a critical transcriptional mediator of the BMP pathway. This was quite striking as this is the first evidence that BMP signaling can be transcellularly signaled between the key players of excitation-inhibition balance in the sensory cortices. Next, I coupled Chromatin immunoprecipitation (ChiP) with RNA sequencing and identified target genes

of BMP2 ligand in cortical neurons. Surprisingly, we found that the SMAD1 transcription factor regulates expression of select activity-induced immediate early genes (IEGs), genes encoding for extracellular matrix components, and glutamatergic synaptic proteins. Therefore, I focused my further experiments on the investigation of synaptic drive onto Parvalbumin interneurons to ask if loss of SMAD1 from Parvalbumin interneurons cause alterations in their synaptic connectivity and cellular properties. By coupling electrophysiological, anatomical and behavioral analyses, I demonstrated that BMP2-SMAD1 signaling is essential to maintain excitation-inhibition in balance in the adult somatosensory cortex.

In summary, this work reveals that developmental signaling molecules are re-used for trans-cellular signaling in neurons to establish synaptic connectivity during the critical periods and maintain excitation-inhibition in balance in the adult cortex.

1. Introduction

1.1 General Introduction

Every organism evolved mechanisms to adapt to their constantly changing environment and to provide the needs of the body for preventing it from going awry. Amongst all, the nervous systems, and especially the brain, is the most plastic organ in the body of organisms. It detects, processes and integrates environmental stimuli on a daily basis, and seemingly miraculously manages to provide stable, reproducible functions as well as plastic adaptations. Besides detecting and integrating information, brain circuits are responsible for diverse functions such as controlling the body movements, instructing emotional states, regulating sleep/wake states, learning new motor skills and forming positive and negative memories. Therefore, studying how brain works has been a fundamental question not only for science but also for other disciplines.

More than a century ago, Ramón y Cajal and Camillo Golgi unraveled the cellular organization of the nervous system for the first time which led them to win the Nobel prize in 1906. While Golgi invented the staining technique and believed in a reticular view of the structure of the nervous system, Cajal demonstrated that the nervous system is not singular but rather consists of individual elements, which are called neurons. Neurons communicate with each other to receive, process and directionally transmit electrical signals in their microcircuits and across brain areas. The main site of communication between neurons are synapses, which were first proposed and named as "synapsis" in 1897 by Charles Sherrington in parallel with Cajal's neuron doctrine. Synaptein, Greek word where "synapsis" was derived, means "bind together or to be connect with".

Building on these important foundations, subsequent decades of research have yielded remarkable insights into anatomical, functional and molecular underpinnings of neuronal wiring. In 1955, Sanford Palay and George Palade for the first time demonstrated the first electron microscopy image of synapses and set the grounds of the current knowledge on the structure of synapses (Palay and Palade 1955). Synapses are the sites where electrical signal is converted into chemical signal as neurotransmitters. Neurotransmitter release from the pre-synaptic site is received by post-synaptic neurons to integrate the information and convert into a response. One key parameter for the classification of neuronal cell types is the identity of neurotransmitters released by the pre-synaptic neuron. The most common neurotransmitter in the mammalian brain is glutamate whereas the majority of inhibitory neurons release GABA. In addition, there is an array of neuropeptides and neuromodulators that contribute to neuronal communication. These signaling molecules elicit changes in the membrane potential of the post-synaptic neuron and trigger signaling events. What is fascinating is that specific temporal patterns and signaling

10

molecules can trigger plasticity events that can modify synaptic and/or neuronal functions on short (seconds to minutes) or long (hours to days) timescales, thus modifying circuit function and animal behavior. Thus, deciphering the molecular codes that instruct and implement the type of plasticity is crucial to understand complex behaviors and the pathophysiology of neurological diseases.

In my work, I used circuits that process sensory information as a model system to study plasticity. The requirement for adaptation to external stimuli can be illustrated by the macroscopic view of one of the sensory areas. Every day, animals open their eyes and are exposed to light which is the main sensory cue for the visual cortex. Sensory stimuli travel from the retina to lateral geniculate nucleus (LGN) in the thalamus and superior colliculus, before reaching the primary visual cortex. Within the mature visual cortex, visual information is primarily transmitted to the layer 4 (L4) neurons through thalamocortical axons. Activation of L4 neurons then elicits responses in the upper layer neurons (L2/3) which exhibit direction- and orientation-specific responses to sensory stimuli. Multiple layers of mechanisms such as involvement of many brain areas, diverse classes of cell types, synaptic connections and molecular programs are evolved to accommodate the needs for passing, segregating and integrating the sensory information.

In the era of Cajal and Golgi, it was only possible to examine neuronal morphology at the level of light microscopy. Thanks to the new technologies, we now live in a time where we can dive into the dynamics of cells at nanoscale and spatiotemporal resolution that was previously unthinkable. Discovery of fluorescent proteins, the advances of high-resolution and multi-photon microscopy, single-cell and multi-omic methods, and most recently spatial methods are rapidly advancing our knowledge about the tremendous diversity and complexity of the neuronal and glial cells in the brain. Such methods even made it possible to dissect the building blocks of the most complex animal species' brain and demonstrated the similarities and differences of the cell types between rodents and the primates. Yet, molecular identities of certain types of cells are conserved amongst species and make them powerful ways for tackling the fundamental questions about our mysterious brain.

Pioneering studies in the field of neuroscience demonstrated how crucial molecular programs are to integrate the sensory information-driven changes in the neuronal activity into the brain circuits. Genome wide associated studies showed that malfunctioning of these molecules are the underlying problems for neurological disorders such as autism or schizophrenia. Moreover, recent studies started to elucidate that formation of memories is dependent on the coding power of such molecules for the formation of new synaptic

connections. Even though for having the potential for being so crucial, the majority of the most molecular programs for neuronal development and plasticity are waiting to be discovered.

My PhD work unraveled that one class of secreted molecules, Bone Morphogenetic Proteins, are essential messengers for neurons to integrate neuronal activity in the form of communication between synapses and the nucleus in the somatosensory cortex. Therefore, in the first part of the following introduction chapter, I will discuss the aspects of activity-dependent circuit plasticity in the cortex. Then, I will introduce the activity-dependent transcriptional programs as one of the molecular mechanisms that direct circuit plasticity. It is noteworthy to mention here that the regulation of neuronal transcriptome and proteome at transcriptional, post-transcriptional and translational levels are key mechanisms of directing neuronal activity-dependent plasticity (Schratt, Tuebing et al. 2006, Mauger, Lemoine et al. 2016, Daswani, Gilardi et al. 2022, Mazille, Buczak et al. 2022). In particular, transcriptional regulation has been shown to be directly involved in the refinement of cortical circuits. Therefore, I will put the emphasis on the activity-dependent transcriptional regulation. As it has been a core mechanism of this dissertation, in the last section I will highlight the literature on the secreted molecules in the context of activity-dependent plasticity, and will further introduce the Bone Morphogenetic Proteins.

1.2 How neuronal activity sculpts cortical circuits during development

Synaptic plasticity is central to the rapid adaptations of the brain to the ever-changing environment. Extensive research has been conducted on cortical plasticity in sensory systems throughout the lifespan. The main differentiation between development and adulthood, as revealed by these studies, is that passive exposure to relevant information is adequate to initiate robust plasticity early in life, whereas in adults, higher-order attentional mechanisms are necessary to facilitate plastic changes. Formerly, development of neuronal circuitries was believed to be regulated by innate genetic programs. However, seminal studies modified this view and demonstrated that both genetic and spontaneously generated activity play a key role. Thus, both, early sensory-evoked activity, as well as spontaneous neuronal activity that takes place before the onset of sensation have critical impact on neuronal wiring.

Spontaneous activity is broadly conserved amongst species form invertebrates to human (Tolonen, Palva et al. 2007, Blankenship and Feller 2010, Akin, Bajar et al. 2019) and across various sensory systems (Ben-Ari, Cherubini et al. 1989, Khazipov and Luhmann

2006). Arguably, the best-known example of spontaneous activity is seen for development of visual circuits where activity arises from the retinal waves. However, how upstream areas contribute to the wiring of cortices is relatively unknown. Interestingly, neuronal activity does not only modify synaptic connectivity but also cell fate specification. Recent studies on the primary somatosensory cortex (S1) have demonstrated that postmitotic L4 neurons exhibit changes in their molecular identity, morphology, and functional properties during the late stages of differentiation (Pouchelon, Gambino et al. 2014). Pouchelon and colleagues demonstrated that restructured thalamic input instructs the genetic identity of L4 neurons in S1. Once inputs are blocked, target L4 neurons repressed expression of the S1 specific genes and acquired an expression profile that resembled neurons in the secondary somatosensory cortex (S2). Strikingly, these genetic changes induced by aberrant thalamic input also led to functional response differences compared to unmodified L4 S1 neurons (see Figure 1.1 for detailed explanation for the flow of cortical information). In another recent study, Cheng and colleagues studied how sensory experience influences development of transcriptomic programs in visual cortex (Cheng, Butrus et al. 2022). They generated a transcriptomic atlas of primary visual cortical cells over six post-developmental time points and mapped gene expression in GABAergic and deep layer glutamatergic neurons as well as non-neuronal cell types prior and during sensory experience. Remarkably, the investigators found that the determination of L2/3 cell types in V1 is influenced by vision, and these cell types exhibit an anatomically layered pattern. The influence of activity on the migration and final specification of cortical interneurons has been also demonstrated (De Marco Garcia, Karayannis et al. 2011, Close, Xu et al. 2012). Another intricate relationship between neuronal activity and cell-type specification has been reported for *Xenopus laevis* embryos where there are only eight classes of neurons which express four types of neurotransmitters. Borodinsky and colleagues demonstrated that during early development, distinct patterns of calcium spikes are generated in these neurons and altering these patterns induced switches in the neurotransmitter release while the identity of the neurons was unchanged (Borodinsky, Root et al. 2004). Collectively, findings from these studies lead to the conclusion that the environment a neuron is exposed to influences its properties at multiple levels, and thereby activity very early on begins to induce homeostatic mechanisms in neuronal circuits. This contrasts the earlier views that neuronal activity only refines networks at late stages of development.
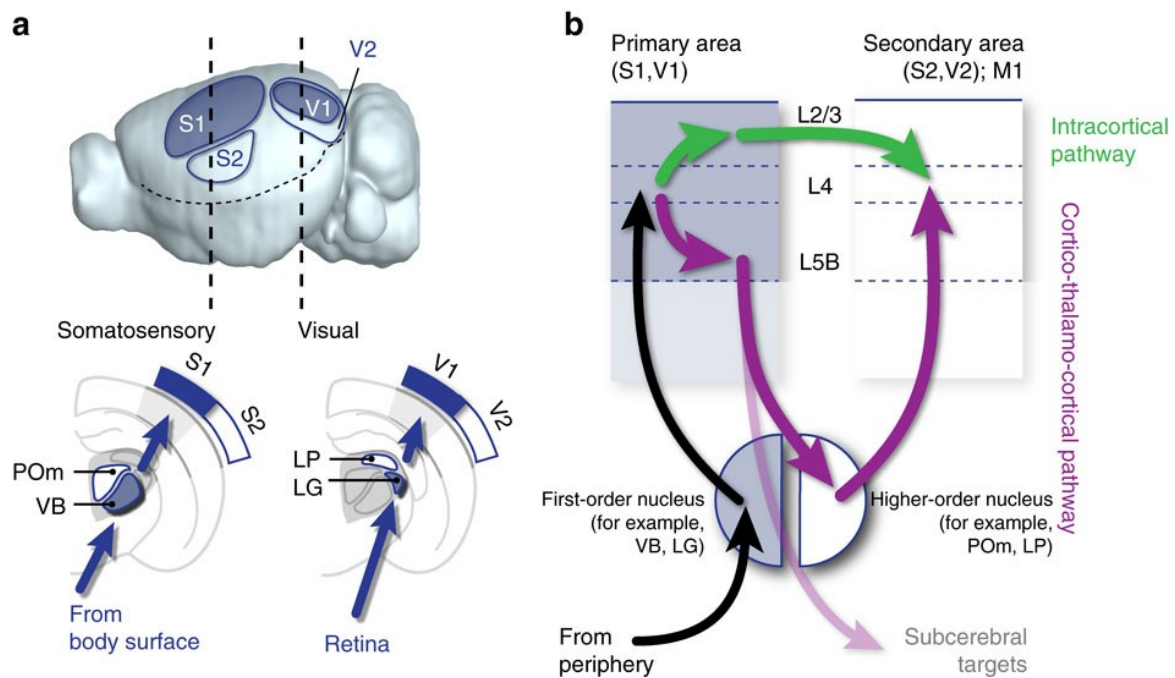
Figure 1.1: Illustration of cortical information flow from primary somatosensory and visual cortices. (a)Exteroceptive, first-order thalamic nuclei (filled in blue) project to primary cortical areas (e.g.S1, V1). Higher-order thalamic nuclei and secondary cortical areas are outlined in blue. POm: posteromedial thalamic nucleus; LG: dorsolateral geniculate nucleus; LP: lateroposterior nucleus; VB: ventrobasalis nucleus. (b) Two main pathways allow inter-areal communications: an intracortical pathway (green) and a cortico-thalamo-cortical pathway (purple), originating from L5B corticospinal neurons and which transits through higher-order thalamic nuclei (Jabaudon 2017).

1.3 The "balance" of excitation and inhibition in mature circuits

A distinguishing characteristic of the mature cortex as opposed to development is its stability. After the critical period plasticity is closed, neuronal circuits become more stable to preserve structure and function. However, exposure to the environmental changes or the learning and acquisition of new and complicated tasks is a life-long process. Therefore, neurons within the exposed networks continue to form and eliminate subsets of synapses.

Studies initially focused on the mechanisms that add new synapses and strengthen synaptic transmission as a cellular correlate of learning. However, it was soon postulated that additional mechanisms must exist that counter increases in synaptic transmission and excitability to maintain the active network in a stable operating range. These mechanisms

are frequently conceptualized in a framework of neuronal excitation-inhibition (E-I) balance. In essence, it was proposed that increases in neuronal excitation must be matched by increased inhibition to keep individual neurons and microcircuits in an optimal range for computation. Thus, operation of circuits with too much excitation would be sub-optimal due to noise, whereas circuits with too much inhibition would lack sensitivity for signal detection. Rubenstein and Merzenich postulated that neurological disorders such as autism could be the result of a disrupted E-I balance (Rubenstein and Merzenich 2003). Conceptually, the E-I balance proposed that generation of too noisy or too quiet circuits, perhaps due to improper GABAergic interneuron functions, would be the underlying causes of such disorders. However, studies modelling autism disorder related genetic alterations in rodents provided heterogenous findings. Thus, future work will be needed to further explore this.

On short time scales, sensory stimuli always lead to an interplay between synaptic excitation and inhibition. Activity changes the membrane potential and the conductance of neurons and the computation of these two mechanisms shapes the spatiotemporal function of cortex. Extensive feed-forward and recurrent excitation are prominent features of neural circuits (Isaacson and Scanziani 2011). Thus, even small adjustments in the delicate balance between excitation and inhibition can spark uncontrollable seizure-like activity in the brain. Even though epilepsy affects around 1-2% of the population, what is quite surprising about it is that most people don't develop such disease. Therefore, changes in the weight of excitation or inhibition must be accompanied by compensatory effects that preserve the excitability of cortical networks. Moreover, associating cortical inhibition primarily with preventing epileptiform activity oversimplifies its broader role. Excitation and inhibition exhibit different patterns across neuronal components such as the soma, dendrites, and axon initial segment, leading to a highly variable ratio depending on the measurement location. In addition, it is important to note that although there is an overall proportionality between excitation and inhibition, their specific ratio also shows dynamic patterns across cortical layers. For example, in layer 2/3, principal cells project their axons horizontally within their own layer, as well as vertically, towards layer 5. Nonetheless, the excitation-inhibition ratio produced by layer 2/3 principal neurons shows discrepancies across layers: it tends to favor inhibition within its own layer but demonstrates a preference for excitation in layer 5 (Adesnik and Scanziani 2010). These observations raise the question how E-I balance is maintained on local and global levels.

1.3.1 Maintaining circuit stability by turning the fast-spiking interneuron knob

In cortical circuits, around 80-90% of the neurons are excitatory which leaves the remaining 10-20% as inhibitory. There is a strong connectivity and a reciprocal relationship between excitatory and inhibitory neurons where they excite or inhibit each other and also themselves. Therefore, GABAergic interneurons are not only stimulated in proportion to the local network activity but also play a direct role in shaping it through their inhibitory feedback.
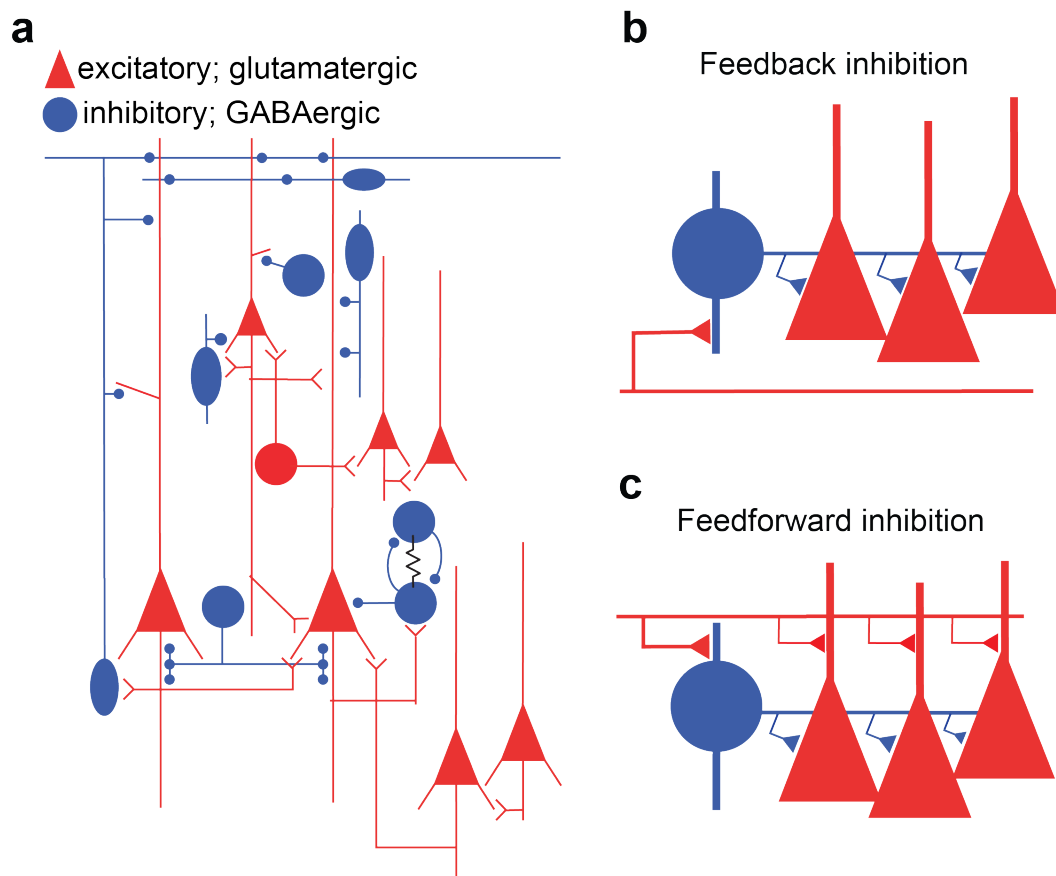
Figure 1.2: Microcircuit motifs of cortical inhibition: a) Simplified scheme of main neuron types and synaptic connections in the neocortex. b) Feedback inhibition arises when cortical principal cells (red) make excitatory synaptic contacts (red) on local interneurons (blue) that in turn form inhibitory synaptic contacts (blue triangles) on the principal cell population. c) Feedforward inhibition is generated when long-range excitatory afferent inputs (red) diverge onto both principal cells and local interneurons. Adapted from (Silberberg, Grillner et al. 2005, Isaacson and Scanziani 2011).

Local cortical circuits are patterned by an array of inhibitory wiring motifs that are similarly used across cortical and sub-cortical regions. Two major forms are called feedback and feedforward inhibition (Figure 1.2). Feedback inhibition occurs when cortical principal cells make synapses onto inhibitory neurons which concomitantly form inhibitory synapses onto the same neuronal population. Thus, activation of principal cells results in a rapid silencing through feedback inhibition. In the case of feedforward inhibition, long-range excitatory inputs (i.e., thalamocortical afferents) are diverged onto both principal cells and inhibitory neurons and thereby excite both populations. This results in the proportional distribution of activity in both populations and allows for matched inhibitory response to excitation in a narrow time window.

Interneurons come in many different flavors and their traditional classification is based on their morphology, anatomy and physiology (Ascoli, Alonso-Nanclares et al. 2008). However, one of the most striking features of this group of neurons is their morphological diversity, in particular with regard to their axonal arborization and, as a consequence, their postsynaptic targets. Different types of GABAergic interneurons, such as 'Basket' cells, 'Chandelier' cells, and 'Martinotti' cells, exert inhibitory control over distinct compartments of principal neurons. For instance, 'Basket' cells target the somatic and perisomatic compartment, 'Chandelier' cells selectively inhibit the axon initial segment, while 'Martinotti' cells preferentially target the apical dendritic tuft. This compartmentalization of inhibition highlights the diverse roles played by these interneurons, which extend beyond their morphological differences. Strikingly, in contrast to the large amount of information that exists on the properties of the various types of cortical inhibitory neurons, knowledge of the specific role that each one plays in orchestrating cortical activity is still limited (Liguz-Lecznar, Urban-Ciecko et al. 2016, Scheyltjens and Arckens 2016). Amongst all, parvalbumin-expressing, fast spiking basket cells, or in short from hereafter referred as PV interneurons, have been shown to be the major regulators of the E-I balance. PV interneurons exert strong control over the excitability of principal cells due to the strategic placement of their axon terminals around the soma. Alongside other cortical inputs, PV interneurons receive similar excitatory signals as their principal cell counterparts, establishing a feed-forward inhibitory circuit (House, Elstrott et al. 2011, Avermann, Tomm et al. 2012, Xue, Atallah et al. 2014). This arrangement enables excitatory input to simultaneously stimulate both the PV basket cell and the pyramidal neuron. Subsequently, the PV interneurons suppress the activity of the principal cell. (Figure 1.3). A crucial factor in this process is the time delay between the arrival of excitatory and inhibitory input at the pyramidal cell, creating a narrow permissive window. Within this window, cumulative

excitatory signals can combine to elicit an action potential in the pyramidal cell. Conversely, if inhibitory input reaches the principal cell before an action potential is generated, the GABA action targeted at the soma will prevent its initiation. Therefore, PV interneurons permit action potential initiation in principal cells only if the excitatory information is synchronized in time and possesses sufficient strength.
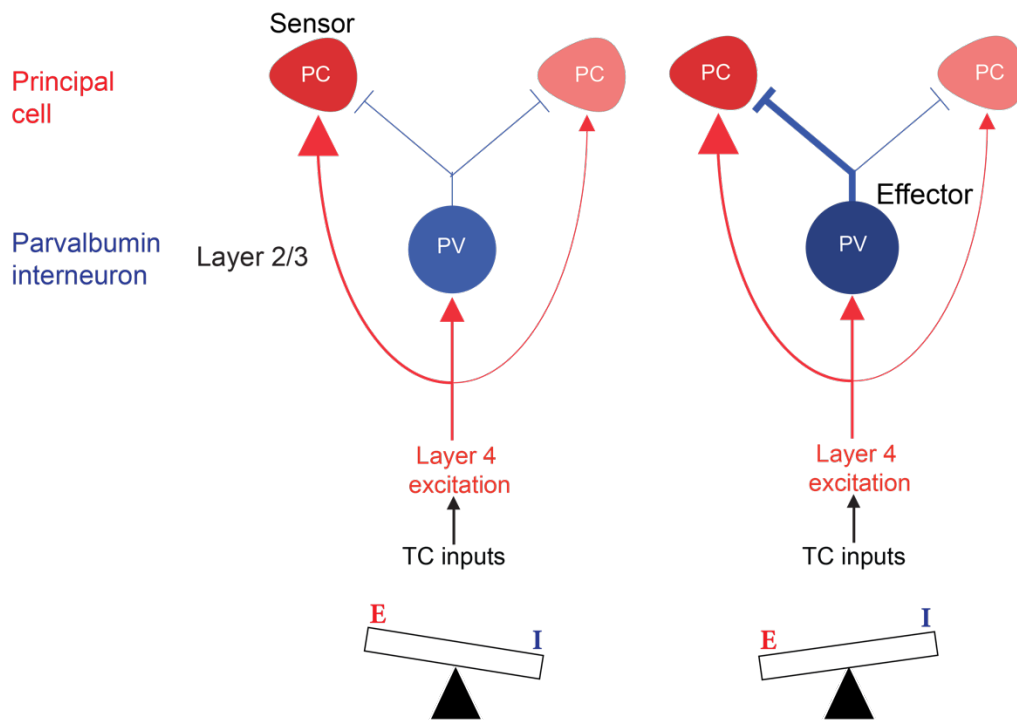
Figure 1.3: Cellular components of equalized E/I ratios in principal cells. Despite divergent axons, Parvalbumin interneurons generate larger inhibition in principal cells receiving more excitation. Accordingly, E/I ratios are equalized across principal cells (Xue, Atallah et al. 2014).

1.3.2 Cellular and molecular properties of fast spiking interneurons controlling circuit stability and plasticity

PV interneurons display characteristic cellular and molecular features which underly their function. One such feature is in their name. Parvalbumin is a calcium binding protein which plays crucial roles for the fast-spiking properties of these neurons due to the kinetics of calcium buffering. Select expression of L-type and P/Q-type calcium channels and fast calcium sensors such as Synaptotagmin-2 (Syt2) at their presynaptic terminals together with acting on GABAA1 receptor on their post-synaptic target principal cells allows their fast inhibitory function. In addition, expression of subtypes of Kv3 family voltage gated channels contributes to the rapid firing of action potentials and neurotransmitter release properties. Interestingly, PV interneurons change their intrinsic and cellular properties in an activity-dependent manner, partially due to these characteristic features in combination with their molecular programs (Campanac, Gasselin et al. 2013, Dehorter, Ciceri et al. 2015, Sun, Ikrar et al. 2016, Joseph, Von Deimling et al. 2021).

One very remarkable feature of cortical PV interneurons is the reticular extracellular structure surrounding their soma and the axon initial segments (AIS), which is called perineuronal nets (PNNs). PNNs were first reported by Camillo Golgi in 1893 and since then the knowledge on the origin and composition of these structures have changed dramatically (Golgi 1989). PNNs are composed of extracellular matrix molecules with similarity to the cartilage in the structure. Main components of PNNs are hyaluranan (HA), link proteins, chondroitin sulfate proteoglycans (CSPGs) and Tenascins. Lecticans are a member of CSPGs which can bind to HA and lectins (Ruoslahti 1996, Iozzo 1998). Glycosaminoglycans (GAG) are covalently attached chains to lectican protein cores through serine residues, forming lecticans such as aggrecan, versican, neurocan and brevican, all of which exist in PNNs (Matsui, Nishizuka et al. 1998, Hagihara, Miura et al. 1999, Carulli, Rhodes et al. 2006). Aggrecan is the commonly existing member of lecticans in all PNNs, whereas others show cell-type specific properties. Amongst those, brevican has been shown to be enriched around the PNNs of PV interneurons in the cortex and hippocampus. To date, several visualization methods for PNNs have been developed such as use of plant lecticans Vicia villosa agglutinin and Wisteria floribunda agglutinin (WFA), which have affinity for N-acetylgalactosamine (Nakagawa, Schulte et al. 1986, Bruckner, Brauer et al. 1993) and mono- or polyclonal antibodies raised against components of the PNNs such as aggrecan or brevican (Wang and Fawcett 2012).

The formation of PNNs occurs as one of the last acts of neural development, coinciding with the closure of the critical periods for plasticity, starting around postnatal day 23 and

lasting for 10 days in mice and rats. In humans, this period spreads from 2 years to 8 years of age (Carulli, Pizzorusso et al. 2010, Oohashi, Edamatsu et al. 2015, Rogers, Rankin-Gee et al. 2018). Tight relationship between the plasticity capacity of neuronal circuits and the PNNs surrounding the PV interneurons have been demonstrated by several studies. Manipulation of PNNs elucidated their impacts on synapses, plasticity, memory, psychiatric conditions and neurological disorders such as epilepsy (Gogolla, Caroni et al. 2009, Sorg, Berretta et al. 2016, Banerjee, Gutzeit et al. 2017, Favuzzi, Marques-Smith et al. 2017, Niekisch, Steinhardt et al. 2019). Recent findings from the studies investigating the emergence of the sensory response and hippocampal engram formation now show that PV interneurons form functional assemblies (Modol, Bollmann et al. 2020) and, proper development of PNNs is essential for the establishment of episodic memories in juveniles (Ramsaran, Wang et al. 2023).

Notably, PNNs not only gate PV interneuron function but also regulate the formation, cellular, and electrophysiological properties of PV interneurons, which are tightly controlled by activity in both developing and adult cortical circuits. Dehorter and colleagues showed that a switch in the Er81 transcription factor from high to low expression levels, triggered by increased network activity, leads to dynamic changes in the firing and cell-intrinsic properties of PV interneurons in the adult cortex (Dehorter, Ciceri et al. 2015). These findings raise questions about how signals direct transcriptional regulation and what other molecular mechanisms underlie the global changes induced in neurons in an activity-dependent manner.

1.4 Activity-dependent transcriptional programs

1.4.1 Relaying trans-synaptic signals to the nucleus

In accordance to their complexity, neurons require highly dedicated genetically defined molecular programs for the establishment and function of their circuits. In contrast to other cell types in the body that continuously go through cell division and grow, neurons are post-mitotic and therefore must stay highly dynamic throughout their lifetime. Therefore, just the repertoire of protein-coding genes which is approximately around 20.000 is not sufficient to explain their proteome diversity providing for very specific synaptic codes or their adaptation capacity. Thus, the excitable properties of neurons allowed them to recognize trans-synaptic signals and utilize diverse molecular programs to maximize their capacity to retain the information. Opening of ligand-gated channels would allow this response to be in milliseconds while second messenger-mediated events would generate responses within the range of seconds to minutes. While there are these fast responses, pioneering studies showed that trans-synaptic signaling also elicits slower and more global

responses through synthesis of new gene products. Neuronal gene expression can be stimulated through various mechanisms such as membrane activity, neurotransmitter signaling, and growth factor activation which also play essential roles in the nervous system development.

The response properties of a neuron to various types of stimuli are closely linked to a rapid and transient gene expression regulation through a group of genes called Immediate Early Genes (IEGs) or Primary Response Genes (PRGs). The initiation of IEG expression can be activated by the entry of calcium through ligand-gated ion channels, for example, N-methyl-D-aspartate-type (NMDA) and specific forms of α-amino-3-hydroxy-5-methyl-4-isoxazolepropionate-type (AMPA) glutamate receptors, and voltage-gated calcium channels, along with the discharge of calcium from intracellular reservoirs (West, Chen et al. 2001). Nevertheless, several investigations have demonstrated that gene transcription is predominantly stimulated by calcium influx through L-type voltage-sensitive calcium channels (L-VSCCs) through several calcium-induced transcriptional programs (Subset of these pathways are illustrated in Figure 1.4). That is believed to occur due to the positioning of L-VSCCs in the cell bodies and adjacent regions of dendrites (Westenbroek, Ahlijanian et al. 1990), which places them closer to the nucleus. Additionally, their calcium conductance and gating characteristics (Wheeler, Groth et al. 2012, Simms and Zamponi 2014) along with their physical association with crucial signaling molecules such as calmodulin, are important for activating transcription (Deisseroth, Heist et al. 1998, Dolmetsch, Pajvani et al. 2001, Ma, Groth et al. 2014).

In 1984, Greenberg and Ziff discovered that the *Fos* gene is rapidly expressed in cells upon stimulation. Considering that inducing its mRNA expression occurred without the requirement for new protein synthesis, it is considered as IEG (Greenberg and Ziff 1984). As being a proto-oncogene and therefore widely regulated in many different cell types, efforts coupled from different fields demonstrated that *Fos* protein is localized in the nucleus and function as a transcription factor (TF). Further studies elucidated that the TF capacity of IEGs is not only restricted with the transcription start sites but rather more selective for distal cis-regulatory elements such as enhancers (Kim, Hemberg et al. 2010). Almost 40 years after the discovery of *Fos* as an IEG*,* we now know that neuronal activity rapidly induces expression of a shared sets of transcription factors. Those include other FOS family proteins FOSB, FOSL1 and FOSL2, Neuronal Per Art Sim Domain Protein 4 (NPAS4) or Early Growth Response Genes (EGR1, EGR2, EGR3). FOS forms heterodimers with JUN, another proto-oncogene, to form AP-1 transcription factor complex and interact directly with FOS binding sites whereas NPAS4 or EGR transcription factor families can recognize distinct binding sites as they belong to separate TF families. Even

though most of the IEGs have TF function, there are also couple of other IEGs identified with different properties. One such example is *Arc* (activity dependent cytoskeleton protein) which has been shown to be enriched in the dendrites and play important roles in synaptic plasticity (Chowdhury, Shepherd et al. 2006).
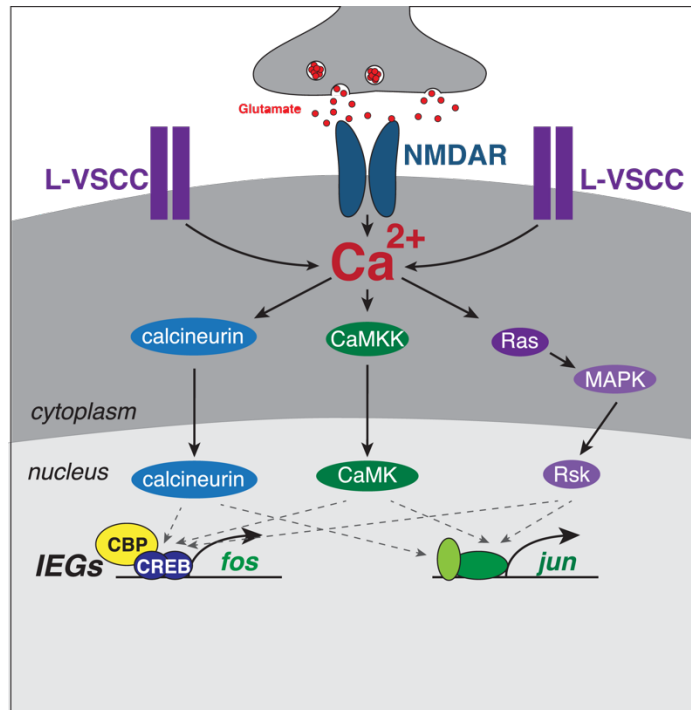
Figure 1.4: Mechanism of action of calcium influx through NMDA receptors (NMDARs) and L-type voltage gated channels. This leads to alteration of various calcium-dependent signaling pathways and concomitant induction of IEGs (Yap and Greenberg 2018).

An additional layer of information gained from seminal studies showed that IEGs with TF functions subsequently induce a second wave of gene expression which are called as late response genes (LRGs) or secondary response gene (SRGs). In contrast to the broad induction of IEGs, late response genes were speculated to be rather cell-type specific to regulate the properties and synaptic connectivity. Until the discovery of NPAS4 regulation in 2008 (Lin, Bloodgood et al. 2008), a brain specific IEG, IEGs have been only demonstrated to control the glutamatergic synapses. Lin et al. showed for the first time that synapse-to-nucleus communication through IEGs is also important for the control of GABAergic synapses on excitatory neurons. Moreover, Spiegel et al. further uncovered the role for NPAS4 on regulation of LRGs in a cell-type specific manner (Spiegel, Mardinly et al. 2014). Complementary to previous demonstrations on the LRGs, Spiegel and colleagues for the first time revealed that shared TFs can bind to distinct gene regulatory regions dependent on the neuron type and thereby control inhibition on excitatory neurons and excitation on inhibitory neurons. All together, these findings had a huge impact on

understanding of how neuronal activity induces global and long-term alterations in neurons and thereby opened the door for investigation of the following questions: Which cellular processes are regulated by activity-dependent transcriptional programs and how does the set of IEG TFs regulate cell type-specific LRGs?

1.4.2 Tailoring synapse-to-nucleus signaling to the circuit functions

Once mature, neuronal circuits regulate body states and functions such as hunger, sleep, pain, fear and social behaviors. Experience-dependent plasticity mechanisms are central for state- and learning-induced behavioral adaptations. The advancement of genetic labeling strategies and single cell-sequencing technologies allowed scientists to access subtypes of cells and manipulate them through molecular tools. These tools facilitated efforts to map activity-dependent transcriptional programs. Mardinly and Spiegel et al. used genetic labelling and isolation of mRNAs from defined subpopulations of neurons and elucidated that when dark-reared mice are exposed to light stimulation, IEGs and LRGs are induced in the primary visual cortex (Mardinly, Spiegel et al. 2016). Shortly after, Hrvatin et al. replicated the same paradigm and captured the changes in the expression levels of IEGs and LRGs in an unbiased way and at the single-cell resolution (Hrvatin, Hochbaum et al. 2018). The former study was restricted to subtypes of neurons whereas the latter one captured both neuronal and non-neuronal cell types of the visual cortex. In addition to being one of the first examples for capturing IEGs upon sensory stimuli, these studies showed that not all IEGs are induced in all cell types but rather some are broader and some are more specific to certain cell types and even different layers of the cortex.

Beyond the understanding of molecular mechanisms, the work on IEGs also provided the foundation for the development of tools to probe the cells and neuronal ensembles contributing to learning processes. From the time FOS has been found as one of the molecular markers of neuronal plasticity, several strategies have been developed for genetic tagging of activated-neurons (DeNardo and Luo 2017). Two successors of these methods were named as FosTRAP and ArcTRAP (Targeted Recombination in Active Populations). TRAP requires two transgenes wherein one expresses tamoxifen inducible Cre recombinase under the promoter of either *Fos* or *Arc*. Second transgene is then a cre-dependent effector gene such as eGFP or tdTomato. Without tamoxifen, cre is retained in the cytoplasm and thereby can't recombine the effector gene. Thus, this strategy provides permanent access and spatiotemporal control of when the cells will be marked. However, this version of TRAP disrupts endogenous Fos and have been shown to have restricted

access to many brain regions. Thereby, by using knock-in strategy, DeNardo et al. developed the most recent version of TRAP, TRAP2 which has been adopted quite well in the fields from studying the physical traces of fear or spatial memories, the engrams (DeNardo, Liu et al. 2019, Pettit, Yap et al. 2022), to which brain areas and their cellular components regulate stress induced sleep disturbances in rodents (Yu, Zhao et al. 2022).

Despite being so powerful and the recent advances both approaches above, methods using single IEG as assays of neural activity also have some disadvantages. IEG-based TRAPping methods have relatively slow temporal resolution of hours to days. Further, certain cell types and brain regions show little FOS or Arc expression, thereby can be difficult to trace the activity brain-wide. To overcome issues of IEG-based tagging of neuronal activity, a robust activity marking (RAM) system has been recently developed and shown to successfully label activated neurons during fear memory formation in the hippocampus(Sorensen, Cooper et al. 2016). This system is designed to have small and more selective activity induced promoter which is derived from minimal Fos promoter, enhancer module of AP1 complex and an Npas4 binding motif. RAM system made suitable for viral delivery approaches and was shown to label activated neurons in several brain regions in both *Drosophila* and mice.

Emerging findings from such studies clearly show that varying patterns of neuronal activity during development or activation of inhibitory neurons could benefit more from rather cell-type specific IEGs (Hrvatin, Hochbaum et al. 2018). Indeed, even though very powerful, currently available TRAP2 line is missing the full landscape of cellular components of engrams as they are restricted to FOS activation (or *Arc*). Therefore, complementary studies combining the measures of FOS levels with calcium imaging in behaving animals (Pettit, Yap et al. 2022) or generation of new reporters from other IEGs are crucial to better understand the cellular, molecular and circuit mechanisms of activity-dependent plasticity. Moreover, several studies also identified primate-specific activity-induced genes (Ataman, Boulting et al. 2016, Qiu, McQueen et al. 2016, Pruunsild, Bengtson et al. 2017). Understanding the function of these genes will be very useful in the aspect of evolution of species-specific activity dependent molecular programs and their contributions to cognitive abilities and genetic factors of neurological disorders in humans.

1.5 Epigenetic control of activity-dependent transcription

1.5.1 Long-lasting gene expression programs through epigenetic control

Although alterations in transcriptional regulation in response to activity are of a relatively brief duration, the retention of acquired behaviors and memories can endure from days to months in mice and from days to decades in humans. This raises the question of how information is stored in the neuron for prolonged periods following the return of activity-dependent gene expression to its baseline level. One potential explanation is that this information is stored by stabilizing the synaptic connectivity, ensuring their persistence long after the period of gene expression induction. Another interesting hypothesis proposes that neuronal activity, in addition to inducing gene expression through the aforementioned mechanisms, can initiate enduring modifications of the genome itself through epigenetic mechanisms, subsequently influencing the gene expression pattern of the neuron and allowing the encoding of memories from previous experiences within the neuronal genome itself. During development and disease states, various epigenetic mechanisms were identified to regulate the cell-type specific gene expression patterns through cis-regulatory elements (CREs) such as promoters and enhancers(Preissl, Gaulton et al. 2022). Different categories of CREs can be distinguished based on their epigenetic attributes, such as DNA methylation, combinations of histone modifications, chromatin accessibility and higher-order chromatin organization (Figure 5). Former bulk sequencing and recent single-cell and spatial-omics technologies demonstrated the power of cell-type specific gene regulatory programs instructed by epigenetic programs, which are highly responsive to environmental changes. Former studies on how IEGs regulate the expression of LRGs showed that IEGs such as FOS/JUN heterodimers or NPAS4 binds to cell-type specific enhancers (Spiegel, Mardinly et al. 2014, Vierbuchen, Ling et al. 2017). These enhancer regions were primed for driving activity-dependent transcription and can become accessible once neurons are activated. In addition, neuronal activity also modifies the state of the chromatin by depositing and exchanging histone acetylation and or methylation marks at CREs, or through rearranging the organization of their chromatin by bringing cell-type specific enhancers to close proximity to the promoters. Recent research has demonstrated that the activation of neurons results in distinct alterations in chromatin that coincide with behavioral encounters, such as the exploration of unfamiliar surroundings or various types of associative learning(Levenson, O'Riordan et al. 2004, Fischer, Sananbenesi et al. 2007, Miller, Campbell et al. 2008). Thus, combination of tagging engrams by using TRAP strategies and single cell omics for studying the neuronal

coding during complex tasks or formation of memories will provide better insights on how the information from transient transcriptomic re-programming is stored for long periods.
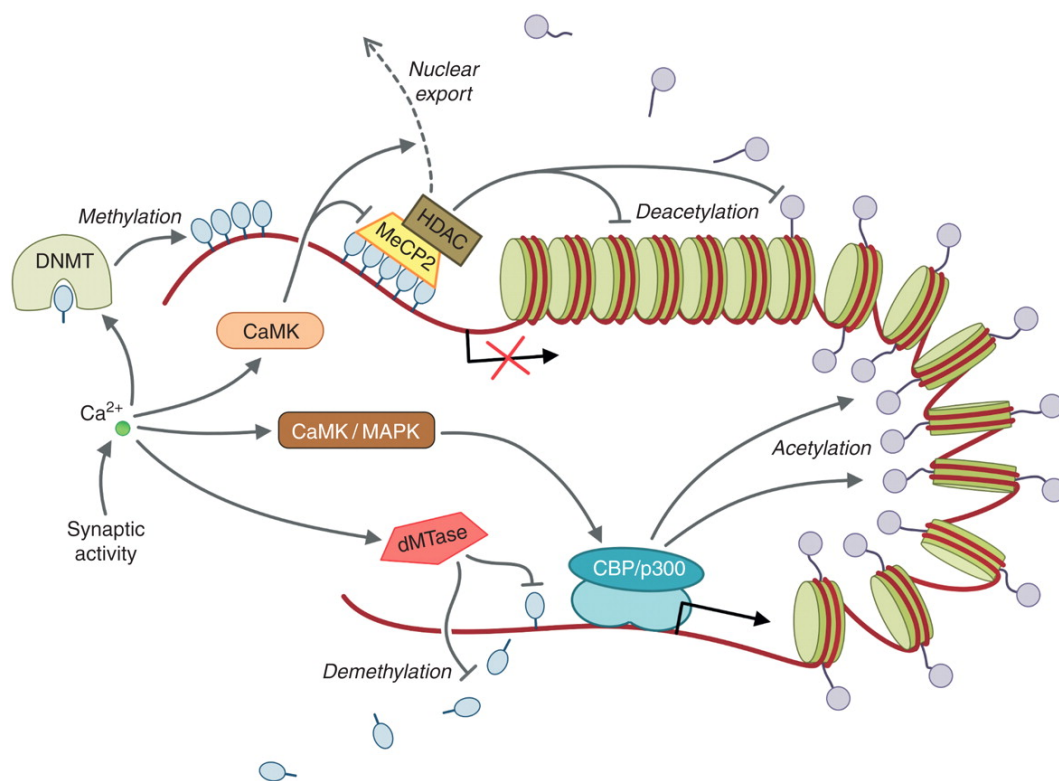
Figure 1.5: Summary of epigenetic mechanisms modified by neuronal activity (Hagenston and Bading 2011).

In addition to the histone modifications, rapid and ever-changing modifications in DNA methylation has also emerged as significant responders of neuronal activity. In mammals, methylation predominantly occurs at CG regions of DNA, referred as mCG. mCG has been shown to be involved in several cellular processes such as proliferation or aging. Interestingly, brain has been found to be enriched for other forms of methylation where methylated cytosine is followed by another nucleotide than guanine and referred as non-CG methylation. Strikingly, neurons were found to accumulate high levels of mCA during the first few weeks of postnatal mouse development when sensory experience plays drastic roles for the formation of neuronal circuits. As in the case of chromatin remodelling, DNA methylation is also under tight control of "writer", "reader" and "eraser" mechanisms. One of the well-known readers of DNA methylations is MeCP2 which is indispensable for the brain development as mutations of that causes a neurodevelopmental disorder which is called Rett syndrome. Interestingly, MeCP2 has also been shown to be regulated by neuronal activity with post-transcriptional modifications and thereby mutations at these sites could explain its importance for the normal brain development (Ebert, Gabel et al.

2013, Lyst, Ekiert et al. 2013). Advanced studies investigating the epigenetic mechanisms on the neuronal transcripts demonstrated that during the critical period plasticity at postnatal development, switch between histone modifications and DNA methylation occurs specifically at the enhancers in subtypes of neurons and thereby modulates fine-tuning of their transcripts (Stroud, Su et al. 2017). Moreover, recent studies demonstrated that DNA methylation has significant contribution to the diversity of brain cell types and the maintenance of their levels are crucial for establishment and persistence of cognitive abilities or strengthening of memories where extensive plasticity events are required (Karaca, Kupke et al. 2020, Liu, Zhou et al. 2021). Collectively, these discoveries suggest that neuronal activity could potentially extend the duration in which it impacts the neuronal transcriptome by altering the activity or interaction of protein complexes involved in the deposition and reading of DNA methylation and histone modification.

1.5.2 Rewinding to basal gene expression through transcriptional repression

Note: parts of this section are extracted from the preview "*The Ying and Yang for the activity-dependent transcription factor Arnt2*", Neuron, (Okur and Scheiffele, 2019).

As aforementioned in the previous chapters, there has been major progress on the identification of gene regulatory elements and transcription factors driving the onset of activity-dependent transcripts in neurons. However, comparably little is known about mechanisms that repress target gene transcription prior to stimulation. Tight repression would minimize noise from background expression and, thus, maximize the dynamic range that can be accomplished in response to stimulation. But how can robust repression be achieved without compromising the dynamics of gene induction in response to stimulation? At activity-dependent promoters, proteins that modify histone composition or histone modifications have important functions in silencing transcription prior to stimulation. For example, the nucleosome remodeler complex NuRD triggers inactivation of promoters (Yang, Yamada et al. 2016) or recruitment of the histone deacetylase HDAC4 represses genes in inactive neurons(Sando, Gounko et al. 2012). Nonetheless, the spatiotemporal regulation of the full repertoire of activity dependent gene regulatory elements in neuronal cells – in particular at the level of enhancers - is poorly understood. The study from Sharma and colleagues(Sharma, Pollina et al. 2019) revealed a dual role for additional additional bHLH-PAS protein, Arnt2, in the repression of Npas4-regulated neuronal transcripts (Figure 6). Yet, Arnt2 itself is not a transcriptional repressor. Thus, Sharma and colleagues went on to identify interactors of Arnt2 that might mediate

transcriptional repression. They discovered as an Arnt2 interaction partner the so-called NCoR2 co-repressor complex that has well-established roles as repressor of transcription in several cell types(Mottis, Mouchiroud et al. 2013). NCoR2 binding regions largely cover the Arnt2-bound regulatory elements, strongly suggesting that Arnt2 indeed recruits NCoR2 for the repression of activity-dependent transcripts prior to stimulation. This study established distal enhancer elements as major contributors to activity-dependent neuronal gene regulation. Interestingly, the chromatin of the Npas4 target sites is largely accessible for transcription factor binding, presumably facilitating rapid gene induction upon stimulation. The extensive functional analysis for the transcription factor Arnt2 demonstrated a powerful repression mechanism that prevents aberrant transcription of activity-dependent genes and hence dysregulation of neuronal circuits. Future studies focusing on how the Arnt2-NCoR2 repressor complex is turned into an activator complex and engages with Npas4 for the transcription of Npas4-dependent genes. This functional conversion may involve posttranslational modifications and/or an interplay between NCoR2 and chromatin remodeling complexes. Notably, Sharma and colleagues also found Arnt2 to interact with Npas3, another bHLH-PAS transcription factor. Npas3 expression is enriched in inhibitory interneurons, thus, providing one additional piece of the puzzle of how cell type-specific responses to neuronal activity might be controlled.
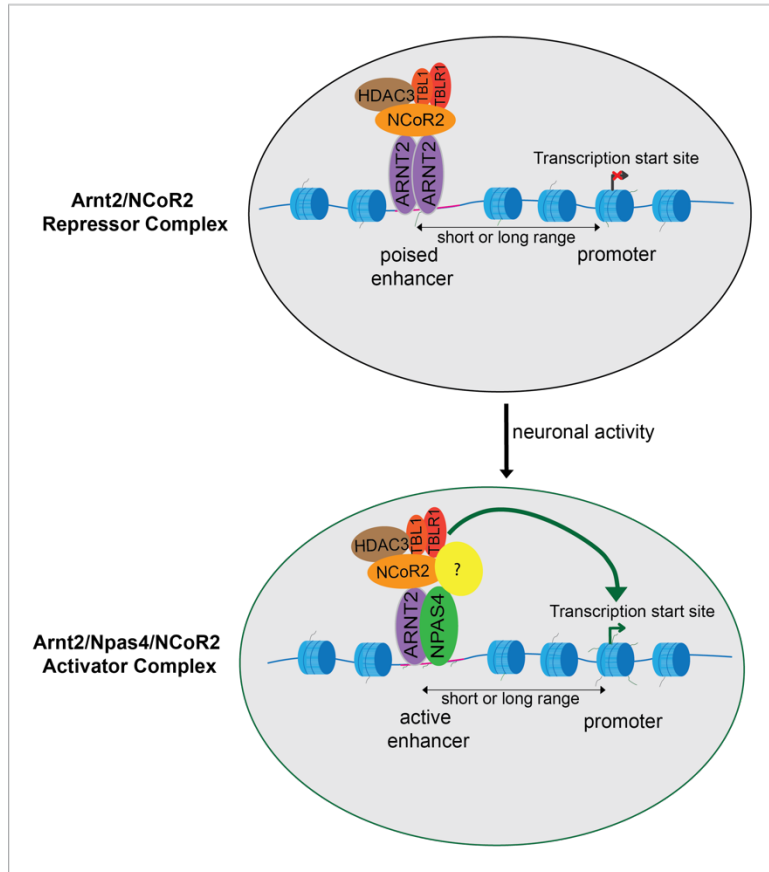
Figure 1.6: Neuronal Activity-Dependent Switch from Repression to Activation. Model for the repression of neuronal activity-dependent genes at enhancers by Arnt2-NCoR2 complexes (NCoR2, HDAC3, TBL1, and TBLR1). Upon reaching a threshold of neuronal stimulation, Arnt2 homodimers are converted to Arnt2-Npas4 heterodimers. The resulting complex containing NCoR2 and presumably additional activators triggers transcription of Npas4-dependent, activity-regulated genes (Okur and Scheiffele 2019).

Overall, this chapter summarizes the progress made for how neuronal activity instructs transcriptional, epigenetic and repression mechanisms and highlights the importance of both cis- and trans-regulators of the DNA. To bridge the gap between activity-regulated transcriptional networks and the circuit functions, future studies employing genome editing strategies such as Crispr/Cas9 to specifically target the identified regulatory regions, or characterization of the behavior of activated neurons under natural behaviors, and activation/silencing of these neurons using TRAP-based genetic tools where the endogenous levels of activity-induced early and late response genes are maintained will fundamentally advance our understanding. One step forward, better characterization of the "second wave" gene products and studying their roles in the intact circuits will provide answers to closing the gap between how the feedback from the nucleus to the synapses

is utilized by neurons to communicate. Thereby, in the next chapter, I will illustrate the secreted molecules identified as products of activity-driven transcriptional networks and in this context, I will further highlight the Bone Morphogenetic Proteins.

1.6 Secreted signaling molecules for neuronal communication

1.6.1 Historical view and the state of the art of activity-dependent secreted factors

It is unquestionable that genes, whose transcription is regulated by neuronal activity, play a crucial role in brain development and function. Amongst the extensively examined activity-regulated secreted molecules, brain-derived neurotrophic factor (BDNF) received substantial attention. Studies in mice lacking BDNF have provided compelling evidence highlighting its indispensable role in various aspects of neuronal function, including survival, differentiation, migration, and dendritic arborization (Ernfors, Lee et al. 1994, Jones, Farinas et al. 1994, Schwartz, Borghesani et al. 1997). Furthermore, BDNF has also been implicated in synaptic development, function, and plasticity, accompanied by alterations in body weight regulation, locomotor activity, and aggression (Korte, Carroll et al. 1995, Patterson, Abel et al. 1996, Lyons, Mamounas et al. 1999, Kernie, Liebl et al. 2000, Carter, Chen et al. 2002, Abidin, Kohler et al. 2006). It is therefore widely accepted that many of the diverse functions of Bdnf, particularly its involvement in synaptic development, function, and plasticity, are under the influence of its activity-dependent expression in neurons(Poo 2001).

The precursor "proBDNF" serves as the source for brain-derived neurotrophic factor synthesis, with the ability to be stored in dendrites or axons (Lessmann, Gottmann et al. 2003). Cleavage of proBDNF was proposed to occur either intracellularly or extracellularly, mediated by specific enzymes (Lee and Chao 2001), leading to the formation of mature BDNF protein. The release of BDNF, comprising both pro and mature forms, is dependent on neuronal activity, introducing a complex dimension to its function(Pang and Lu 2004). Interestingly, BDNF and proBDNF were proposed to exert opposing effects on cellular function. ProBDNF is secreted under pathological and non-pathological conditions and exhibits a preference for binding to the p75NTR receptor, resulting in long-term depression (LTD) facilitation and apoptosis induction (Friedman 2010). However, some rigorous studies suggest that at least in some cell types only mature BDNF can be secreted(Matsumoto, Rauskolb et al. 2008). Conversely, mature BDNF selectively binds

to tyrosine kinase receptors (TrkB), promoting cell survival, facilitating long-term potentiation (LTP), and enhancing spine complexity (Zagrebelsky, Holz et al. 2005, Volosin, Song et al. 2006). Co-expression of p75NTR and TrkB receptors augments neurotrophin binding affinity, enabling precise ligand discrimination(Bibel, Hoppe et al. 1999). Thus, proBDNF can be regarded as part of a regulatory mechanism that modulates BDNF activity under non-pathological conditions. Additionally, truncated forms of the TrkB receptor act as dominant negative inhibitors, internalizing and clearing BDNF from the synapse, thereby regulating BDNF signaling (Haapasalo, Sipola et al. 2002).

The intricate regulation of Bdnf expression in the nervous system, which is under tight control of temporal, spatial, and stimulus-specific factors, is substantiated by the complexity of its gene structure. The Bdnf gene comprises a minimum of eight distinct promoters that initiate transcription of multiple unique mRNA transcripts. Interestingly, each transcript consists of an alternative 5' exon spliced to a common 3' coding exon that encompasses the complete open reading frame for the BDNF protein (Aid, Kazantseva et al. 2007). By utilizing alternative promoters, splice donors, and polyadenylation sites, the Bdnf gene has the capacity to generate at least 18 distinct transcript isoforms. Remarkably, despite this diversity, all of these Bdnf mRNAs encode an identical BDNF protein. The functional implications underlying the transcriptional organization of the Bdnf remain enigmatic; however, a compelling hypothesis suggests that the production of multiple mRNAs encoding the same protein enables multilayered regulation of BDNF expression. This regulation could involve differential mRNA stability and translatability, or differential subcellular localization of the mRNA(s) or protein. Substantiating this notion, it is well-established that the various Bdnf promoters exhibit differential responsiveness to neuronal activity, with promoter IV-dependent Bdnf transcription accounting for the majority of activity-induced Bdnf expression in the cortex (Timmusk, Palm et al. 1993, Timmusk, Belluardo et al. 1994, Tao, Finkbeiner et al. 1998).

As being an activity-regulated gene, BDNF has been shown to be target for several transcriptional programs downstream of calcium influx, without surprise including IEGs (Bito, Deisseroth et al. 1996, Gaiddon, Loeffler et al. 1996). Initial studies demonstrated a critical role for BDNF on the regulation of the inhibitory inputs onto glutamatergic neurons(Hanover, Huang et al. 1999, Huang, Kirkwood et al. 1999). In addition to those, selective role for BDNF on the promotion of inhibition onto soma of the glutamatergic neurons through PV interneurons have been also elucidated(Inagaki, Begum et al. 2008, Bloodgood, Sharma et al. 2013). As serving the first example of secreted molecules on

the regulation of activity-dependent plasticity mechanisms, BDNF opened the door for the investigation of other growth factors and secreted factors in neuronal wiring.
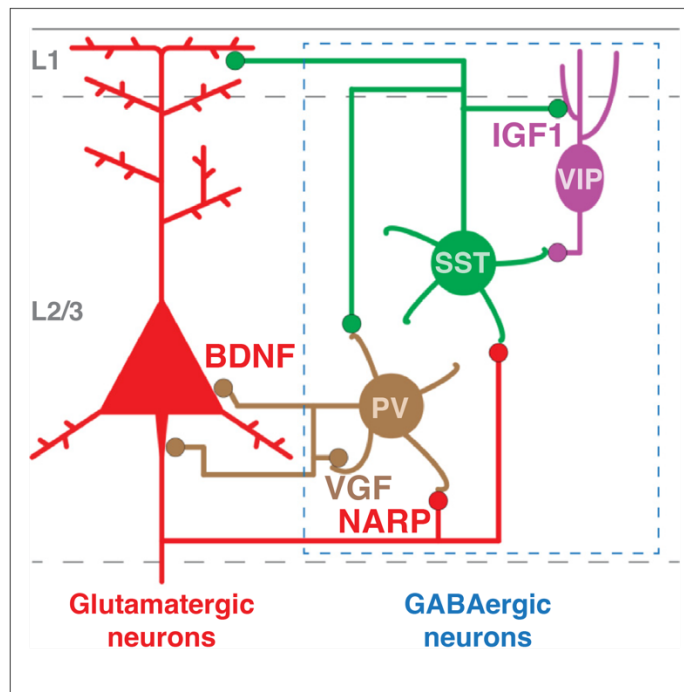
Figure 1.7: A simplified diagram of a cortical microcircuit in layer 2/3. Glutamatergic pyramidal neurons (Pyr, red) and subtypes of GABAergic neurons that express Parvalbumin (PV, brown), Somatostatin (SST, green) and Vasoactive Intestinal Protein (VIP, purple). Examples of experience-induced genes *Bdnf*, *Igf1*, *Narp* and *Vgf* are highlighted. These secreted molecules promote specific sets of synapses that potentially regulate the firing rates of glutamatergic principal neurons. Secreted molecules are placed next to the synapses that they regulate and are color-coded by the cells in which they are experience-induced (Adapted from Gray and Spiegel, Current Opinion in Neurobiology, 2019).

To date, a handful of sensory-induced secreted molecules are identified as critical regulators of synaptic connectivity in cortical circuits. Figure 7 above highlights some of these identified molecules from different neuronal subtypes. One of these molecules, Insulin Growth Factor 1 (IGF1) has been shown to be induced in Vasoactive Intestinal Protein (VIP) interneuron type in the visual cortex after light exposure(Mardinly, Spiegel et al. 2016). Local action of IGF1 on VIP interneurons promotes inhibitory drive in a cell-autonomous way. In contrast to this cell-autonomous action of IGF1, Neuronal pentraxin (NARP/Nptx2) has been shown to be an activity-induced secreted molecule from glutamatergic neurons and concentrated on the excitatory synapses on PV interneurons

in a perineuronal net dependent way(Chang, Park et al. 2010, Pelkey, Barksdale et al. 2016). Most recent studies investigating the cell-type specific targets and function of FOS in mechanisms involved in the regulation of state-dependent circuit modifications and engram formation found that, Fos induction regulates bidirectional perisomatic inhibition onto hippocampal CA1 neurons through a secreted neuropeptide Secretogranin II (Scg2) (Yap, Pettit et al. 2021, Pettit, Yap et al. 2022). Interestingly, Martijn and colleagues demonstrated that increases in the activity of PV interneurons also leads to upregulation of both Scg2 and Vgf neuropeptide transcripts, and furthermore found VGF as critical regulator of PV-PV peri-somatic synapses (Selten, Bernard et al. 2023). Collectively, these surprising findings highlight the importance of the growth factors on their role in cell-type specific synaptic rearrangements for the operation of neuronal networks.

1.6.2 Multitasking in the nervous system: A new role for Bone Morphogenetic Proteins as trans-cellular messengers?

First discovered in 1965 by Marshall Urist as mix of proteins that appear to be responsible for bone formation, Bone Morphogenetic Proteins (BMPs) are now well known for their function in neuronal cell fate determination during development (Bond, Bhalala et al. 2012). More than two decades ago, first evidence that BMPs play crucial roles in synapse formation and stability was obtained for *Drosophila melanogaster* neuromuscular junction (Aberle, Haghighi et al. 2002, Marques, Bao et al. 2002). Mutations in Wishful thinking (wit), the *Drosophila* homolog of BMP type II receptor, resulted in significantly smaller synapses. However, no evident morphological abnormalities were detected in either muscle or neurons. Subsequent studies shed light on additional components of the classical TGFβ signaling cascade. Motor neuron terminals at the neuromuscular junction (NMJ) exhibited a concentration of the type I receptor, thickveins (Tkv). Notably, mutations in tkv, saxophone (another type I BMP-receptor, sax), and gbb (glass bottom boat, a *Drosophila* BMP homolog) produced similar synaptic phenotypes, characterized by reduced neuromuscular synapse size, aberrant synaptic ultrastructure, decreased synaptic transmission, and functional alterations. Interestingly, these effects coincided with a lack of phosphorylated Mad (*Drosophila* SMAD) in motor neurons. Moreover, synaptic phenotypes resembling those observed in mutants were also observed in mad and co-SMAD medea (med) mutants, which are downstream components of the *Drosophila* BMP signaling pathway. Remarkably, targeted expression of these genes specifically in motoneurons was sufficient to restore the synaptic phenotypes, implying the control of *Drosophila* neuromuscular synapse growth through the classical BMP signaling cascade. This signaling cascade initiates SMAD phosphorylation, nuclear translocation, and

induction of target gene expression in the presynaptic cell (Figure 8). Selective introduction of the wild-type gene into neuronal cells proved effective in rescuing the synaptic phenotype observed in mutants of wit, tkv, or sax. Interestingly, the expression of Gbb, considered a retrograde signal derived from muscle, in neurons led to the rescue of neurotransmission defects and a partial recovery of synaptic growth. Nevertheless, restoring Gbb specifically in the muscle only partially reversed the synaptic growth phenotype, while the neurotransmission defects persisted (McCabe, Marques et al. 2003). These findings confirm the crucial role of muscle-derived Gbb in synaptic growth, while suggesting that the synaptic transmission defects observed in gbb mutants are not solely attributable to its retrograde signaling function.
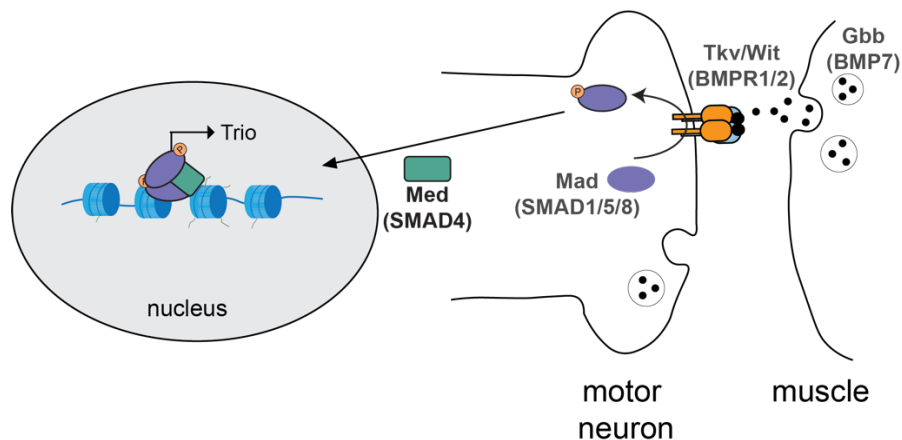
Figure 1.8: Canonical BMP signaling for regulation of growth and stability of synapses at *Drosophila* neuromuscular junction. Descriptions in the parentheses are for mammalian homologs of the pathway. Adapted from (Abbott and Nelson 2000).

The role of BMP pathway for the regulation of synapses in invertebrates brought attention. Coinciding emergence of crucial roles for neurotrophic factor BDNF in synapse development, function and plasticity lead to the exploration of other growth factor signaling pathways such as Wnt and TGFβ and revealed that multiple growth factors display crucial roles at synapses and in neuronal plasticity (Salinas 2003, Sun, Gewirtz et al. 2010). In mice, two studies investigated the role for BMP signaling in postnatal developing mammalian brain. Kalinovsky and colleagues investigated the specificity of the synaptic connections in the ponto-cerebellar circuit and for the first time demonstrated that retrograde BMP4 signaling regulates axon-target interactions (Kalinovsky, Boukhtouche et al. 2011). Shortly after, Xiao and colleagues investigated the signaling pathways specifying nerve terminal size and fast synaptic neurotransmission and found BMP signaling as regulators of the synapse morphology and function at the calyx of Held of the auditory system (Xiao, Michalski et al. 2013). Despite some technical challenges with assessing the phosphorylated SMAD transcription factor complex, surprisingly in both

studies presynaptic pSMAD1/5/8 levels appeared to not be altered. Thus, these observations suggest that the role of BMP signaling on synapse development and function at post-developmental stages of some of the mammalian nervous systems are non-canonical. Indeed, non-canonical (i.e., not mediated through pSMAD) actions of BMP signaling through LIM domain kinase 1 (LIMK1) pathway have been implicated as the dysregulation of synapses in Fragile X mental retardation protein knockout mice. This study found Bmpr2 as downstream target of an RNA binding protein FMRP which is mutated in the Fragile X syndrome and showed alterations in the LIMK-driven cytoskeletal rearrangements and thereby result in synaptic abnormalities(Kashima, Roy et al. 2016). More recently, Aihara and colleagues found BMPR2 as key regulator of the stabilization of the dendrites extended by mitral cells during the development of olfactory bulb. They also found that this selective role of the BMP signaling on the dendrite stabilization is facilitated through LIMK pathway and in the co-existence of glutamatergic inputs (Aihara, Fujimoto et al. 2021).

At the start of my studies, a link of the BMP pathway and neuronal activity-dependent plasticity was unknown. However, some studies demonstrated the importance of BMP/TGFβ signaling for learning and cognition in adult circuits. (Sun, Thomas et al. 2007, McBrayer, Dimova et al. 2015). Given that BMP signaling components are essential for the patterning of the nervous systems at embryonic development (Bier and De Robertis 2015), it has been difficult to either obtain postnatal phenotypes or separate the phenotypes from its developmental functions. In developing neurons, activity-dependent mobilization of the BMP pathway was reported by Higashi and colleagues who overexpressed an EGFP-tagged BMP4 ligand in cultured hippocampal neurons and demonstrated secretion of BMP4 from dense core vesicles clustered on axons (Higashi, Tanaka et al. 2018). These experiments highlighted a potential link of activity-induced synapse regulation through BMP4-BMP receptor type 1a (BMPR1a) pathway and the cross-talk of the canonical pathway with neuronal activity.

Classical signaling pathways that operate with arrays of ligands and receptors like BMP, Wnt, Hedgehog; their components are expressed extensively, with receptors for most pathways found in nearly all cell types, and the ligands for these pathways distributed in subsets of cells. Interestingly, despite the universal expression of the components, pathway activation is tightly regulated, confined to specific cell types within precise spatiotemporal contexts. Multiple mechanisms have been shown to restrict activation of such pathways from the modulation of extracellular ligand concentrations through the formation of morphogenetic gradients, secreted inhibitors, and factors in the extracellular

matrix allows spatial and temporal control of signaling (Rogers and Schier 2011, Bier and De Robertis 2015). Moreover, by controlling the phosphorylation of effector proteins, pSMAD1/5/8 in the case of BMPs or selective activation or silencing particular sets of their targets, cells can regulate the amplitude and dynamics of their individual pathway responses (Axelrod, Miller et al. 1998, Lim-Tio and Fuller 1998, Shaul and Seger 2007). Furthermore, different ligand variants could bind to and interact with different receptor variants with different strengths which facilitates preferential activation of different cell types based on the receptor variants they express. It is fascinating that these three mechanisms could operate individually or in combination (Figure 9).
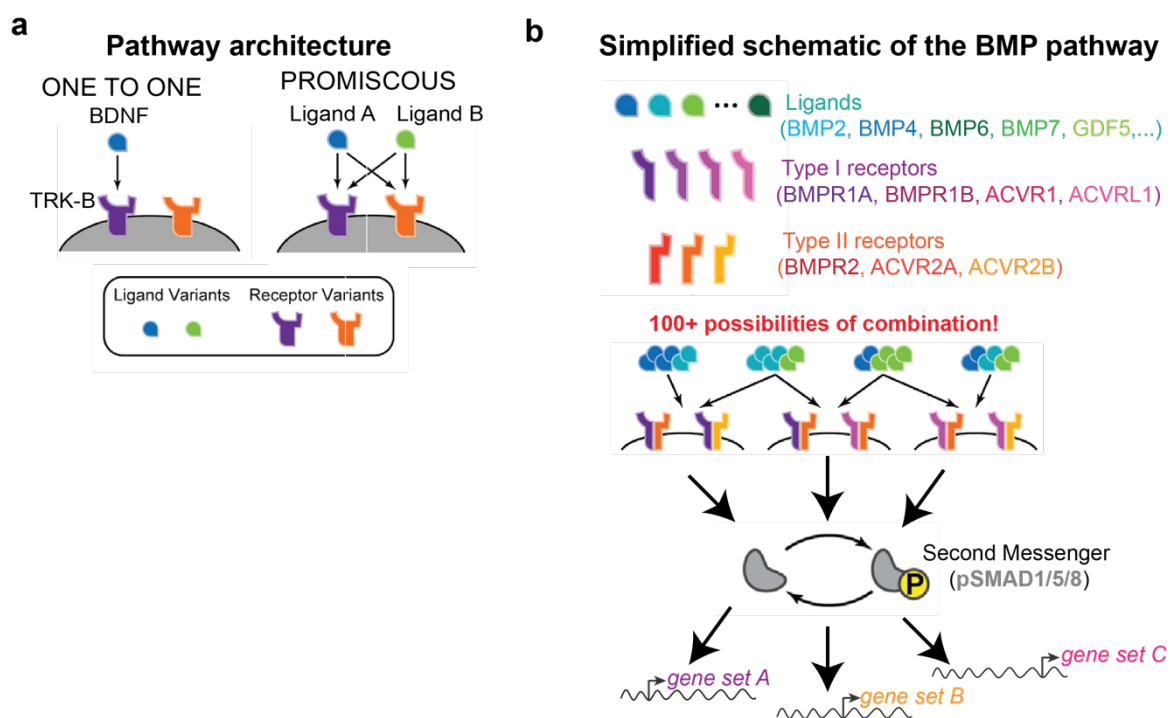
Figure 1.9: Promiscuous ligand-receptor interactions in the BMP pathway and its combinatorial power to provide spatio-temporally controlled cellular responses. Adapted from (Su, Murugan et al. 2022).

Neural circuits are perfect platforms for such combinatorial codes to be used as each one of them have multicellular patterns. For example, in the olfactory system, promiscuous ligand-receptor interactions have been shown to sense a great diversity of odorants by enabling a limited number of receptors through a combinatorial code (Duchamp-Viret, Chaput et al. 1999, Malnic, Hirono et al. 1999, Goldman, van Naters et al. 2005, Hallem and Carlson 2006). For neuronal circuits, it is fundamental to activate the right cells at the right time and place for information processing and integration. Therefore, gaining insights

into these pathways in the neuronal circuits which can serve as computational devices to receive the information specifically addressed them will facilitate our understanding for how the brain works.

1.7 The dissertation project

A famous Turkish poet once wrote "*To live! Like a tree alone and free, and like a forest, sisterly.*" (Nazim Hikmet Ran, 2002). Like forests, neural circuits also have evolved as harmonious systems. For the generation of the neuronal networks during development and maintenance of this harmony later in the adult, neurons utilize the power of their cellular, molecular and synaptic diversity. We are starting to better understand the interplay of neuronal activity with specification of neuronal subtypes or segregation of neuronal circuits during development (Pouchelon, Gambino et al. 2014, Guillamon-Vivancos, Anibal-Martinez et al. 2022). For mature circuits in the adult organism, the impact of the diverse forms of neuronal computation such as sensory information processing or associative learning on the neurons have been long appreciated. Processing such a multitude of stimuli poses a challenge to maintain a balanced network function despite alterations in synaptic connectivity and network activity. Thus, compensatory mechanisms have to come into play that ensure the preservation of network function.

In the neocortex, stability is preserved by the prompt actions of excitatory principal cells and inhibitory interneurons. It has been well-studied how principal cells adapt to the changes in activity (Huang, Kirkwood et al. 1999, Bloodgood, Sharma et al. 2013), but much less is known about how this is accomplished by interneurons. Seminal studies found PV interneurons as a core component of the excitation-inhibition balance and showed that depending on the activity state of the principal cells they are targeting, parvalbumin interneurons modify their synaptic outputs onto them. This suggests that there has to be an information exchange between the principal cells and parvalbumin interneurons. Extensive studies on this subject found Neuregulin-1 (NRG1) and its tyrosine kinase receptor ErbB4 as key communication pathway involved during critical-period plasticity (Sun, Ikrar et al. 2016). However, if and how such signaling pathways are involved in the stabilization of neuronal activity in the adult cortex remains to be discovered.

The aim of this project was to uncover trans-cellular signaling pathways as ways for communication between principal cells and Parvalbumin interneurons which modify PV interneuron function. I focused on Bone Morphogenetic Protein (BMP) pathway which has

strong power to generate diverse signaling readouts due to its ligand-receptor promiscuity. Moreover, BMP signaling has great potential to provide cell-type specific responses due to large numbers of ligand heterodimers expressed in the brain. By combining several approaches and utilizing advanced tools, I investigated if the canonical BMP pathway is mobilized in glutamatergic neurons in response to increased network activity and its consequences on their synaptic connectivity with PV interneurons. Thus, following results chapters of this thesis will describe the following results:

1) Examination of the contribution of canonical BMP pathway in maintenance of excitation-inhibition balance in the adult mouse somatosensory cortex

2) Assessing whether BMP pathway contributes to the developmental acquisition of the synapse- and plasticity properties of PV-INs

2. Results

2.1 Preface

The following result chapter describes the work carried out in close collaboration with several people. Below I will illustrate the individual contributions of each person involved in the projects investigated during my PhD thesis.

Peter Scheiffele supervised both of the projects, submitted manuscripts have been written amongst co-authors of the studies.

Control of neuronal excitation-inhibition balance by BMP-SMAD1 signaling

Zeynep Okur[1], Nadia Schlauri[1,†], Vassilis Bitsikas[1], Myrto Panopoulou[1], Kajari Karmakar[1,††], Dietmar Schreiner[1], Peter Scheiffele[1]*

For this project, I generated samples for ChIP-sequencing and RNA-sequencing and critically involved in post-hoc processing of analyzed data, conducted experiments for histology and quantification, generation of PV interneuron specific Smad1 loss of function mouse model, validations, action potential measurements and analyses of PV interneurons, behavioral analyses of seizure mice.

Genetically encoded synapse marking probe validations and quantifications were perfomed by Nadia Schlauri, a master student who worked under my supervision. In vivo EEG recordings and analyses were performed in close collaboration with Vassilis Bitsikas, a postdoc in Alex Schier lab. miniEPSC and miniIPSC recordings and analyses were performed in collaboration with Myrto Panopoulou, a postdoc in the lab. Some of the *in vitro* and *in vivo* Fluorescence in situ hybridization (FISH) experiments and quantitative RT-PCR experiments were performed by Kajari Karmakar, a postdoc in the lab. Design and *in vitro* validations of BRE reporters and FingR probes were carried out in close collaboration with Dietmar Schreiner.

LTP of inhibition at PV interneuron output synapses requires developmental BMP signaling

Evan Vickers[1,3], Denys Osypenko[1], Christopher Clark[1,4], Zeynep Okur[2], Peter Scheiffele[2], Ralf Schneggenburger[1, 5]

For this project, Evan Vickers and Denys Osypenko performed all the slice electrophysiology recordings. I performed Fluorescent in Situ Hybridization (FiSH) against the Ntrk2 and Cacna1a for the auditory cortex from mouse brain sections and performed quantitative analysis. Christopher Clark performed RNA-sequencing from Fluorescent

Activated Cell Sorted (FACS) parvalbumin interneuron nuclei and I was also involved in the investigation of the sequencing data.

2.2 Control of neuronal excitation-inhibition balance by BMP-SMAD1 signaling

Summary

Throughout life, neuronal networks in the mammalian neocortex maintain a balance of excitation and inhibition which is essential for neuronal computation. Deviations from a balanced state have been linked to neurodevelopmental disorders and severe disruptions result in epilepsy. To maintain balance, neuronal microcircuits composed of excitatory and inhibitory neurons sense alterations in neural activity and adjust neuronal connectivity and function. Here, we identified a signaling pathway in the adult mouse neocortex that is activated in response to elevated neuronal network activity. Over-activation of excitatory neurons is signaled to the network through the elevation of BMP2, a growth factor well-known for its role as morphogen in embryonic development. BMP2 acts on parvalbumin-expressing (PV) interneurons through the transcription factor SMAD1, which controls an array of glutamatergic synapse proteins and components of peri-neuronal nets. PV interneuron-specific impairment of BMP2-SMAD1 signaling is accompanied by a loss of PV cell glutamatergic innervation, underdeveloped peri-neuronal nets, and decreased excitability. Ultimately, this impairment of PV interneuron functional recruitment disrupts cortical excitation – inhibition balance with mice exhibiting spontaneous epileptic seizures. Our findings suggest that developmental morphogen signaling is re-purposed to stabilize cortical networks in the adult mammalian brain.

Bone Morphogenetic Protein signaling is mobilized by neuronal network activity in adult neocortex

To identify candidate trans-cellular signals that are regulated by neuronal network activity in mature neocortical neurons, we examined secreted growth factors of the bone morphogenetic protein family (BMPs), which had been implicated in cell fate specification and neuronal growth during development (Marques, Bao et al. 2002, McCabe, Marques et al. 2003, Keshishian and Kim 2004, Ting, Herman et al. 2007, Kalinovsky, Boukhtouche et al. 2011, Xiao, Michalski et al. 2013, Higashi, Tanaka et al. 2018, Aihara, Fujimoto et al. 2021). Amongst four bone morphogenetic proteins (BMP2,4,6,7) examined, *Bmp2* mRNA was significantly upregulated in glutamatergic neurons upon stimulation (3.5 +/- 0.5 fold, Extended Data Fig. 1a-d). A similar activity-dependent elevation of BMP2 was observed

at the protein level in neurons derived from a *Bmp2* HA-tag knock-in mouse (*Bmp2^{HA/HA}*, Extended Data Fig. 1e-g). BMPs are well known for their function as developmental morphogens and in fate specification of neuronal progenitors, where they direct gene regulation in recipient cells through SMAD transcription factors (Fig. 1a) (Hogan 1996, Liem, Tremml et al. 1997, Shi and Massague 2003, De Robertis and Kuroda 2004, Mukhopadhyay, McGuire et al. 2009, Rowitch and Kriegstein 2010). Interestingly, the canonical BMP- target genes *Id1* and *Smad6* were significantly upregulated in stimulated neocortical cultures, a process that was blocked by addition of the extracellular BMP-antagonist Noggin (Extended Data Fig. 1h, i). In the neocortex of adult mice, key BMP signaling components continue to be expressed with the ligand BMP2 exhibiting highest mRNA levels in glutamatergic neurons (Extended Data Fig. 2a-c). To test whether BMP-target gene transcription is activated in response to elevated neuronal network activity in adult mice, we chemogenetically silenced upper layer PV interneurons in the barrel cortex (Fig. 1b). This local reduction of PV neuron-mediated inhibition results in increased neuronal network activity (Devienne, Picaud et al. 2021, Goldenberg, Schmidt et al. 2022) accompanied by a 4- to 8-fold transcript increase for the activity-induced primary response genes *cfos* and *Bdnf* (Fig. 1c). Importantly, this chemogenetic stimulation also resulted in upregulation of four critical SMAD1/5-dependent BMP target genes (*Id1*, *Id3*, *Smad6* and *Smad7*) (Fig. 1c). To monitor BMP target gene activation with temporal and cell type-specific resolution *in vivo*, we developed a novel temporally-controlled BMP-signaling reporter (Fig. 1d). We combined BMP-response element sequences (4xBRE) from the *Id1* promoter (Lewis and Prywes 2013) with the small molecule (LMI070)-gated miniX^{on} cassette (Monteys, Hundley et al. 2021) to drive a nucleus-targeted eGFP (Extended Data Fig. 3a). Thus, the level of nuclear eGFP reports activation of BMP-signaling during a time window specified by LMI070 application (Extended Data Fig 3a-c). Notably, chemogenetic stimulation in presence of LMI070 resulted in a 3-fold increase in eGFP intensity in PV interneurons (Fig. 1e-g). In aggregate, these results demonstrate that increased cortical network activity mobilizes BMP2 signaling to alter transcriptional responses in PV interneurons in the adult mouse barrel cortex.

BMP-SMAD1 signaling controls transcriptional regulation of synaptic proteins

During development, the combinatorial action of various BMP ligands and receptors directs cell type-specific target gene regulation through SMAD transcription factors, but also SMAD-independent functions have been described (Massague 2000, Butler and Dodd 2003, Marques, Haerry et al. 2003, McCabe, Marques et al. 2003, Eaton and Davis 2005, Ting, Herman et al. 2007, Kalinovsky, Boukhtouche et al. 2011, Higashi, Tanaka et al. 2018, Su, Murugan et al. 2022, Vicidomini and Serpe 2022). In neocortical neurons,

BMP2 stimulation (20 ng/ml for 45 minutes) resulted in SMAD1/5 activation in both, glutamatergic and GABAergic neurons (Extended Data Fig. 4a-c). To uncover SMAD1 target genes in postmitotic mammalian neurons, we performed chromatin immunoprecipitation sequencing (ChiP-seq) for Smad1/5 from naïve and BMP2-stimulated neocortical cultures (Fig. 2a). We found 349 BMP2-responsive (> 2-fold increase and p.adj value < 0.05) SMAD1/5 binding sites and 167 sites that were bound constitutively (stimulation independent, < 2-fold increase and p.adj value< 0.05) (Fig. 2b and Supplementary Table 1). Importantly, BMP2-responsive peaks were associated with promoter elements whereas the majority of constitutive SMAD1/5 binding regions were promoter-distal. To explore whether SMAD1 triggers *de novo* activation of target genes or rather modifies transcriptional output of active genes, we mapped active regulatory elements by performing ChiP-seq for histone 3 acetylated at lysine 27 (H3K27ac), a chromatin modification that marks active promoters and enhancers. By intersecting H3K27ac ChiP-seq signals with SMAD1/5 peaks (Fig. 2b-e), we found that the majority of BMP2-responsive regulatory elements are already active in naïve cultures. By comparison, constitutively bound regions exhibited only low H3K27ac signal (Fig. 2b, c) suggesting that they are transcriptionally silent. Sequence analysis confirmed enrichment of the SMAD1/5 DNA binding motif in the BMP2-responsive gene regulatory elements (Fig. 2d). The impact of BMP2-induced SMAD1/5 recruitment on transcriptional output was examined by RNA-sequencing (Fig. 2a). Differential gene expression analysis identified 30 and 147 up-regulated transcripts 1 and 6 hours after BMP2-stimulation, respectively (Extended Data Fig. 4c, Supplementary Table 2). 50% of the regulated genes 1 hour after BMP2-stimulation had direct Smad1/5 binding at their promoters and included negative feedback loop genes of the BMP signaling pathway (*Id1*, *Id3* and *Smad7*). 25% of differentially regulated genes 6 hours after BMP2-stimulation had direct Smad1/5 binding. (Extended Data Fig. 4d). Conditional knock-out of *Smad1* in post-mitotic neurons was sufficient to abolish upregulation of these genes in response to BMP2 signaling and reduced their expression in naïve (unstimulated) neurons (Fig. 2f and Extended Data Fig. 4e,f Supplementary Table 3). Direct transcriptional targets of BMP-SMAD1 signaling in neocortical neurons included an array of activity-regulated genes such as *Junb*, *Trib1* and *Pim3*, key components of the extracellular matrix (*Bcan, Gpc6*) and glutamatergic synapses (*Lrrc4*, *Grin3a*) (Fig.2e, Extended Data Fig. 4d). Moreover, neuronal *Smad1* ablation was accompanied by broad gene expression changes beyond de-regulation of direct SMAD1 target genes (Fig. 2g). Top GO terms enriched amongst the upregulated genes were "glutamatergic synapse" and transcription factors under the term "nucleus" (Fig. 2h). Furthermore, de-regulated genes include the majority of neuronal activity-regulated rapid primary (rPRG) and secondary (SRG) activity-response genes (Fig. 2i).

43

Thus, SMAD1 is the key downstream mediator of BMP signaling in mature neurons and its neuronal loss of function results in a severe imbalance of neuronal network activity *in vitro*.

Synaptic innervation and excitability of PV interneurons are controlled by SMAD1

PV interneurons in neocortical circuits are key regulators of excitation – inhibition balance and glutamatergic synapse formation onto PV interneurons and peri-neuronal nets (PNNs) surrounding these cells are modified in response to changes in neuronal network activity (Li, Lu et al. 2011, Favuzzi, Marques-Smith et al. 2017). To test whether SMAD1 regulates synapse formation onto PV interneurons, we generated conditional *Smad1* knock-out mice. Postnatal ablation of *Smad1* in PV interneurons (*PV^cre/+::Smad1^fl/fl*; *Smad1^ΔPV* mice) did not alter PV cell density or distribution in the somatosensory cortex of adult mice (Extended Data Fig. 5a-c). We then adopted genetically encoded intrabodies (Fibronectin intrabodies generated by mRNA display, FingRs) directed against PSD-95 and gephyrin (GEPH) to quantitatively map synaptic inputs to PV interneurons *in vivo* (Gross, Junge et al. 2013) (Extended Data Fig. 6a-c). FingR probes were selectively expressed in PV interneurons in layer 2/3 of barrel cortex using cre recombinase-dependent adeno-associated viruses (Fig. 3a-g, Extended Data Fig. 6a-c and Supplementary Movie 1). In *Smad1^ΔPV* mice, we observed a 40% reduction in morphological glutamatergic synapse density onto PV interneurons (Fig. 3b, c). This was accompanied by a comparable reduction in mEPSC frequency but no change in mEPSC amplitude in acute slice recordings (Fig. 3d-f). The density of peri-somatic PV-PV synapses (identified by synaptotagmin-2 and FingR GPHN co-localization) was also reduced (Fig. 3h, i), but there was no significant change in mIPSC frequency or amplitude in PV cells of *Smad1^ΔPV* mice, likely due to compensatory inhibition derived from other interneuron classes (Fig. 3j-l). Thus, SMAD1 is required for normal functional glutamatergic innervation of layer 2/3 PV interneurons, resulting in reduced glutamatergic input to these cells in *Smad1^ΔPV* mice.

Neuronal activity-induced regulation in PV interneurons modifies the elaboration of PNNs and parvalbumin expression (Li, Lu et al. 2011, Dehorter, Ciceri et al. 2015, Dehorter, Marichal et al. 2017, Favuzzi, Marques-Smith et al. 2017, Devienne, Picaud et al. 2021, Joseph, Von Deimling et al. 2021), and our ChiP-Seq analysis identified the PNN component brevican (*Bcan*) as one of the direct SMAD1 targets in neuronal cells. In *Smad1^ΔPV* mice, the elaboration of PNNs around PV interneurons and parvalbumin protein expression were significantly reduced (Fig. 4a-c). This results in a significant reduction in the density of parvalbumin-immuno-reactive cells in layer 2/3, despite the normal density of genetically-defined PV interneurons (Extended Data Fig. 5a-c). Through organizing PNNs, Brevican has been implicated in regulating plasticity and excitability of PV

interneurons (Favuzzi, Marques-Smith et al. 2017). Interestingly, the firing rate of SMAD1-deficient PV interneurons in response to current injections was significantly reduced in the barrel cortex of adult mice (Fig. 4d-f and Extended Data Fig. 5d, note that firing rate was unchanged in young animals, Extended Data Fig. 5e). This reduced firing frequency most likely is explained by a reduction in input resistance in the $Smad1^{\Delta PV}$ cells (Extended Data Fig. 5d). Thus, in the absence of BMP-SMAD1 signaling PV interneurons not only receive less glutamatergic drive but are also less excitable. These cellular alterations resulted in a severe overall disruption of cortical excitation – inhibition balance. As compared to control littermates, $Smad1^{\Delta PV}$ mice exhibited hyperactivity in open field tests and frequently exhibited spontaneous seizures when introduced into novel environments (Fig. 4g, h). Video-coupled EEG recordings with electrodes over the barrel cortex (Supplementary Movie 2) revealed marked high amplitude activity bursts at the time of seizure followed by a refractory period (Fig. 4i). Overall, our results demonstrate that elevated network activity in the somatosensory cortex of adult mice triggers the upregulation of BMP2 in glutamatergic neurons which balances excitation by controlling synaptic innervation and function of PV interneurons through the transcriptional factor SMAD1.

Discussion

Despite being exposed to a wide range of sensory stimulus intensities, cortical circuits exhibit remarkably stable activity patterns that enable optimal information coding by the network. This network stability is achieved by homeostatic adaptations that modify the excitability of individual neurons, scale the strength of synapses, as well as microcircuit-wide modifications of excitatory and inhibitory synapse density (Turrigiano and Nelson 2004, Marder and Goaillard 2006, Spiegel, Mardinly et al. 2014, Froemke 2015, Iascone, Li et al. 2020, Chen, Li et al. 2022). These multiple adaptations occur at various time-scales, from near instantaneous adjustments of excitation and inhibition during sensory processing (Okun and Lampl 2008), to slower modifications of synaptic connectivity upon longer-term shifts in circuit activation as they occur during sensory deprivation but also in disease states (Rubenstein and Merzenich 2003, Keck, Keller et al. 2013, Cellot and Cherubini 2014, Spiegel, Mardinly et al. 2014, Nelson and Valakh 2015, Mardinly, Spiegel et al. 2016). Thus, both rapid cell intrinsic, as well as long-lasting trans-cellular signaling processes have evolved to ensure cortical network function and stability.

Differential recruitment of PV interneuron-mediated inhibition has emerged as a key node for the control of excitation – inhibition balance and cortical plasticity (Takesian and Hensch 2013, Xue, Atallah et al. 2014, Zhou, Liang et al. 2014). We here demonstrate that elevated neuronal network activity in the somatosensory cortex of adult mice triggers BMP

target gene expression in PV interneurons. The transcription factor SMAD1, directly binds to and regulates promoters of an array of glutamatergic synapse proteins and components of the perineuronal nets, such as brevican. Thus, BMP2-SMAD signaling provides a trans-neuronal signal to adjust functional PV interneuron recruitment and excitability that ultimately serve to maintain excitation – inhibition balance and stabilize cortical network function in adult neocortex. In developing auditory cortex, genetic deletion of type I BMP-receptors from PV interneurons is associated with a loss of spike-timing dependent LTP at PV interneuron output synapses onto principal neurons of layer 4 whereas basal GABAergic transmission was unchanged (Vickers, Osypenko et al. 2020). This suggests a selective role for BMP2-SMAD1 signaling in controlling glutamatergic input connectivity to PV interneurons.

Importantly, transcriptional regulation through BMP2-SMAD1 signaling significantly differs from the action of activity-induced immediate early genes. As secreted growth factor, BMP2 derived from glutamatergic neurons relays elevated network activity to PV interneurons through the activation of an array of SMAD1 target genes. Rather than ON/OFF responses, the majority of direct SMAD1 targets exhibit active enhancer and promoter elements and are already expressed under basal conditions. However, SMAD1 activation results in an elevation of transcriptional output, indicating a graded gene expression response to BMP2.

In early development, BMP growth factors act as morphogens that carry positional information and differentially instruct cell fates (Hogan 1996, De Robertis and Kuroda 2004, Mukhopadhyay, McGuire et al. 2009). The combinatorial complexity arising from the substantial number of BMP ligands and receptors has the power to encode computations for finely tuned cell-type-specific responses (Klumpe, Langley et al. 2022, Su, Murugan et al. 2022). Our work suggests that the spatiotemporal coding power, robustness, and flexibility which evolved for developmental patterning is harnessed for balancing plasticity and stability of neuronal circuits in the adult mammalian brain. Notably, additional BMP ligands besides BMP2 are selectively expressed in neocortical cell types (Extended Data Fig. 2b). Moreover, an array of type I and type II BMP receptors are detected across neocortical cell populations. This suggests that BMP-signaling might control additional aspects of cell-cell communication in the mammalian neocortex.

Disruptions in excitation – inhibition balance and homeostatic adaptations have been implicated in neurodevelopmental disorders as there is reduced GABAergic signaling and a propensity to develop epilepsy in individuals with autism (Rubenstein and Merzenich 2003, Cellot and Cherubini 2014, Nelson and Valakh 2015, Exposito-Alonso and Rico 2022). Considering that BMP-signaling pathways can be targeted with peptide mimetics (Carlson, Keck et al. 2022) they may provide an entry point for therapeutic interventions in

neurodevelopmental disorders characterized by disruptions in PV interneuron innervation, excitation – inhibition balance, and seizures.
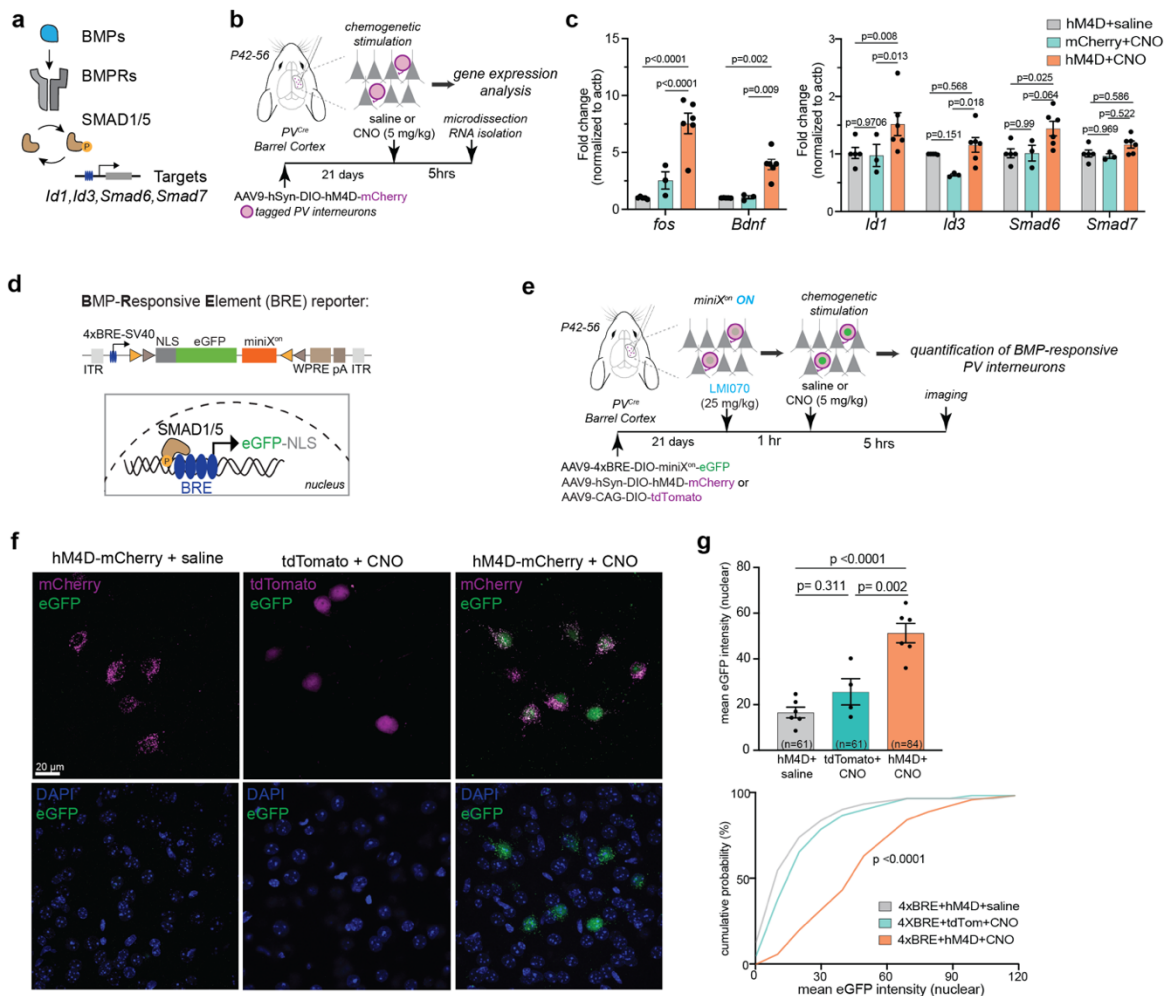
Fig. 1

Fig. 1. Neural activity elevation elicits BMP signaling in PV interneurons of the adult barrel cortex. (**a**) Illustration of BMP pathway components (adopted from (Su, Murugan et al. 2022)). (**b**) Schematic representation of chemogenetic neuronal activity manipulation protocol in adult barrel cortex. **(c)** Expression of immediate early genes *cFos* and *Bdnf* and SMAD1/5 target genes *Id1*, *Id3*, *Smad6*, and *Smad7* in barrel cortex of chemogenetically stimulated and control mice (N=3-6 mice/group). Two-way ANOVA with Tukey's post hoc test. **(d)** Schematic representation of viral vector for expression of nuclear eGFP reporter (NLS-eGFP) under control of BMP reporter element (4xBRE) and the miniX^{on} splicing cassette. **(e)** Experimental paradigm. **(f)** Representative images of 4xBRE-driven eGFP signal in the nucleus of layer 2/3 PV interneurons marked by cre-dependent expression of hM4Di-mCherry or tdTomato, respectively. **(g)** Quantification of BRE signaling reporter readout in chemogenetically stimulated and control PV interneurons. Bar graph for mean ± SEM of nuclear eGFP intensity per mouse (N=4-6 mice/group, n=61-84 cells per condition, Kruskal-Wallis test with Dunn's multiple comparisons) and cumulative distribution of eGFP reporter intensity per PV interneuron (Komolgorov-Smirnov test).
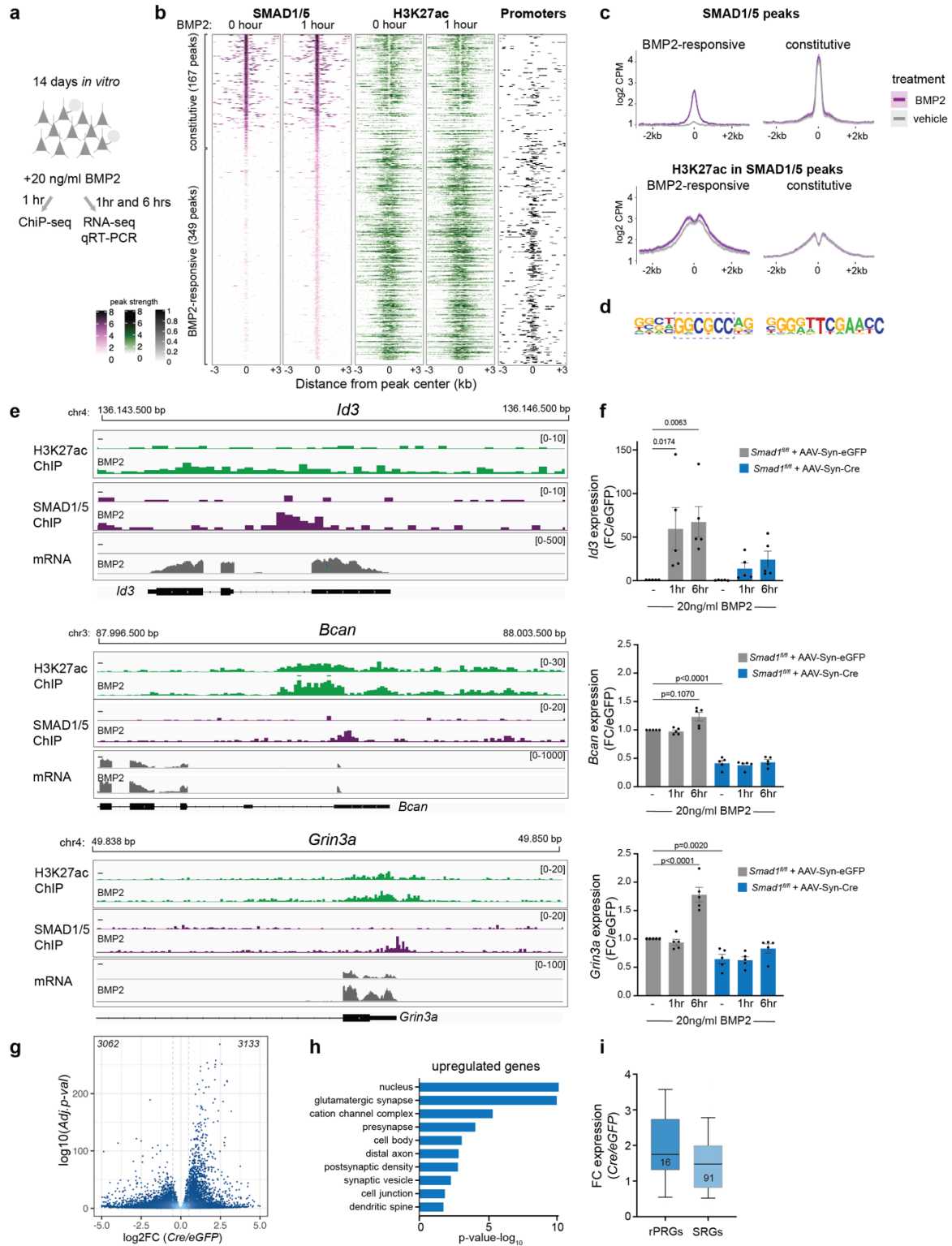
Fig. 2. BMP2-SMAD1 signaling regulates synaptic components and is required for stable cortical networks. (a) Schematic representation of BMP2 stimulation experiments from neocortical cultures. **(b)** ChiP-seq analysis of naïve (0 hour) and growth factor-stimulated (1hour 20ng/ml BMP2) neocortical neuron cultures at DIV14. Heatmaps in purple display peak strength of SMAD1/5 binding, heatmaps in green show H3K27ac binding at SMAD1/5 peak regions. The right column (in black) displays position of promoter elements. Each binding site is represented as a single horizontal line centered at the SMAD1/5 peak summit, color intensity correlates with sequencing signal for the indicated

49

factor. Peaks are ordered by decreasing Smad1/5 peak intensity. **(c)** Mean normalized ChiP-seq signal for SMAD1/5 and H3K27ac plotted for BMP2-responsive and constitutive SMAD1/5 binding sites. Gray lines indicate signal obtained from vehicle-treated cultures and purple lines signal obtained from BMP2-stimulated cultures. **(d)** Top enriched motifs detected for BMP2-responsive (left) and constitutive (right) SMAD1/5 peaks. **(e)** Examples of IGV genome browser ChiP-seq tracks displaying H3K27ac (green), SMAD1/5 (purple) and RNA-seq signal for SMAD1/5 targets *Id3*, *Bcan* and *Grin3a* in naïve (-) and BMP2-stimulated cultures. **(f)** qPCR analysis of mRNA expression of *Id3*, *Bcan* and *Grin3a* mRNAs in AAV-Syn-eGFP infected *versus* AAV-Syn-Cre infected *Smad1$^{fl/fl}$* neocortical cultured neurons. Fold change (FC) relative to unstimulated cells is shown for 1 hour and 6 hours stimulation with 20ng/ml BMP2. **(g)** Vulcano plot of differential gene expression in naïve *Smad1$^{fl/fl}$* cortical cultures infected with AAV-Syn-iCre infected *versus* AAV-Syn-eGFP. Dashed lines indicate log$_2$FC:0.4 and -log10Adj.-p-val: 2 chosen as thresholds for significant regulation. Number of significantly down- and up-regulated genes are indicated on the top. **(h)** Top ten enriched cellular component gene ontology terms for genes upregulated in conditional *Smad1* mutant cells (*Smad1$^{fl/fl}$* infected with AAV-Syn-iCre) in unstimulated cortical cultures. **(i)** Expression levels of neuronal activity-regulated rapid Primary Response Genes (rPRGs) and Secondary Response Genes (SRGs) as defined in (Tyssowski, DeStefino et al. 2018) in conditional *Smad1* mutant cells (*Smad1$^{fl/fl}$* infected with AAV-Syn-iCre) compared to control AAV-Syn-eGFP infected cultures. The bar graphs show the means ± SEM (N=5 per condition, one-way ANOVA with Dunnett's multiple comparisons).

Fig. 3
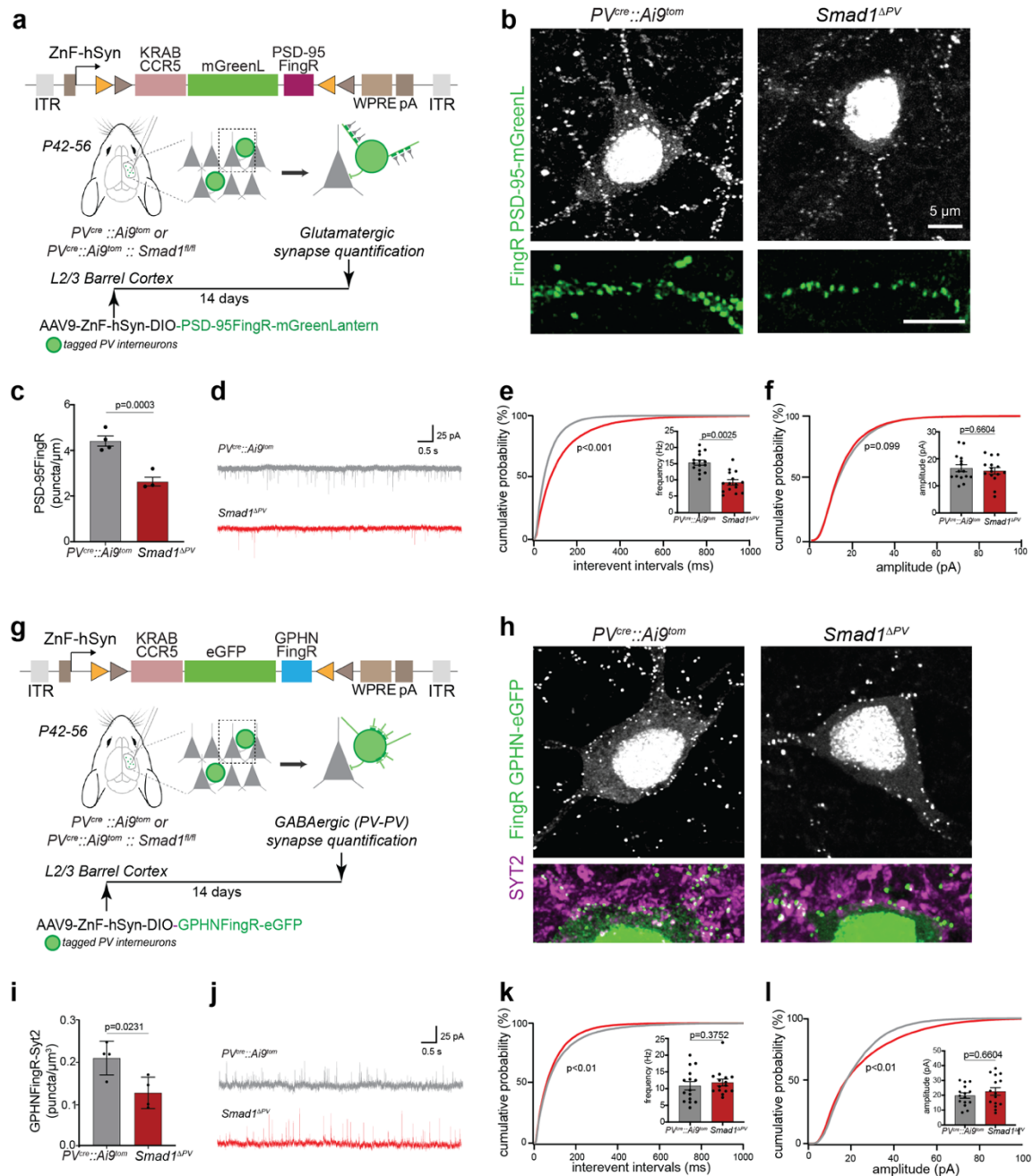
Fig. 3. SMAD1 regulates glutamatergic innervation of PV interneurons. (a) Schematic representation of AAV-driven, cre-recombinase-dependent intrabody probes for glutamatergic (PSD-95FingR-mGreenL) synapses. Intrabody expression is driven from human synapsin promoter (hSyn) fused to a CCR5 zinc finger binding site (ZnF). Intrabody coding sequences (FingRs) are fused to mGreenLantern and a CCR5-KRAB transcriptional repressor for autoregulation of probe expression. Thus, excess probe accumulates in the nucleus. **(b)** FingRPSD-95mGreenLantern-marked synapses formed onto control ($PV^{cre}::Ai9^{tom}$) and $Smad1$ conditional knock-out ($Smad1^{\Delta PV}$) PV interneurons and corresponding dendritic stretches. **(c)** Quantification of glutamatergic synapse density on the dendrites of PV interneurons. Number of synapses was normalized to dendritic length (Mean and SEM from N=3-4 animals per genotype, n=40 cells per genotype, unpaired t-test). Note that the vast majority of PSD-95FingR-mGreenLantern-marked structures co-localize with the presynaptic marker vGluT1 (see FigS6A). **(d)** Representative traces of mEPSC recordings from control (gray) and $Smad1^{\Delta PV}$ (red) PV

interneurons in acute slice preparations from adult mice. **(e)** Frequency distribution of interevent intervals (Kolmogorov-Smirnov test) and mean mEPSC frequency (mean ± SEM for n=15 cells/genotype, from N=4 mice. Kolmogorov-Smirnov test). **(f)** Frequency distribution of mEPSC amplitudes (Kolmogorov-Smirnov test) and mean mEPSC amplitude (mean ± SEM for n=15 cells/genotype, from N=4 mice. Kolmogorov-Smirnov test). **(g)** Schematic representation of AAV-driven, cre-recombinase-dependent intrabody probes for GABAergic (GPHNFingR-eGFP) synapses, fused to eGFP and a CCR5-KRAB transcriptional repressor for autoregulation of probe expression. Thus, excess probe accumulates in the nucleus. **(h)** Synapses formed onto control (*PV^{cre}::Ai9^{tom}*) and *Smad1* conditional knock-out (*Smad1^{ΔPV}*) PV interneurons. **(i)** Quantification of PV-PV GABAergic synapse density on PV interneuron somata. Number of GPHNFingR-eGFP / Synaptotagmin2 (SYT2) – containing structures was normalized to soma volume (mean and SEM from N=3-4 animals per genotype, n=78 cells, unpaired t-test). **(j)** Representative traces of mIPSCs recorded from control (in gray) and *Smad1^{ΔPV}* (red) PV interneurons in acute slice preparations. **(k)** Frequency distribution of interevent intervals (Kolmogorov-Smirnov test) and mean mIPSC frequency (mean ± SEM for n=15 cells/genotype, from N=4 mice. Kolmogorov-Smirnov test). **(l)** Frequency distribution of mIPSC amplitudes (Kolmogorov-Smirnov test) and mean mIPSC amplitude (mean ± SEM for n=15 cells/genotype, from N=4 mice. Kolmogorov-Smirnov test).

Fig. 4
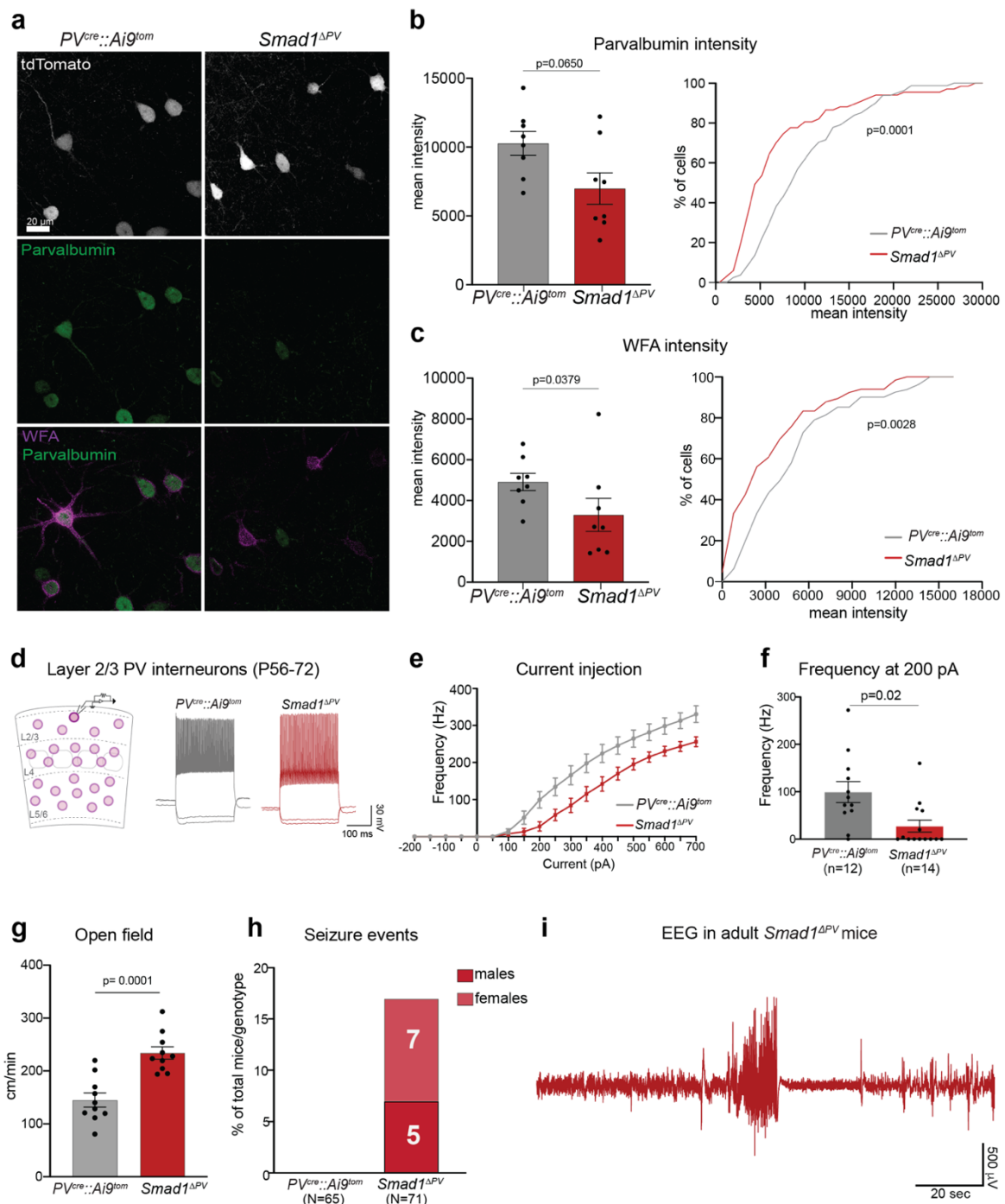
Fig. 4. Loss of SMAD1 in PV interneurons results in disruption of E/I balance in the adult mice. (a) Parvalbumin immunoreactivity and Wisteria floribunda agglutinin (WFA)-binding to the PNNs in adult control ($PV^{cre}::Ai9^{tom}$) and $Smad1$ conditional knock-out ($Smad1^{\Delta PV}$) mice. **(b)** Quantification of parvalbumin immunoreactivity per cell in $PV^{cre}::Ai9^{tom}$ (gray) and $Smad1^{\Delta PV}$ (red) mice. Bar graphs with mean intensity per mouse (N=8/genotype) and cumulative distribution of mean intensity per cell (n=81 cells for $PV^{cre}::Ai9^{tom}$, n=67 cells for $Smad1^{\Delta PV}$ mice). Kolmogorov-Smirnov test for bar graph and cumulative distribution). **(c)** As in B but plotting WFA staining intensity. **(d)** Experimental strategy and example traces from current-clamp recordings of control (in gray) and $Smad1^{\Delta PV}$ (red) PV interneurons in acute slice preparations. **(e)** Comparison of firing frequencies of layer 2/3 PV interneurons at given currents and **(f)** Mean firing frequency in

response to 200 pA current injection in cells from $PV^{cre}::Ai9^{tom}$ (gray) and $Smad1^{\Delta PV}$ (red) mice (N=4 mice, n=12 cells for $PV^{cre}::Ai9^{tom}$ and N=4, n=14 cells for $Smad1^{\Delta PV}$, Kolmogorov-Smirnov test). **(g)** Quantification of the velocity in open field from adult $PV^{cre}::Ai9^{tom}$ (gray) and $Smad1^{\Delta PV}$ (red) mice (N=10 mice/genotype, unpaired t-test). **(h)** Number of $PV^{cre}::Ai9^{tom}$ control (0 out of 65 mice) and male and female $Smad1^{\Delta PV}$ (red) mice (12 out of 71 mice) displaying spontaneous seizures during cage changes. **(i)** Representative 2.5 minutes EEG trace obtained from a $Smad1^{\Delta PV}$ mouse. All bar graphs show the means ± SEM.

Extended Data Fig. 1
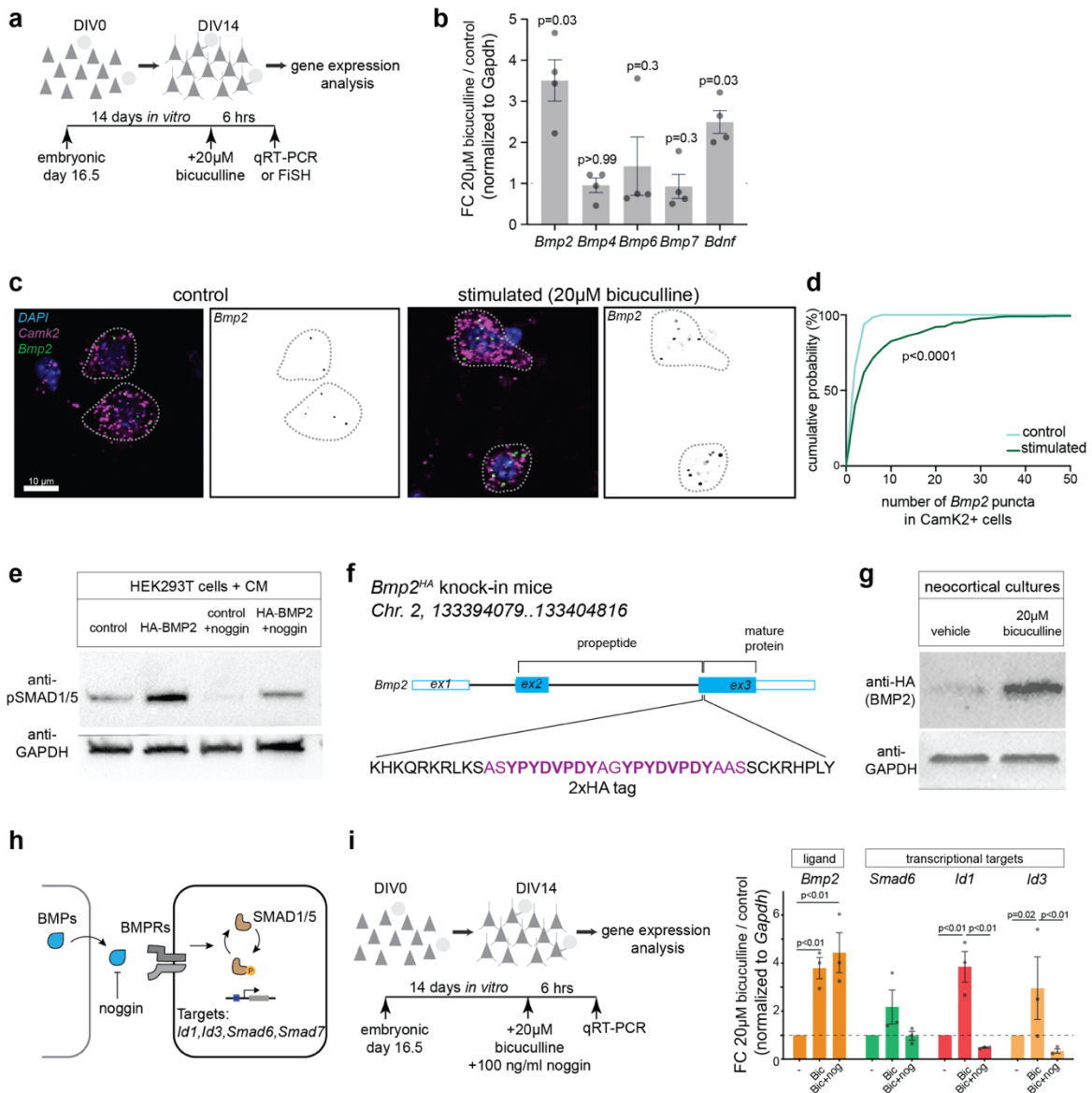
Extended Data Fig. 1. Elevation of neuronal network activity triggers BMP2 upregulation in neocortical glutamatergic neurons *in vitro*. (a) Schematic representation of cortical cultures and pharmacological activity manipulation. **(b)** qPCR assessment of *Bmp2*, *Bmp4*, *Bmp6*, Bmp7 and *Bdnf* transcripts in DIV14 neocortical cultures treated with 20 μM bicuculline for 6 hours expressed as fold-change (FC) compared to untreated cultures. All expression values were normalized to *Gapdh* (N=4 independent cortical cultures, total of 3 technical replicates, Mann-Whittney test). **(c)** *Bmp2* transcript levels by fluorescence in situ hybridization (FiSH) in *Camk2*-positive glutamatergic neurons in naïve and stimulated neocortical cultures). **(d)** Cumulative distribution of *Bmp2* FiSH signal per cell in control and stimulated neurons (N=3 independent cortical cultures, Komolgorov-Smirnov test). **(e)** Confirming functional signaling for HA-epitope-tagged BMP2 in cultured cells. Western blot for phosphorylated SMAD1/5 (anti-pSMAD1/5) in cultured human embryonic kidney cells (HEK293T) treated with conditioned medium (CM) from control or HA-BMP2-expressing cells containing or lacking 100 ng/ml noggin. **(f)** Illustration of Crispr-based knock-in strategy for introduction

of an epitope tag into the endogenous mouse *Bmp2* locus. A double HA tag sequence and flanking homology arms were encoded in a single stranded DNA oligo and were inserted in *Bmp2* exon 3 (ex3) at a Crispr/Cas9 cleavage site through homology-directed repair. The 2x HA tag is positioned at the N-terminus of the mature BMP2 protein. Resulting homozygous *Bmp2^{HA/HA}* knock-in mice were viable and fertile. **(g)** Western blot with anti-HA antibodies of lysate from cultured neocortical neurons from *Bmp2^{HA/HA}* knock-in mice (DIV14) either naïve or treated for 24 hours with 20μM bicuculline (N=3 independent cortical cultures). BMP2^{HA} expression levels *in vivo* could not be reliably assessed, likely due to its low abundance in the complex tissue samples. **(h)** Illustration of inhibition of BMP-signaling by the extracellular antagonist noggin. **(i)** qPCR assessment of *Bmp2*, *Smad6*, *Id1* and *Id3* transcripts expressed as fold-change in bicuculline (bic, 20μM for 6 hours) and Bic+Nog (20μM bicuculline and 100 ng/ml noggin for 6 hours) compared to naïve cultures (N=3 independent cortical cultures, total of 3 technical replicates, two-way ANOVA).
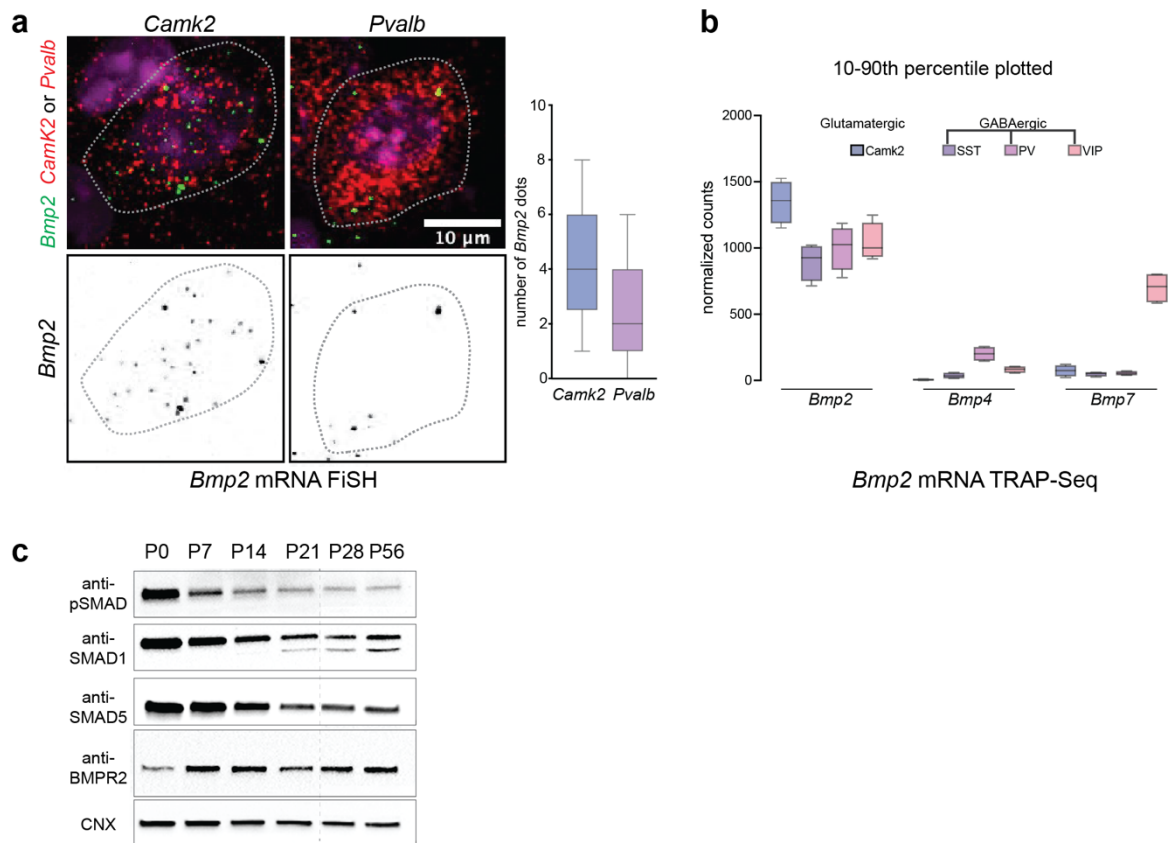
Extended Data Fig. 2. Expression of BMP signaling components in the adult mouse neocortex. (a) Quantification of *Bmp2* mRNA expression *Camk2*^{+} and *Pvalb*^{+} neurons in layer 2/3 of mouse barrel cortex (P25-30) assessed by FiSH (N=3 mice, n=57 cells/*Camk2*+ and n=45 cells/*Pvalb*+) (**b**) mRNA expression of *Bmp2*, *Bmp4*, *Bmp7* in P25 mouse neocortex in genetically-defined *Camk2*^{+} principal neurons and somatostatin[+] (SST), PV, and Vasoactive intestinal peptide[+] (VIP) interneurons extracted from SPLICECODE database of TRAP-Seq analysis (Furlanis, Traunmuller et al. 2019). (**c**) Developmental expression levels assessed by Western blot of BMP receptor type 2 (BMPR2), transcriptional mediators (SMAD1 and SMAD5) and their active complex (pSMAD1/5/9) in the mouse neocortex (postnatal day 0 to postnatal day 56).
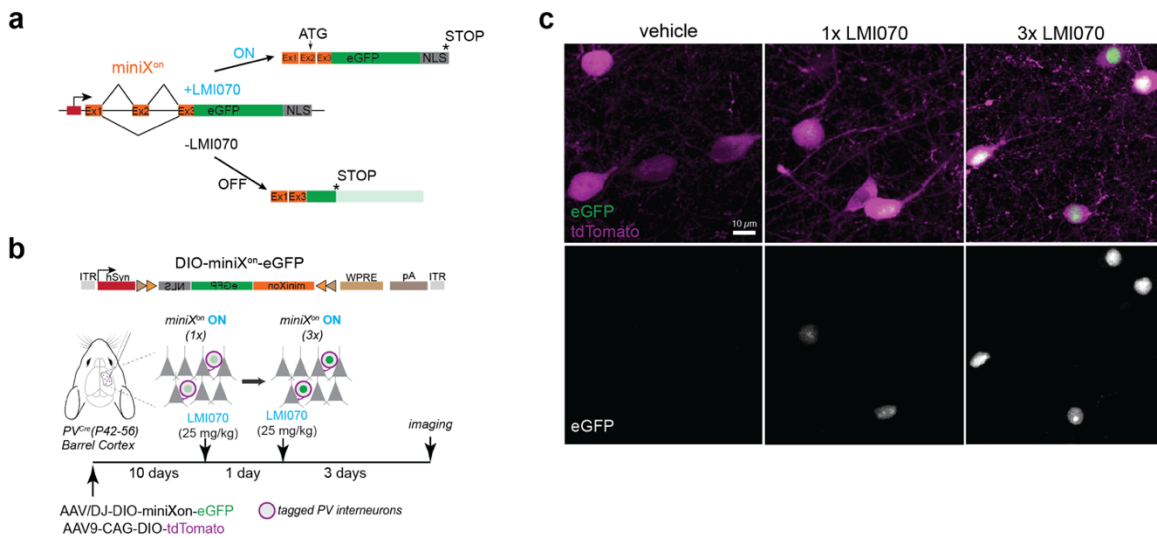
Extended Data Fig. 3. Chemically-gated, cre recombinase-dependent AAV expression system. (a) Schematic illustration of miniX^on regulation of protein expression (Monteys, Hundley et al. 2021). In presence of the small molecule LMI070, alternative splicing of the cassette shifts to include a translational start codon in exon 2 (Ex2) and, thus, turns on expression of nuclear targeted eGFP reporter protein (NLS-eGFP). In absence of LMI070, translation does not occur in the correct reading frame. **(b)** Schematic diagram for cre-dependent expression of miniX^on constructs in PV interneurons by AAV injection into the barrel cortex of adult *PV^cre* mice. **(c)** Representative images for nuclear NLS-eGFP expression in PV interneurons of mice treated by oral gavage with vehicle or 25 mg/kg LMI070 (1x or 3x in 24 hours intervals).
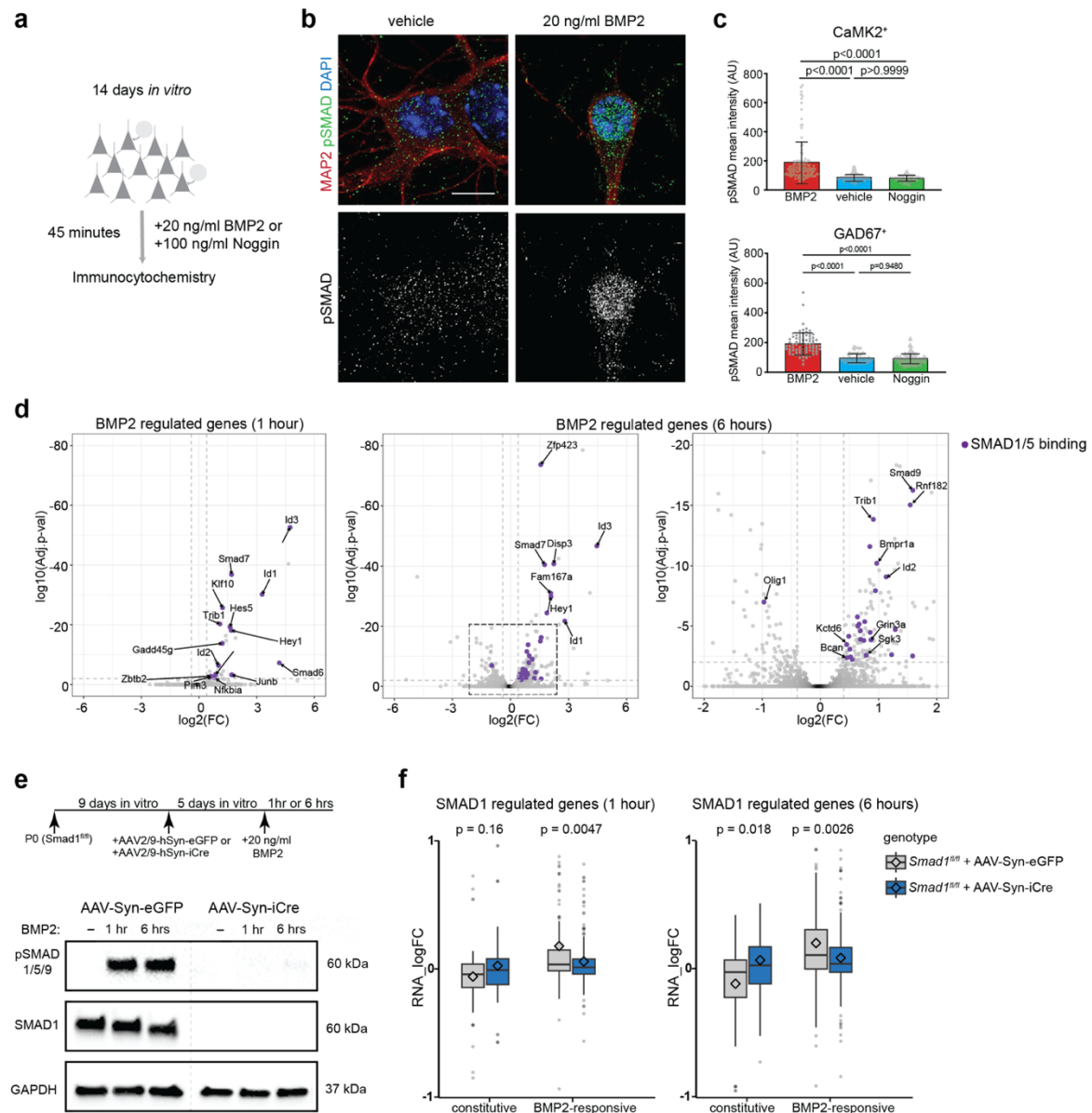
Extended Data Fig. 4. BMP-SMAD1 signaling in neocortical neurons. (a) Schematic representation of cortical cultures and BMP pathway manipulations. **(b)** Immunostaining of naïve or BMP2-stimulated (20ng/ml for 45 minutes) cultured neocortical neurons (DIV14) with antibodies to the neuronal marker microtubule associated protein-2 (MAP2) and pSMAD1/5/9 (activated SMAD). **(c)** Quantification of nuclear pSMAD intensity in cultured CaMK2^{+} glutamatergic neurons and GAD67^{+} GABAergic neurons from BMP2-treated (20ng/ml 45 minutes), vehicle-treated and noggin-treated (100 ng/ml, minutes) cortical cultures (N=3 independent cultures, one-way Anova followed by Tukey's multiple comparisons test, the bar graphs show then means ± SEM.) **(d)** Vulcano plot of RNA-seq expression data from neocortical cultures (DIV14) stimulated with BMP2 (20ng/ml) for one hour (left) or 6 hours (middle and right). Log2 fold change (FC) of expression values for stimulated over non-stimulated cells and log10 adjusted p-values are displayed. Direct SMAD1/5 targets identified in ChiP-seq that are significantly regulated were marked in purple and are indicated by arrow. Gray dashed lines indicate 30% change and adj. p-value of 0.01 which were used as cut-offs to consider genes significantly regulated. Black dashed lines indicate the 2 fold change and log10 adj.p-values less than 20 which were used as cut-offs to highlight genes moderately but significantly changed (right). **(e)**

Experimental design and Western blot for detection of SMAD1 and pSMAD1/5/9 protein levels in control (AAV-Syn-eGFP) and neuron-specific Smad1 conditional knock-out (AAV-Syn-iCre) cultured neocortical neurons (DIV14), either naïve (-) or treated with recombinant BMP2 (20 ng/ml) for 1 hr or 6 hrs (representative of N=3 independent cortical cultures). **(f)** Box plots showing the fold change of gene expression in neocortical cultures (DIV14) assessed by RNA-seq plotted for genes with constitutive and BMP2-responsive SMAD1/5 binding events as identified by ChiP-seq. Horizontal black lines mark the median, whiskers indicate standard deviations and diamonds mark the mean of the fold changes (N=4 cultures/condition, p-values were obtained with Wilcoxon test).

a $PV^{cre}::Ai9^{tom}$ $Smad1^{\Delta PV}:PV^{cre}::Ai9^{tom}::Smad1^{fl/fl}$

b Density of PV-INs

c Density of parvalbumin positive PV-INs

Legend: $PV^{cre}::Ai9^{tom}$ (grey), $Smad1^{\Delta PV}$ (red)

d

PV interneurons (P56-72)	$PV^{cre}::Ai9^{tom}$	$Smad1^{\Delta PV}$	p-value	significance
RMP (mV)	-75.25 ± 1.6	-76.8 ± 1.7	p=0.81	ns
IR (MΩ)	136.78 ± 7.1	113.0 ±8.4	p=0.02	*
Capacitance (pF)	44.96 ± 3.7	48.61 ± 1.9	p=0.19	ns
AP-threshold (mV)	-40.1 ± 1.8	-39.81 ± 1.0	p=0.83	ns
APmax (mV)	45.15 ± 2.4	48.23 ± 2.0	p=0.03	*
AHP amplitude (mV)	12.85 ± 0.5	16.74 ± 1.2	p=0.02	*
Half-width (ms)	0.42 ± 0.03	0.47 ± 0.02	p=0.49	ns
MFF	330.67 ± 22.4	256 ± 13.0	p=0.04	*
number of cells (n)	12	14		

e Current injection (P26-P30)

PV interneurons (P26-30)	$PV^{cre}::Ai9^{tom}$	$Smad1^{\Delta PV}$	p-value	significance
RMP (mV)	-72.5 ± 1.0	-71.0 ± 0.9	p=0.16	ns
IR (MΩ)	99.2 ± 5.3	93.8 ± 5.1	p=0.98	ns
Capacitance (pF)	37.1 ± 1.4	38.0 ± 1.8	p=0.82	ns
MFF	288.3 ± 9.1	290 ± 11.7	p=0.36	ns
number of cells (n)	23	21		

Extended Data Fig. 5. Normal PV interneuron density but decreased parvalbumin protein immunoreactivity in barrel cortex of $Smad1^{\Delta PV}$ mice. (a) Representative images of coronal sections of adult mouse (P56-P72) barrel cortex of $PV^{cre}::Ai9^{tom}$ mice (left) and $Smad1^{\Delta PV}$ mice (right) displaying nuclear DAPI, tdTomato, and anti-parvalbumin immunoreactivity. **(b)** Quantification of density of tdTomato⁺ PV interneurons across layers in barrel cortex of $PV^{cre}::Ai9^{tom}$ mice (left) and $Smad1^{\Delta PV}$ mice (N=4-5 mice/genotype, n=2 sections per genotype, mean cell density/mouse and SEM, two-way Anova followed with Sidak's multiple comparisons test). **(c)** Quantification of density of parvalbumin immunoreactive PV interneurons across layers in barrel cortex of $PV^{cre}::Ai9^{tom}$ mice (left) and $Smad1^{\Delta PV}$ mice (N=6-7 mice/genotype, n=2 sections per genotype, mean cell density/mouse and SEM, two-way ANOVA followed with Sidak's multiple comparisons test). **(d)** Intrinsic and action potential properties of layer 2/3 PV interneurons from P56-72 $PV^{cre}::Ai9^{tom}$ mice and $Smad1^{\Delta PV}$ mice. RMP: resting membrane potential, IR: input resistance, MFF: maximum firing frequency, AP: action potential, AHP: afterhyperpolarization (N=4 mice, n=12 cells for $PV^{cre}::Ai9^{tom}$ and N=4, n=14 cells for $Smad1^{\Delta PV}$, Kolmogorov-Smirnov test). **(e)** Comparison of firing frequencies of PV

interneurons at given currents and their intrinsic properties from P26-30 $PV^{cre}::Ai9^{tom}$ mice (gray) and $Smad1^{\Delta PV}$ mice (red). RMP: resting membrane potential, IR: input resistance, MFF: maximum firing frequency (N=4 mice, n=23 cells for PVcre::Ai9tom and N=4 mice, n=21 cells for $Smad1^{\Delta PV}$ mice, Kolmogorov-Smirnov test).

a

Xph20-eGFP

5 µm

FingR PSD-95-eGFP

FingR PSD-95-mGreenL

FingR PSD-95-mGreenL
vGlut1

b Quantification of dendritic glutamatergic synapses onto PV interneurons

1 — FingR — vGlut1 — PV tdT+ → tdTomato positive PV cell with postsynaptic binder, presynaptic antibody marker and nuclear stain (DAPI)

2 — ~ 30 µm → Filament detection with tdTomato channel masks dendrite and allows measurement of selected stretch

3 → Spots are masked in mGreenLantern channel and spots in distance closer to 1 µm in distance are quantified

c Quantification of GABAergic PV-PVsynapses formed onto the soma of PV interneurons

— FingR — SYT2 — PV tdT+

1 tdTomato positive PV cell with postsynaptic binder, presynaptic antibody marker and nuclear stain (DAPI)

2 Surface detection with tdTomato channel masks soma and allows removal of processes

3 Spots are masked in eGFP channel and Syt2 channel, overlap of spots with DAPI signal is removed

4 Masked spots that are closer to 1 µm in distance to the soma are selected

5 Apposed spots in eGFP (binder) and SYT2 (presynaptic marker) channel are quantified and density is normalized to the soma volume

Extended Data Fig. 6. Optimization of intrabody labelling and quantification of synaptic innervation of PV interneurons. We optimized the original FingR-PSD-95-eGFP constructs (Gross, Junge et al. 2013) by introducing the neuron-optimized fluorophore mGreenLantern (Campbell, Nabel et al. 2020), and placing the cDNA under control of the neuron-specific synapsin promoter. We then compared FingR-PSD-95-mGreenLantern with FingR-PSD-95-eGFP and a PSD-95 paralog-specific Xph20-EGFP intrabody (Rimbault, Breillat et al. 2021) by stereotaxic injection of cre-dependent AAVs into the barrel cortex of adult (P56-P72) PV[cre] mice. **(a)** Representative images of PV interneurons expressing Xph20-eGFP, PSD-95FinGR-eGFP, PSD-95FingR-mGreenLantern. Scale bar in top panel is 5 µm. Co-immunostaining with the glutamatergic presynaptic marker VGlut1 (magenta) reveals extensive overlap with the postsynaptic FingR-PSD-95-mGreenLantern marker. **(b)** Illustration of 3D quantification protocol for glutamatergic synapses on PV interneuron dendrites with IMARIS software. **(c)** Quantification protocol developed in IMARIS to quantify peri-somatic GABAergic synapses labelled with FingRGPHN-eGFP intrabodies and co-stanined with Syt2 on PV interneurons.

LTP of inhibition at PV interneuron output synapses requires developmental BMP signaling

Evan Vickers[1,3], Denys Osypenko[1], Christopher Clark[1,4], Zeynep Okur[2], Peter Scheiffele[2], Ralf Schneggenburger[1, 5]

[1] Laboratory of Synaptic Mechanisms, Brain Mind Institute, School of Life Science, École Polytechnique Fédérale de Lausanne (EPFL), 1015 Lausanne, Switzerland

[2]: Biozentrum, University of Basel, 4056 Basel, Switzerland

[3] present address: Institute of Neuroscience, University of Oregon, Eugene, OR 97403,

USA

[4] present address: Institute for Regenerative Medicine, University of Zürich, 8952

Schlieren, Switzerland

[5] Address correspondence to: Dr. Ralf Schneggenburger (ralf.schneggenburger@epfl.ch)

Abbreviated title:

BMP signaling and plasticity of inhibition

Abstract

Parvalbumin (PV)-expressing interneurons (PV-INs) mediate well-timed inhibition of cortical principal neurons, and plasticity of these interneurons is involved in map remodeling of primary sensory cortices during critical periods of development. To assess whether bone morphogenetic protein (BMP) signaling contributes to the developmental acquisition of the synapse- and plasticity properties of PV-INs, we investigated a conditional/conventional double KO mice of BMP-receptor 1a (BMPR1a; targeted to PV-INs) and 1b (BMPR1a/1b (c)DKO mice). We report that spike-timing dependent LTP at the synapse of PV-INs onto principal neurons of layer 4 in the auditory cortex was absent, concomitant with a decreased paired-pulse ratio (PPR). On the other hand, baseline synaptic transmission at this connection, and action potential (AP) firing rates of PV-INs were unchanged. To explore possible gene expression targets of BMP signaling, we measured the mRNA levels of the BDNF receptor TrkB and of P/Q-type Ca^{2+} channel - subunits, but did not detect expression changes of these genes in PV-INs of BMPR1a/1b (c)DKO mice. Our study suggests that BMP-signaling in PV-INs during and shortly after the critical period is necessary for the expression of LTP at PV-IN output synapses, involving gene expression programs that need to be addressed in future work.

Introduction

The neocortex of mammals contains specific classes of excitatory and inhibitory neurons(Rudy, Fishell et al. 2011, Markram, Muller et al. 2015, Zeisel, Munoz-Manchado et al. 2015, Tasic, Yao et al. 2018). Amongst the inhibitory interneurons, PV-INs can sustain high - frequency AP firing, and show fast membrane potential signaling and

temporal precision at their input - and output synapses (Hu, Gan et al. 2014). PV-INs form output synapses largely on soma-near compartments of principal neurons (Kubota, Kondo et al. 2015),

and the resulting GABA release causes well-timed inhibition of cortical principal neurons (Gabernet, Jadhav et al. 2005, Cruikshank, Urabe et al. 2010). Furthermore, the output synapses of PV-INs can undergo long-term potentiation (Maffei, Nataraj et al. 2006, Lourenco, Pacioni et al. 2014, Vickers, Clark et al. 2018) as well as long-term depression (LTD; ref.(Vickers, Clark et al. 2018)). Plasticity of inhibition, in part provided by PV-INs, has been related to critical period plasticity in the visual (Hensch 2005, Maffei, Nataraj et al. 2006, Kuhlman, Olivas et al. 2013), somatosensory (Li, Gainey et al. 2014) and auditory cortex (Vickers, Clark et al. 2018). It is likely that the physiological properties of PV-INs are gradually acquired during postnatal development (Doischer, Hosp et al. 2008), driven by specific gene expression changes (Okaty, Miller et al. 2009). Nevertheless, little is known about the molecular mechanisms which determine the developmental acquisition of the physiological properties of PV-INs, including their fast-firing properties, synaptic connectivity, and the plasticity at their output synapses.

Here, we investigate a possible role of BMP-receptor signaling for the development of these functional properties of PV-INs. BMPs are members of the TGF-beta superfamily of growth factors, with widespread roles for the embryonic development and patterning of various mammalian tissues (Zhao 2003, Dutko and Mullins 2011, Cardozo, Almuedo-Castillo et al. 2019), including the nervous system (Augsburger, Schuchardt et al. 1999, Liu and Niswander 2005). In the mammalian CNS, BMP-receptors (BMPRs) and their ligands are expressed up to early adulthood (Zhang, Mehler et al. 1998, Sato, Mikawa et al. 2010, Miyagi, Mikawa et al. 2011), suggesting that BMP signaling fulfills further roles in later brain development. Indeed, a role for BMP signaling in the elimination of excitatory synapses (Kalinovsky, Boukhtouche et al. 2011, Higashi, Tanaka et al. 2018) and in the development of mono-innervation at a large excitatory connection in the auditory brainstem, has been reported (Xiao, Michalski et al. 2013, Kronander, Clark et al. 2019). Earlier genetic studies showed that BMP signaling drives the growth of motor nerve terminals at the *Drosophila* neuromuscular junction (Aberle, Haghighi et al. 2002, Marques, Bao et al. 2002, McCabe, Marques et al. 2003). Together, these studies suggest a role for BMP signaling in guiding the establishment of specific synaptic connectivity at excitatory connections in the mammalian brain and in the periphery.

Evidence for a role of BMP signaling in the development of inhibitory interneurons is also emerging. A previous study showed that BMP-signaling in the OLIG lineage of neuronal /

oligodendrocyte precursors determines the number of oligodendrocytes and Calbindin-positive interneurons (Samanta, Burke et al. 2007), and it was shown that exogenous BMP4 can act on PV-INs or their precursors to contribute to the morphological differentiation of PV-INs (Mukhopadhyay, McGuire et al. 2009). However, it is unknown whether BMP signaling in PV-INs is necessary for the development of the functional properties of this class of interneurons. Here, we use genetic tools, patch-clamp recordings and single-cell gene expression analyses to address this question.

Results

Fast firing properties of PV-INs are largely independent of BMP-signaling

Mature PV-INs can sustain high-frequency AP firing, and show fast release kinetics and spike-timing dependent plasticity at their output synapses (see Introduction). To investigate whether the developmental acquisition of these functional properties depends on BMP

signaling in PV-INs, we genetically deleted two critical BMP-type 1 receptor subunits, BMPR1a and BMPR1b. We interbred a conventional BMPR1b KO mouse (Yi, Daluiski et al. 2000) with a conditional BMPR1a KO mouse (BMPR1a$^{lox/lox}$; ref. (Mishina, Hanks et al. 2002), targeted to PV-INs by the use of PV^{Cre} mice; ref. (Hippenmeyer, Vrieseling et al. 2005)). To facilitate analysis, PV-INs were genetically labelled with a tdT reporter line (Ai9; see Materials and Methods). In auditory cortex, onset of Cre-mediated recombination in PV^{Cre} mice occurs at ~ P13. Therefore, we focused our analysis to an age of P19 – P24. This age corresponds to a developmental period shortly after the critical period for the remodeling of sound frequency representation in primary auditory cortex at P11 - P14 (de Villers-Sidani, Chang et al. 2007, Barkat, Polley et al. 2011). We assume that in (c)DKO mice, the removal of BMPR1a in the Cre-expressing PV-INs will, in the background of BMPR1b$^{-/-}$ mice, lead to an arrest of BMP-signaling.

We recorded tdTomato-positive PV-INs in slices of primary auditory cortex of BMPR1a/1b (c)DKO mice, and in control littermate mice. Control mice had at least one functional allele of BMPR1a and - 1b (see Materials and Methods). At the age investigated here, PV-INs in control mice exhibited high-frequency AP firing upon positive current injection, with maximal firing rates of 138 ± 7 Hz (Fig. 1A, B, G; n = 7 PV-INs). In PV-INs from BMPR1a/1b (c)DKO mice, the maximal firing frequency was higher (162 ± 8 Hz; Fig. 1D, E, G), but this trend did not reach statistical significance (p = 0.09; Fig. 1G; n = 7 and n = 17 recordings from N = 7 control - and N = 13 (c)DKO mice). Furthermore, curves of instantaneous AP-frequency versus AP number, and of time-averaged AP frequency versus injected current amplitude appeared similar between control- and (c)DKO mice (Fig. 1B, E). Accordingly,

neither the maximal adaptation, nor the firing rate gain (i.e. slope of AP frequency versus injected current) were significantly different in BMPR1a/1b (c)DKO mice as compared to control mice (Fig. 1H; p = 0.08 and p = 0.86 respectively). Thus, fast AP firing of PV-INs, a property which must be acquired developmentally before the age recorded here, was not affected in BMPR1a/1b (c)DKO mice.

We furthermore analyzed the membrane resistance and membrane time constant using negative current injections. The membrane resistance was larger in BMPR1a/1b (c)DKO mice as compared to control (Fig. 1C, F), but this effect was moderate (an increase of ~ 25%), and on the edge of statistical significance (p = 0.04; Fig. 1I, left). The membrane time constant was not different between the two genotypes (average values of ~ 8 ms in both genotypes; Fig. 1I, right; p = 0.27, Mann-Whitney's test). Taken together, the developmental acquisition of the high AP firing frequency in PV-INs, nor of their fast, subthreshold membrane potential signaling seemed to depend strongly on BMP-receptor signaling in these cells. Nevertheless, we cannot exclude that differences appear in BMPR1a/1b (c)DKO mice with further development.

Changes in release probability at the output synapses of PV-INs
We next investigated whether the properties of synaptic transmission at inhibitory synapses formed by PV-INs onto L4 principal neurons in auditory cortex are altered in the (c)DKO mice. We performed paired whole-cell recordings; PV-INs were identified by their tdTomato fluorescence, and postsynaptic principal neurons by their characteristic morphology and by their AP firing properties (Vickers, Clark et al. 2018). We found that unitary IPSCs in control mice covered a large range of amplitudes across paired recordings (~ 10 - 500 pA), with an average amplitude of 149 ± 23 pA (n = 29; N = 18; Fig. 2A, B, left), in good agreement with previous work (Vickers, Clark et al. 2018). In BMPR1a and -1b (c)DKO mice, the unitary IPSC amplitude also covered a large range, with an average value of 157 ± 21 pA (n = 37; N = 24), that was indistinguishable from the IPSC amplitude in control mice. We furthermore investigated the BMPR1b single KO mice (sKO). This was necessary to control for non-specific effects that might result from the constitutive deletion of BMPR1b from cells other than PV-INs in the cortical network. The unitary IPSC amplitude in BMPR1b sKO mice was 109 ± 46 pA (n = 13 and N = 6), and a Kruskal-Wallis test reported no significant effect of genotype across the three groups (p = 0.99, Fig. 2B). Thus, the baseline strength of synaptic transmission at the PV-IN to principal neuron synapse was unchanged upon removal of BMPR1a and -1b from PV-INs.

In a subset of recordings, we evoked a second presynaptic AP at an interval of 20 ms to study the paired-pulse ratio of synaptic transmission, as an indicator of presynaptic release probability (PPR; defined as IPSC2/IPSC1). We found that PPR was decreased in BMPR1a/1b (c)DKO mice (Fig. 2A, bottom; Fig. 2C). ANOVA showed that PPR was significantly different across the three genotype groups (p = 0.0073). Further post-hoc statistical testing showed that (c)DKO mice and control mice had significantly different PPR (p = 0.005; Tukey's post-hoc test). This finding suggests that the release probability at PV-IN output synapses of (c)DKO mice is increased. In BMPR1b sKO mice, the PPR was in-between the values for control mice and (c)DKO mice, but not significantly different from neither of them (p = 0.1 and 0.35 respectively; Tukey's post-hoc test). These data indicate that the conditional removal of BMPR1a from PV-INs (in the background of the BMPR1b sKO mice) caused the observed changes in PPR.

An increased release probability is expected to cause an increased unitary IPSC amplitude, if other quantal parameters of transmission had been unchanged. Nevertheless, in the overall dataset, the unitary IPSC amplitude was indistinguishable between control-, and BMPR1a/1b (c)DKO mice (see above; Fig. 2B). A masking of the effects of a changed release probability could be caused by small opposing effects of either the quantal size q, and/or of the readily-releasable vesicle pool available at the PV-IN to L4 principal neuron connection. To test for such changes, we performed a variance - mean analysis, using baseline IPSC data obtained at stimulation frequency of 0.1 Hz (see below, Fig. 3A-C for examples). We found that the variance - mean value was 36 ± 4 pA (n = 29 and N = 18) and 26 ± 2 pA (n = 37 and N = 24) in control- and BMPR1a/1b (c)DKO mice, but this trend did not reach statistical significance (p = 0.1; Mann-Whitney test). In principle, a smaller variance - mean ratio would indicate a lower quantal amplitude q. Nevertheless, a small decrease in IPSC variance would also be expected for a reduced readily-releasable pool (Clements and Silver 2000, Meyer, Neher et al. 2001).

Deficient spike-timing dependent iLTP in the absence of BMP-signaling in PV-INs
We next investigated spike-timing dependent long-term plasticity at the inhibitory synapses formed by PV-INs onto L4 principal neurons (Vickers, Clark et al. 2018). After establishing a baseline unitary IPSC amplitude for a given paired recording (Fig. 3A, left), we applied repeated AP stimuli in the postsynaptic - then presynaptic order at an interval of 5 ms (50 times, 0.2 Hz; "post-pre induction"; Fig. 3A, middle). This induced a long-lasting potentiation of the unitary IPSC amplitude by 40 ± 8 % (n = 9, N = 6; Fig. 3D, left), similar to previous results (Vickers, Clark et al. 2018). In the BMPR1a and -1b (c)DKO mice, the same protocol failed to induce LTP of inhibition in most recordings (Fig. 3B), and

occasionally caused long-term depression (LTD) of inhibition. Because the amount of plasticity observed in (c)DKO mice was close to zero in many recordings, we next performed a statitical analysis to determine if the change in IPSC amplitude after the induction protocol was significant. This revealed that in recordings from BMPR1a/1b (c)DKO mice, the change in IPSC amplitudes was in most cases not significant ($p > 0.05$, unpaired t-test; see Fig. 3D, dataset in the middle, open circles; $n = 7$ out of $n = 8$ recordings). Conversely, in the recordings from control mice, significant iLTP was observed in $n = 8$ out of $n = 9$ recordings ($p < 0.05$, unpaired t-test; Fig. 3D, data set on the left, cross symbols). The group average revealed a decrease in IPSC amplitude to -6 ± 4 % in (c)DKO mice ($n = 8$, $N = 6$; Fig. 3D, middle). In the BMPR1b sKO mice, LTP was indistinguishable from that of control mice (Fig. 3C; Fig. D, right; $n = 8$, $N = 5$). ANOVA reported a significant effect of genotype on iLTP (Fig. 3D; $p = 0.027$). Tukey's post-hoc test found that the magnitude of iLTP was significantly smaller in BMPR1a/1b (c)DKO mice as compared to control mice ($p = 0.044$), and as compared to the BMPR1b sKO mice ($p = 0.046$; Fig. 3D). These findings suggest that BMP-receptor signaling in PV-INs at ~ P15 - P20 is a pre-requisite for the development of cellular mechanisms that enable spike-timing dependent LTP at PV-IN output synapses.

In a subset of the recordings, we again applied paired stimuli to measure possible changes in PPR after the induction of LTP. In the control mice, the PPR was significantly reduced after the induction of LTP ($p = 0.046$, $n = 4$; Fig. 3E, left), consistent with a presynaptic locus of expression for LTP of inhibition (Vickers, Clark et al. 2018). In (c)DKO mice, the PPR was not significantly changed after the induction protocol ($p = 0.39$, $n = 5$; Fig. 3E, middle), consistent with an absence of LTP in this genotype (Fig. 3D). Furthermore, the PPR before induction was smaller than in the control mice (see also Fig. 2C). Finally, in BMPR1b sKO mice, the PPR was decreased by LTP induction ($p = 0.008$, $n = 8$ Fig. 3E, right). These findings are consistent with the notion of an increased release probability in BMPR1a/1b (c)DKO mice (Fig. 2C), and that this increased release probability could occlude the expression of LTP at the output synapses of PV-INs.

Expression of TrkB is unchanged in PV-INs of BMPR1a/1b (c)DKO mice
Activation of BMP-receptors modifies gene expression in target cells by SMAD-dependent signaling cascades (Miyazono, Kamiya et al. 2010). In BMPR1a/b (c)DKO mice, we observed alterations in presynaptic release probability and of LTP at PV-IN output synapses (Figs 2, 3). Transmitter release at PV-IN output synapses is mediated by P/Q-type Ca^{2+} channels (Hefft and Jonas 2005, Zaitsev, Povysheva et al. 2007), and spike-timing dependent LTP of inhibition involves retrograde BDNF signaling from principal

neurons onto nerve terminals of PV-INs (Vickers, Clark et al. 2018). Thus, we probed whether the mRNA levels coding for the P/Q - type Ca^{2+} channel subunit -1A (Cacna1A) and for the BDNF receptor TrkB (Ntrk2) might be altered in BMPR1a/1b (c)DKO mice. We used fluorescent *in-situ* hybridization (FISH) on sections from control - and (c)DKO mice; PV-INs were detected with a tdTomato FISH probe based on the Cre-dependent expression of this reporter gene in PV-INs. We found that the density of PV-INs in the auditory cortex was unchanged in BMPR1a/b (c)DKO mice as compared to control mice (Fig. 4A, C). To investigate the mRNA expression levels of Cacna1a and Ntrk2, we counted the puncta within the somata of tdTomato - positive neurons (Fig. 4B). In n = 9 cells analyzed from one control - and one (c)DKO mouse each, we did not observe a difference in the number of puncta normalized by cell surface (Fig. 4D, left). Repeated measurements in n = 32 cells from N = 3 control mice, and in n = 35 cells from N = 4 BMPR1a/1b (c)DKO mice, did not indicate a significant change in the expression of Ntrk2 in PV-INs (Fig. 4D right, p = 0.4; Mann-Whitney test). Similarly, the mRNA expression of Cacna1a was unchanged between control mice, and BMPR1a/1b (c)DKO mice (Fig. 4E; p = 0.86; Mann-Whitney test).

To further test for the functional expression of presynaptic P/Q-type Ca^{2+} channels at the nerve terminals of PV-INs, we measured unitary IPSCs in paired recordings, and applied the specific P/Q-type Ca^{2+} channel toxin -agatoxin-iva (Iwasaki, Momiyama et al. 2000). We found that the block of synaptic transmission by -agatoxin was unchanged between control - and BMPR1a/1b (c)DKO mice (97 ± 1.5 %, n = 2; and 97 ± 1.0 %, n = 6; p = 0.99; Fig. 4F, G). Thus, consistent with unaltered Cacna1A transcript levels, P/Q-type Ca^{2+} channels continue to be the predominant Ca^{2+} channels at the output synapses of PV-INs of BMPR1a/1b (c)DKO mice.

Discussion

Layer 4 of sensory cortices receives information from thalamus via excitatory synapses on principal neurons, and this thalamocortical drive includes a powerful feedforward inhibition mediated by PV-INs (Gabernet, Jadhav et al. 2005, Cruikshank, Urabe et al. 2010). In the input layers of auditory cortex, the timing of AP firing is relevant (Wehr and Zador 2003, Zhou, Mesik et al. 2012, Moore and Wehr 2013), and marked spike-timing dependent plasticity occurs both at excitatory synapses, and at inhibitory synapses formed by PV-INs onto principal neurons in layer 4 of the auditory cortex (D'Amour and Froemke 2015, Vickers, Clark et al. 2018). In the auditory cortex of rodents, exposure to a predominant sound frequency during a critical period at P11 - P14 leads to enhanced representation of that sound frequency (de Villers-Sidani, Chang et al. 2007, Barkat, Polley et al. 2011, Vickers, Clark et al. 2018). We previously found that at an age immediately following the

critical period (P15 - P22), induction protocols with reversed AP sequences (pre - post *versus* post - pre) cause opposing forms of long-term plasticity at the output synapses of PV-INs (Vickers, Clark et al. 2018). Upon further development, at an age of 4 - 5 weeks, however, both spike-timing sequences cause long-term *potentiation* at the PV-IN output synapses (Vickers, Clark et al. 2018). Thus, the direction of plasticity at the output synapses of PV-INs is developmentally regulated, and a symmetric learning rule of potentiation of inhibition is attained in more mature animals. A symmetric learning rule with potentiation of inhibition is, in turn, expected to stabilize neuronal networks (Vogels, Sprekeler et al. 2011). Nevertheless, the molecular mechanisms that drive developmental changes of long-term plasticity at inhibitory synapses have been unknown.

Previous work showed that BMP signaling occurs in developing PV-INs and contributes to the morphological differentiation of PV-INs (Mukhopadhyay, McGuire et al. 2009), but the effects of interrupting BMP signaling on the functional properties of PV-INs had not been studied. We used conditional genetic inactivation of BMPR1a in PV-INs, in the background of BMPR1b sKO mice, and studied these mice at P19 - P24, about 7 - 10 days after the onset of Cre-expression in PV-INs at ~ P13. In BMPR1a/1b (c)DKO mice, there were no consistent effects on the passive membrane properties of PV-INs, nor on the high rate of AP-firing that these neurons can generate (Fig. 1). On the other hand, spike-timing dependent LTP of inhibition upon post - pre induction protocols was absent, and there was a concomitant reduction of PPR indicating an increased release probability at the output synapses of PV-INs (Fig. 3). In BMPR1b single KO mice, no deficits of LTP of inhibition were observed (Fig. 3D). These data show that developmental BMP-signaling in PV-INs determines presynaptic properties of the output synapses of PV-INs, including release probability, and spike-timing dependent long-term potentiation.

Given a role of BMP-signaling in determining the properties of the output synapses of PV-INs, it is tempting to speculate in which neuronal compartments of PV-INs BMP-receptors are localized, and which is the source of BMP that activates these receptors. At the *Drosophila* neuromuscular junction, evidence for a retrograde BMP signaling direction from postsynaptic - to presynaptic compartments was obtained by genetic approaches (McCabe, Marques et al. 2003, Ball, Warren-Paquin et al. 2010). However, because of a lack of suitable antibodies for immunohistochemistry of BMP-receptors, we have not been able to study the localization of BMP-type 1 receptors in PV-INs. Single-cell genome-wide expression data suggests that BMPR1b is strongly expressed in astrocytes but only weakly expressed in various neuron types, whereas BMPR1a is more strongly expressed in neurons, including PV-INs (see https://www.brainrnaseq.org/ established by ref. (Zhang,

Chen et al. 2014), and http://greenberg.hms.harvard.edu/project/gene-database/ established by ref. (Hrvatin, Hochbaum et al. 2018). This might suggest that amongst the two type-1 BMP-receptors investigated here, BMPR1a is mainly responsible for initiating BMP-signaling in PV-INs early postnatally; however, further experiments with the single conditional KO are necessary to reinforce this conclusion.

We have previously found that LTP of inhibition involves the activation of TrkB receptors, most likely localized on the presynaptic nerve terminals of PV-INs (Vickers, Clark et al. 2018). Previous work has also shown that BDNF signaling can influence critical period plasticity by acting on inhibitory neurons in the visual cortex (Huang, Kirkwood et al. 1999). Furthermore, earlier *in-vitro* experiments have reported that BMPs and neurotrophins, such as BDNF and NT3, can act synergistically in neurons (Gratacos, Checa et al. 2001), and that BMP2 can increase the expression of the NT3 receptor TrkC in peripheral neurons (Kobayashi, Fujii et al. 1998, Zhang, Mehler et al. 1998) (Schnitzler, Mellott et al. 2010). For these reasons, we started to investigate whether Ntrk2, the gene coding for trkB, shows a misregulated expression on the mRNA level in PV-INs of BMPR1a/1b (c)DKO mice. However, we did not find significant changes in transcript levels of Ntrk2 in PV-INs of BMPR1a/1b (c)DKO mice (Fig. 4). Nevertheless, it remains possible that BMP-signaling in PV-INs regulates the expression level of TrkB on the protein level, and/or that a scaffolding protein necessary for the correct subcellular localization and function of the BDNF receptor TrkB is regulated by BMP-signaling in PV-INs.

We also analyzed the expression of Cacna1a, the gene which codes for the -subunit of voltage-gated P/Q type Ca^{2+} channels. P/Q-type Ca^{2+} channels are expressed in PV-INs both on the soma-dendritic compartment and at the nerve terminal (Hefft and Jonas 2005, Zaitsev, Povysheva et al. 2007, Rossignol, Kruglikov et al. 2013, Vecchia, Tottene et al. 2014). We found that the mRNA levels of Cacna1A were not changed significantly in PV-INs, and correspondingly, synaptic transmission at the output synapses of PV-INs continued to be highly sensitive to the P/Q-type Ca^{2+} channel blocker agatoxin-IVa (Fig. 4). Thus, the target genes downstream of BMP- and SMAD-signaling in PV-INs need to be systematically investigated in future studies, possibly using genome-wide screening approaches. Identifying target genes whose expression is regulated by BMP-signaling in PV-INs might allow further insights into the signaling pathways that enable a presynaptic, BDNF-dependent form of LTP at the output synapses of these interneurons (Vickers, Clark et al. 2018).

PV-INs are characterized by the high AP firing frequency they can sustain (Hu, Gan et al. 2014), a property which is acquired during postnatal development (Doischer, Hosp et al. 2008, Okaty, Miller et al. 2009). We did not find clear effects on the high AP firing frequency that these neurons can support, nor on the membrane time constant of PV-INs in BMPR1a/1b (c)DKO mice (Fig. 1). The input resistance of PV-INs was moderately increased in BMPR1a/b (c)DKO mice (Fig. 1I), which might suggest a slower developmental maturation towards a low membrane resistance in adult animals (Doischer, Hosp et al. 2008).

Taken together, we find that developmental BMP-signaling in PV-INs determines presynaptic properties of the output synapses of these interneurons, including release probability and spike-timing dependent LTP of inhibition. A symmetric "learning rule" of long-term *potentiation* of inhibition regardless of the exact sequence of pre- and postsynaptic APs is established at ~ P28 (ref. (Vickers, Clark et al. 2018)), and this symmetric learning rule is likely beneficial for the stability of neuronal networks (Vogels, Sprekeler et al. 2011). Thus, it is possible that developmental BMP-signaling in PV-INs, which supports LTP of inhibition, is a prerequisite for certain types of homeostatic plasticity in cortical networks (Maffei, Nataraj et al. 2006, Xue, Atallah et al. 2014). This hypothesis could be tested in future systems-level investigations of cortical function using BMP-receptor mutants.

Author contributions

E.V., C.C., and R.S. designed the research. E.V., D.O. and C.C performed and analyzed electrophysiological experiments. Z.O. performed FISH experiments; Z.O. and P.S. analyzed FISH experiments. E.V., P.S. and R.S wrote the paper. E.V and D.O prepared figures 1-3; Z.O. and D.O. prepared figure 4. All authors reviewed the manuscript.

Additional Information
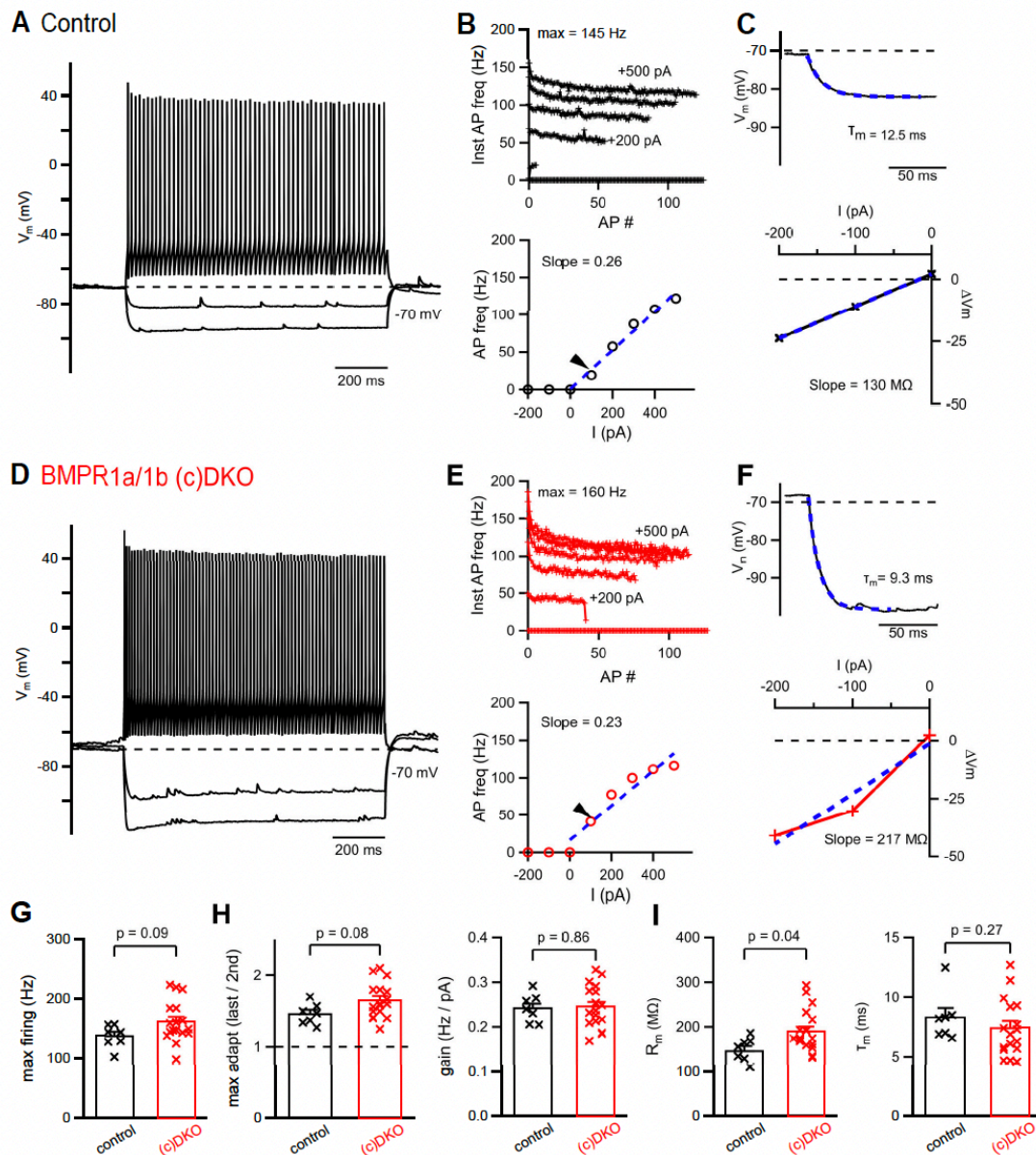
Figures

Figure 1. AP-firing properties and passive membrane properties of PV-INs are largely unchanged in BMPR1a/1b (c)DKO mice.

(**A**) AP-firing of a PV-IN in a control mouse of age P22, in response to 1-s current steps to - 200, - 100 and + 200 pA. (**B**) Instantaneous AP frequency (top) and plot of AP-frequency as a function of injected current (bottom). (**C**) Exponential fit (dashed blue line) to the membrane potential (V_m) relaxation caused by a -100 pA current injection, to determine the membrane time constant (τ_m; top), and plot of the steady-state V_m value as a function

of the injected current to determine membrane resistance (slope = 130 MΩ in this example). The data in (A-C) are from the same recording. (**D-F**) Same as (A-C), but for a recording of a PV-IN in a BMPR1a/1b (c)DKO mouse of age P19. (**G**) Individual - and average data of the maximal AP firing frequency in control mice (left, black data points) and in BMPR1a/1b (c)DKO mice (right, red data points). (**H**) Individual - and average data for maximal adaptation (left), and for the firing rate gain (right). The latter was calculated as the slope in the plots of AP-firing versus injected current (B, E, bottom). (**I**) Individual - and average data for membrane resistance (left) and membrane time constant (right). For the number of recordings (n) and number of mice (N), and the statistical tests used, see Results.
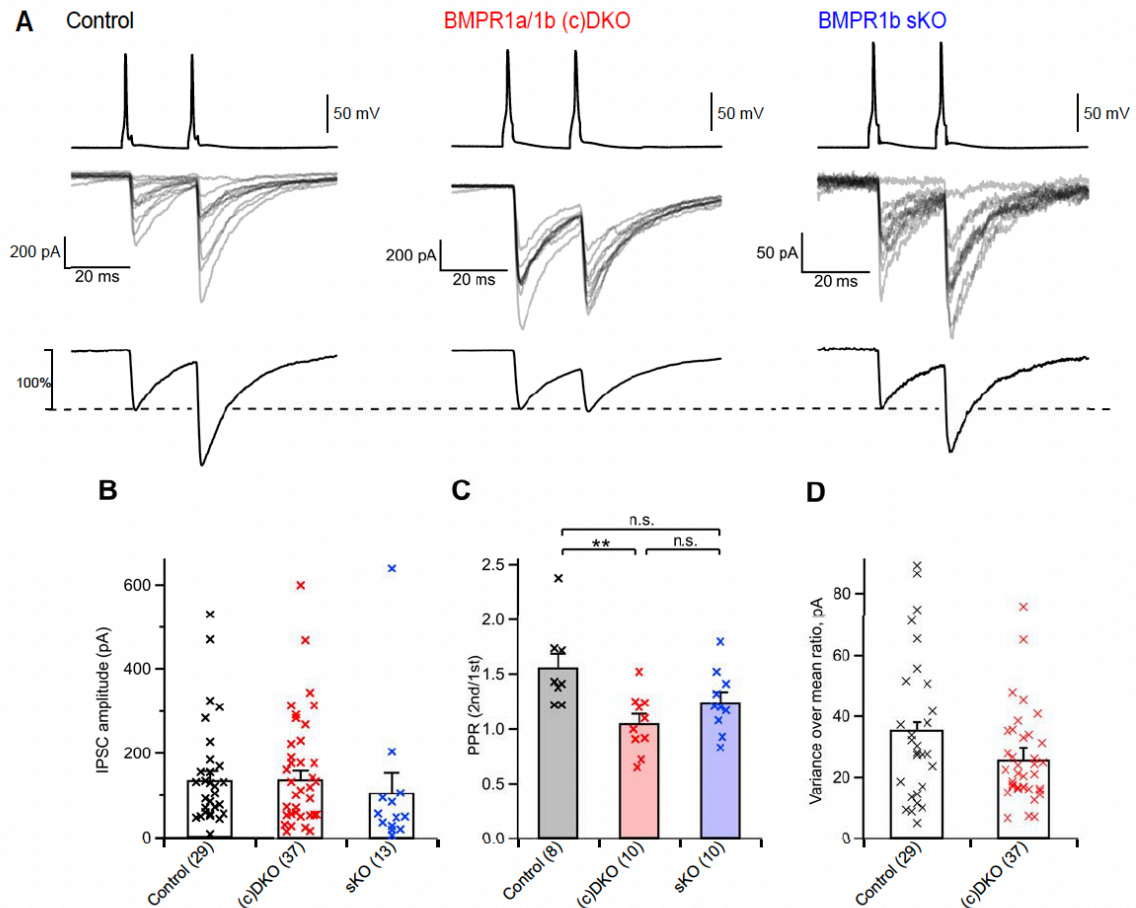
Figure 2. Knock-out of BMP-type1 receptors in PV-INs leads to an increased release probability, but does not affect baseline synaptic transmission at PV-IN output synapses.

(A) APs evoked by brief current injections in PV-INs (V_m traces on top), and the resulting IPSCs in a postsynaptic principal neuron of layer 4 (middle). The bottom panels show peak-normalized IPSCs averaged from a larger number of stimulations (n = 40 - 60). From left to right, example paired recording from a control mouse at P23, from a BMPR1a/1b (c)DKO mouse at P21, and from a BMPR1b sKO at P22. (B) Individual - and average values of unitary IPSC amplitudes recorded in paired recordings in control mice (left); in BMPR1a/1b (c)DKO mice (middle) and in BMPR1b sKO mice (right). A Kruskal-Wallis test did not find a significant difference between the groups (see Results). (C) Individual - and average data for paired-pulse ratio (PPR) in a subset of recordings in which paired stimulation was applied, for the same genotypes as in (B). (D) Individual- and average

values of the IPSC variance - mean ratio of the IPSC peak amplitudes, in control mice (left) and in BMPR1a/1b (c)DKO mice (right).

In panels B-D, the number of recordings ("n") is indicated on the x-axis; for the number of animals ("N") see Results. For statistical tests and p-values, see Results. **, $p < 0.01$; n.s., not significant.
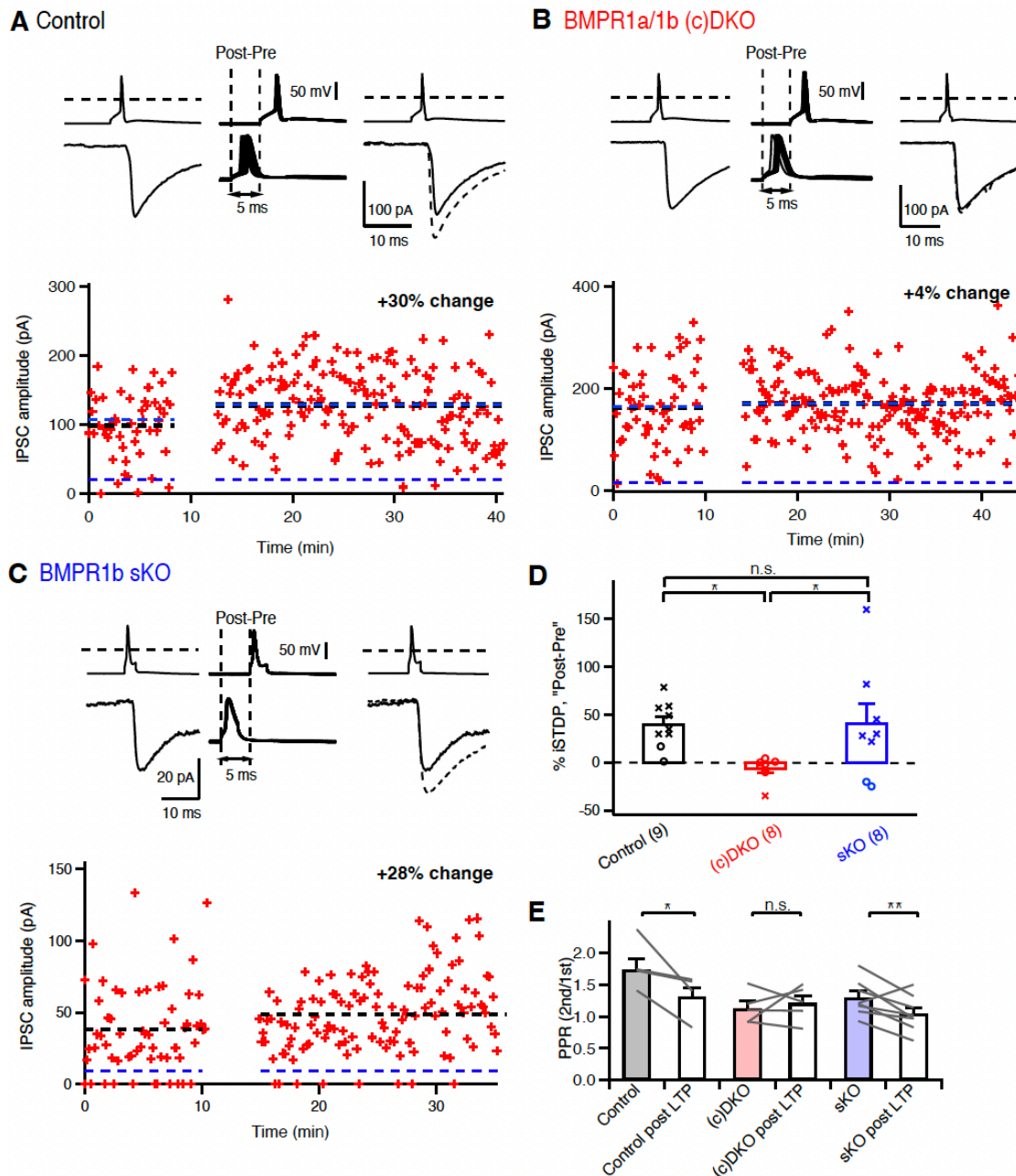
Figure 3. Knock-out of BMP-type 1 receptors in PV-INs impairs spike-timing dependent LTP at PV-IN output synapses.

(A-C) Example of spike-timing dependent plasticity experiments with "post - pre" AP stimulation in paired recordings from a control mouse at P21 (A), from a BMPR1a/1b (c)DKO mouse at P20 (B), and from a BMPR1b sKO mouse at P21 (C). The traces on the top of each panel show presynaptic APs (in mV; top), and postsynaptic IPSCs during baseline (left, in [pA]), pre- and postsynaptic APs during the induction of spike-timing dependent plasticity (middle, in mV), and again IPSCs and presynaptic APs after the

induction period (right, in [pA], same scale as left). Continuous IPSC traces represent average IPSCs during baseline; dashed IPSC traces represent the average IPSCs during the post-induction period. The plots on the bottom are IPSC stability plots. Thick dashed lines represent the average IPSC amplitude for baseline - and post-induction times. The amount of spike-timing dependent plasticity for each example is indicated. The lower thin dashed lines represent the threshold amplitude below which IPSCs were regarded as failures (see ref. 11). (**D**) Individual - and average values of spike-timing dependent plasticity measured in control mice (left, black data points), in BMPR1a/1b (c)DKO mice (middle, red data points), and in BMPR1b sKO mice (right, blue data points). Significantly - and non-significantly changed IPSC amplitudes are indicated by cross - and open symbols, respectively (t-test; $p < 0.05$ and $p > 0.05$ respectively). For the statistics of the group comparisons, and for n and N numbers, see Results. (**E**) Individual - and average values of PPR for a subset of recordings in which paired presynaptic stimuli were given. For each genotype, PPR under baseline conditions (left bar with color), and following the induction of spike-timing dependent plasticity (right open bar) is given. Left two bars, data from n = 4 recordings in control mice; middle two bars, data from n = 5 recordings in BMPR1a/1b (c)DKO mice; right two bars, data from n = 8 BMPR1b sKO mice. **, $p < 0.01$; *, $p < 0.05$; n.s., not significant.
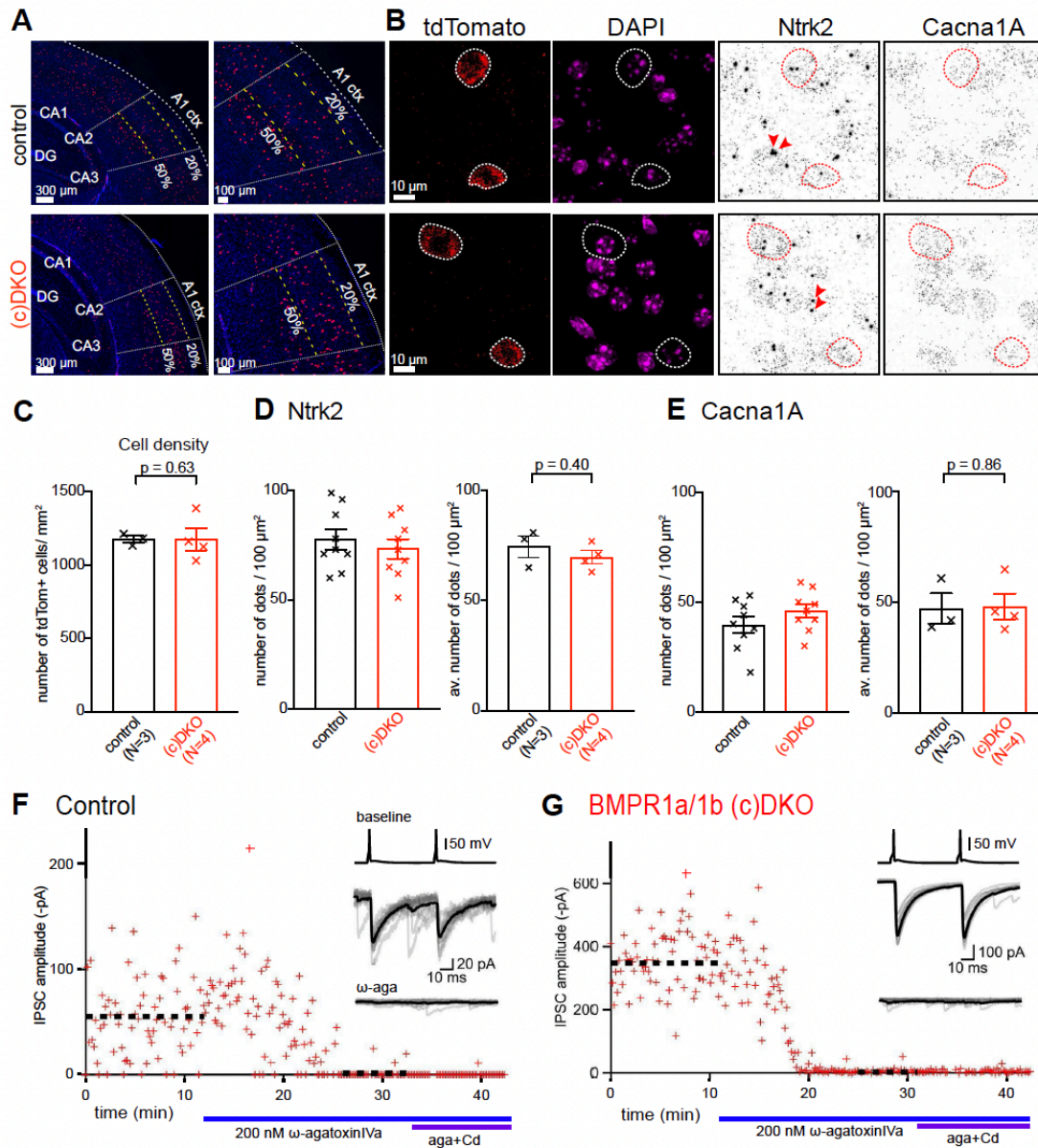
Figure 4. Expression levels of TrkB and P/Q-type Ca^{2+} channels are unchanged in PV-INs of BMPR1a/1b (c)DKO mice.

(A) FISH images of coronal brain sections at two magnifications (left, and right), for a control mouse at P25 (bregma, ~ -2.1 mm), and for a BMPR1a/1b (c)DKO mouse at P25 (bregma, ~ - 2.4 mm). The red and the blue channels show the FISH probe for tdTomato (indicating PV-INs) and DAPI, respectively. "A1 ctx", auditory cortex. (**B**) FISH images at higher magnification for a control mouse at P25 (top) and for a BMPR1a/1b (c)DKO mouse at P25 (bottom), showing, from left to right, the tdTomato probe channel with two PV-positive neurons each, the DAPI channel, the Ntrk2 channel, and the Cacna1A probe

channel. Red arrowheads show nascent transcripts of Ntrk2 in the nucleus which were excluded from the quantifications. (**C**) The density of PV-INs within 20 - 50% depth of auditory cortex was unchanged between N = 3 control mice (left, black data points), and N = 4 BMPR1a/1b (c)DKO mice (right, red data points). (**D**) Left, individual - and average data of the normalized number of Ntrk2 transcript dots for n = 9 PV-INs each from a control mouse (black data points), and from a BMPR1a/1b (c) DKO mouse (red data points). Right, averaged data from N = 3 control mice (left) and from N = 4 BMPR1a/1b (c)DKO mice (right). (**E**) Similar data as in (D), here for Cacna1A transcript levels, the gene which codes for the -subunit of the P/Q-type Ca^{2+} channel. (**F, G**) Example paired recordings in which the P/Q-type Ca^{2+} channel blocker -agatoxinIVa (200 nM) was applied, followed by the application of the same toxin plus 100 µM $CdCl_2$. Note that unitary IPSCs are almost completely blocked by -agatoxin-IVa in both genotypes. The inset shows traces of presynaptic APs (top, only for control conditions), and of postsynaptic IPSCs before - (middle) and after application of -agatoxinIVa (bottom). For statistical analysis and number of recordings, see Results.

3. Discussion and future directions

3.1 Conclusions

In my PhD thesis, I focused on understanding how neurons in the sensory circuits communicate to each other in response to neuronal activity in both developing and the adult brain. My work revealed new insights into the activity-induced molecular mechanisms of the excitation-inhibition balance and discovered new roles of the Bone Morphogenetic Proteins.

In a collaborative effort, we studied if BMP pathway could play role for the plasticity of the PV interneurons during the critical period of plasticity in the auditory cortex. Spike timing dependent plasticity (STDP) has been shown to be developmentally regulated in a sensory-experience dependent manner and in particular, inhibitory long-term depression (iLTD) has been proposed as key mechanism of disinhibition (Vickers, Clark et al. 2018). Output synapses of PV interneurons were shown as the major regulators of such disinhibitory plasticity mechanisms in L4, the input layer of thalamocortical connections. In our study, we showed that acquisition of those synapses and their plasticity mechanism are controlled by the BMP pathway.

In combination to the first evidence of BMP pathway being useful for plasticity mechanisms in the developing brain, I screened the expression patterns of the components of BMP pathway in the RNA-sequencing datasets generated from subtypes of cortical neurons, and found that BMP ligands are preferentially expressed in different neuronal subtypes. Strikingly, I found BMP2 being predominantly expressed in the glutamatergic neurons and being mobilized with elevated network activity. By generating genetically-encoded BMP reporters, I demonstrated that PV interneurons respond to the elevated BMP. By using an unbiased approach, we investigated the transcriptional targets of BMP2-SMAD1 in cortical neurons and found that BMP2 induce SMAD1 to bind to the promoters of their target genes which I mainly found as the components of the glutamatergic synapses. This made me to hypothesize that BMP2-SMAD1 signaling in the adult cortex would be regulating the glutamatergic drive onto PV interneurons. Due to the exceptionally high density of the synapses in the cortex, it was impossible to investigate the dendritic synapses onto PV interneurons with conventional methods. To overcome this issue, we made an effort to advance currently available synaptic protein binders to make them genetically encoded and suitable for in vivo and cell-type specific synapse marking. This effort made us generate a very reliable and easy to apply viral-based tools to visualize glutamatergic and GABAergic synapses in vivo. By applying these tools in combination with slice

electrophysiology, I showed that conditional loss of SMAD1 from PV interneurons results in reduced glutamatergic synaptic input on the PV interneuron dendrites and cause an imbalance in their synaptic excitation and inhibition as their overall inhibitory synaptic drive was unchanged. Moreover, I found that this reduction in the glutamatergic drive also has consequences on their cell-intrinsic and excitability features. Furthermore, these alterations resulted in increased susceptibility of SMAD1 mutant mice to display spontaneous epileptic seizures.

Taken together, this thesis uncovers essential roles for BMP pathway for activity-induced plasticity mechanisms of the PV interneurons and thereby makes major contributions to understanding how the cortical circuits keep the harmony while they are responding to the various forms of activity. Many very exciting questions arise from these findings and open the door for further questions, which I will discuss in the following chapters.

3.2 Deciphering the combinatorial code of BMP pathway in the neuronal circuits

Morphogen signaling pathways including BMP are essential during the development and regulate the transcriptional programs by generating gradients of morphogens to instruct specific cellular programs. Despite enormous amount of information on the components and interactions that comprise these signaling pathways, we still do not understand what specific signal processing capabilities each pathway provides, why different pathways use distinct molecular architectures, and how to predictively control the activity of these pathways in specific cell types.

My findings demonstrated that BMP pathway is used in the regulation of the neuronal circuits in the adulthood and strongly suggested that BMP2 is released from the glutamatergic neurons upon neuronal activity. It is quite an interesting finding as this has great potential for further insights into how neurons use the promiscuity of the BMP pathway to convey a particular signal to regulate complex behaviors. Therefore, it is necessary to investigate this question by trying to find out the source of BMP ligands and their cell-type specific transcriptional programs in parallel to each other. I will therefore elaborate some of the ways that could be used to address these questions.

3.2.1 Functions hidden in the structural complexity: Integration of multiple signaling mechanisms

When it comes to the signaling pathways, it is almost impossible to think that their function is independent of each other. For instance, if we take neuronal cFos induction during neuronal plasticity as an example, we know that its transcription can be triggered by several growth factors and calcium signaling, in part relying on the MAPK pathway. BMP-receptors regulate transcription through the phosphorylation of SMAD transcription factors. However, interestingly, SMADs are also phosphorylated downstream of MAPK, highlighting a potential convergence of neuronal activity-dependent signaling and the BMP pathway.

Receptor-regulated SMAD transcription factors (SMAD1 and SMAD5, R-SMADs) display unique features. They are composed of MH1 and MH2 (Mad-homology) domains where the MH1 domain mediates the DNA binding and interaction with other TFs while the MH2 domain interacts with other proteins such as chromatin remodelers or inhibitory SMADs. In addition to their C-terminal phosphorylation site which is the site of BMP-receptor-mediated activation, R-SMADs bear a linker site where several amino acids were identified to be phosphorylated via kinase pathways (Figure 3.1).
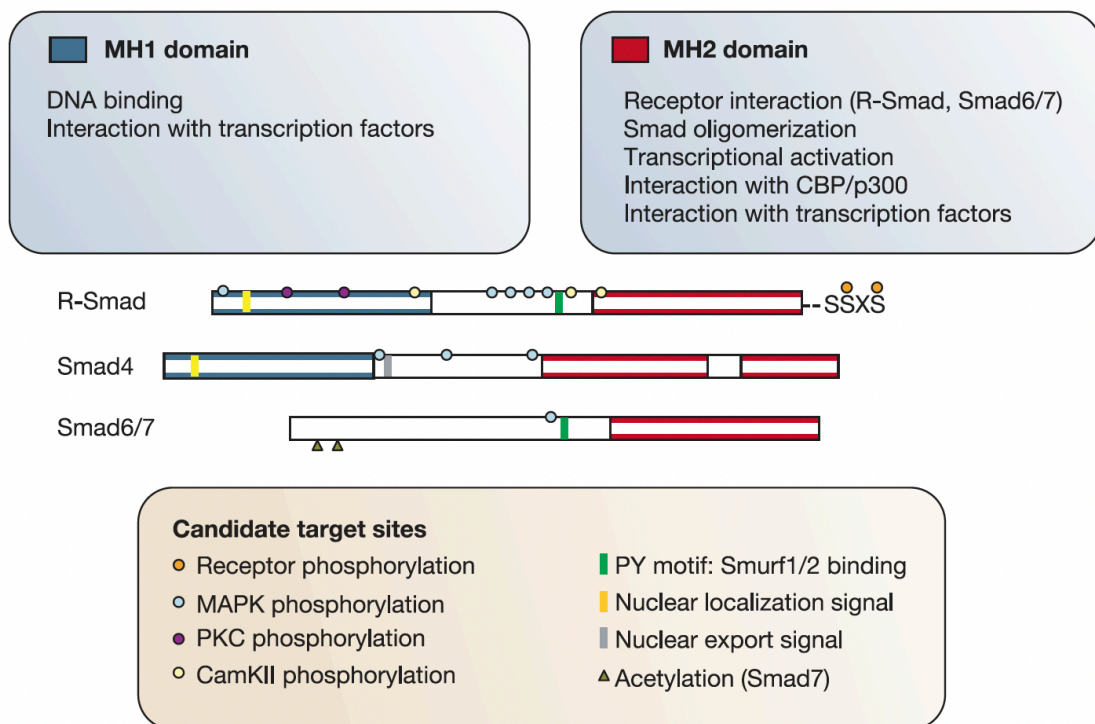
Figure 3.1: Structural organization and role of the domains of SMADs (R-SMAD: SMAD1/5 for BMP and SMAD2/3 for TGFβ, SMAD4: co-SMAD, SMAD6/7: inhibitory SMADs), and candidate target sites for kinase pathways. Such pathways include Erk

MAPK and cJun-N-terminal kinase (JNK), as well as CamK2 and Protein Kinase-C (PKC). The significance of candidate MAPK phosphorylation sites in Smad4 and Smad6/Smad7 is not known (Derynck and Zhang 2003).

The linker phosphorylation of R-SMADs caught a lot of attention as it holds potential for SMADs to integrate various types of signals. Towards understanding the mechanism and consequences of such regulation, Sapkota and colleagues demonstrated that linker phosphorylation of SMAD1 by MAPK enables binding of the ubiquitin-ligase Smurf1 and SMAD degradation (Sapkota, Alarcon et al. 2007). This study showed that MAPK restricts the nuclear activity of SMAD1 by either sending it for degradation or retaining it in the cytoplasm. While the function of linker phosphorylation was described in non-neuronal cells, it would provide an intriguing mechanism for neurons that the activation or strength of BMP signaling is tuned by neuronal activity at the level of SMAD proteins. In developing sensory neurons there is in fact evidence for SMAD1 dual phosphorylation by BMP and neurotrophic growth factor (NGF) signaling at the C-terminus and the linker, respectively (Finelli, Murphy et al. 2013). While C-terminal phosphorylation of SMAD1 induced the downstream ERK1/2 signaling of MAPK pathway through transcriptional regulation, ERK1/2 specific phosphatase and in turn restricted axon growth. It would be very interesting to test if calcium-dependent pathways or activity-induced neurotrophic factors such as BDNF could also induce linker phosphorylation of SMAD1 in mature neurons and what behavioral aspects are regulated through linker-phosphorylation-dependent downstream events of the BMP pathway.

In addition to their canonical role in the transcriptional regulation, SMADs were also shown to regulate some miRNAs either by binding to their promoter elements or interacting with miRNA processing proteins (Davis, Hilyard et al. 2008, Davis, Hilyard et al. 2010, Kang and Hata 2012). For instance, BMP4 stimulation of vascular smooth muscle cells was suggested to post-transcriptionally elevate mature miR-21 levels (Davis, Hilyard et al. 2008). Further investigations on how SMADs regulate post-transcriptional processing of miRNAs indicated that SMADs may interact with p68 in the Drosha complex to promote pre-miR cleave (Figure 3.2). Sequence analysis from twenty miRNAs regulated by BMP4 stimulation uncovered a conserved, RNA-SMAD binding element (R-SBE) 5′-CAGAC-3′. Interestingly, this sequence has been initially identified as the consensus sequence for binding of the receptor mediated SMADs on DNA (Massague, Seoane et al. 2005). Such regulatory mechanisms of SMADs on controlling miRNA levels could play crucial roles in neurons express an array of miRNAs with diverse expression patterns in neuronal sub-types (He, Liu et al. 2012).

Moreover, functions of some miRNAs were investigated in loss-of-function studies. Thus, miR-138 expression has been shown to be activity-induced in neurons and was suggested to play important roles in the synaptic plasticity of PV interneurons. Interestingly, miR-134 was found to be strongly upregulated in epilepsy patients and mouse models (Schratt, Tuebing et al. 2006, Morris, Reschke et al. 2019). In my studies I performed some experiments to investigate whether BMP2 stimulation would induce changes in the levels of mature miRNAs in cortical neurons and if these changes are directly regulated by SMAD1. I performed miRNA-sequencing from control and SMAD1 mutant cortical neurons with or without BMP2 stimulation. From this analysis, I confirmed that deletion of SMAD1 in cortical neurons lead to upregulation and downregulation of several miRNAs. Interestingly, I found miR-134 as the most significantly upregulated miRNA, presumably due to the hyperexcitable cortical network of $SMAD1^{KO}$ neurons. However, in my analysis, I did not identify any miRNAs significantly regulated by BMP2 stimulation. Our findings therefore suggest that in neurons SMAD1 is not essential for BMP-dependent regulation of miRNA maturation. If BMP4 or other BMPs are the main stimulus for miRNA regulation through SMADs in neurons remains to be addressed in future studies.
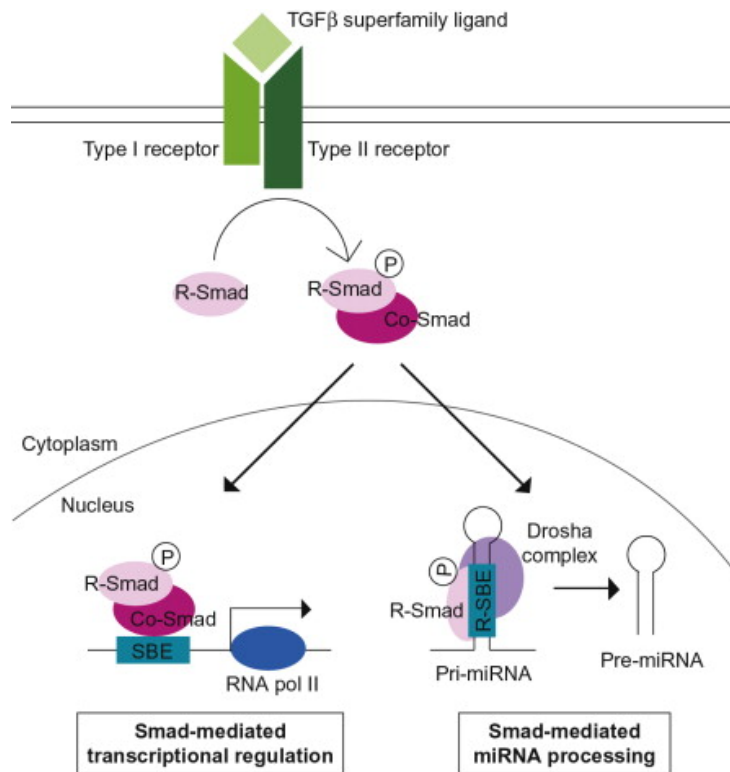
Figure 3.2: Regulation of miRNA by TGFβ/BMP signaling. Stimulation with TGFβ family of ligands such as BMP4 results in phosphorylation and translocation of Smads into the nucleus. Smads modulate gene transcription by binding to SBE. Alternatively, Smads directly associate with R-SBE of pri-miRNA and facilitate a cleavage by Drosha (Kang and Hata 2012).

3.2.1 Hunting the BMPs in the brain

Publicly available RNA-sequencing datasets from subtypes of cortical cells revealed that expression of BMP ligands is highly selective for different cell types (Mardinly, Spiegel et al. 2016, Hrvatin, Hochbaum et al. 2018, Furlanis, Traunmuller et al. 2019). In these datasets, we found BMP2, BMP4 and BMP7 as being expressed in neurons. BMP2 shows the highest expression and is mostly found in glutamatergic neurons, whereas BMP4 and BMP7 are predominantly expressed in PV interneurons and VIP interneurons, respectively.

BMP ligands can form homo- and heterodimers, while latter one has been shown to activate the pathway more potently than the former one (Dalessandro and Wang 1994, Hazama, Aono et al. 1995). During bone formation *in vivo*, BMP2/BMP7 and BMP2/BMP6 heterodimers were shown to be more potent than BMP2 homodimers (Israel, Nove et al. 1996). A similar finding has been observed for BMP7:GDF7 heterodimer function during the roof plate-mediated repulsion of commissural axons

in the spinal cord and guiding the establishment of their trajectory (Butler and Dodd 2003). It has also been proposed that heterodimers may have stronger signaling activity due to the assembly of receptor complexes formed by different type I and type II receptors, rather than dimers of the same ones(Little and Mullins 2009). Moreover, BMP2/4 sub-group has been shown to have higher affinity for type I receptors, whereas BMP5/6/7 has preference for type II receptors (Isaacs et al., 2010; Kirsch, Nickel, & Sebald, 2000).

An additional layer of regulation is the interaction of extracellular binding partners with BMP ligands. Noggin, one of the extracellular antagonists of BMP ligands, displays much higher inhibitory activity towards BMP homodimers as compared to the heterodimers *in vitro (Zhu, Kim et al. 2006).* Thus, it was proposed that only heterodimers that acquire sufficient receptor binding affinity in an environment of extracellular antagonists can elicit a signaling response. All together, these findings strongly argue for a combinatorial code that cells use to access and respond to the information that is provided by signaling molecules in their environment. Indeed, in a recent study Bauer and colleagues demonstrated that in developing *Drosophila* wing disc, *Dpp*(BMP2/4)/*Gbb*(BMP5/6/7/8) heterodimers are the active and crucial signal for obtaining optimal signaling and long-range BMP distribution (Bauer, Aguilar et al. 2023).

Given the reciprocal relationship of principal cells and PV interneurons in the upper layers for balancing excitation and inhibition, it is tempting to further investigate if PV interneurons differentially respond to BMP ligands and the interplay of BMP homo-, heteromers, and antagonists. One possibility to experimentally address this would be through combining multiple genetic and viral-based tools. Due to its pivotal role in the development, the study of the BMP2 function in the adult brain requires tools for acute loss of BMP2 from adult neuronal cells under precise spatiotemporal control. There has been a systematic effort to generate Cre mouse lines for genetic manipulation of neuronal subpopulations. One such transgenic line has been generated by insertion of a tamoxifen-dependent CreERT2 recombinase under control of the Cux2 promoter which allows to target layer 2/3 and L4 neurons in the mouse neocortex with temporal control (Harris, Hirokawa et al. 2014, Gil-Sanz, Espinosa et al. 2015). This tool enables conditional ablation of BMP2 selectively from upper layer pyramidal cells in the neocortex of adult mice. Combining this spatiotemporally controlled ablation of BMP2 with the BRE-reporter system I generated as a readout, it would be possible to directly test whether indeed pyramidal cell-derived BMP2 serves as trans-cellular

signal in response to elevated network activity. A second read-out for such experiments would be to quantitatively assess synapse formation onto PV cell dendrites. To this end, we recently developed and characterized a new version of FingR intrabodies that target the postsynaptic protein PSD-95 in PV interneurons. To develop this PVFingR-PSD95 (in short PVFingR), we made a constitutive version of FingR-PSD-95 by replacing the promoter with an enhancer sequence (E2) which was identified to be selective for PV interneurons and successfully drive expression of various types of reporters (Vormstein-Schneider, Lin et al. 2022). By knocking out BMP2 from principal cells and investigating the glutamatergic synaptic inputs on PV interneurons, we can further dissect out if BMP2 secretion from principal cells plays roles in the regulation of synaptic plasticity of PV interneurons.

The experiment described above would test whether PV interneurons respond to BMP2 that is secreted from principal cells. However, it is possible that BMP2 could also be secreted from other interneurons where BMP2 expression was detected as well. BMP2 can form heterodimers with BMP4 or BMP7, which may differentially induce signaling cascades. It has been our long interest to visualize endogenous BMP ligands in the brain at the protein level. To this end, we generated a knock-in mouse line where we inserted two HA tags at the N-terminus of the mature BMP2 polypeptide. This would allow for identification of neurons that express and secrete BMP2. However, thus far, we failed to obtain reliable signals in immunohistochemistry, presumably due to the very low BMP2 levels expressed in the somatosensory cortex. Due to the structural and functional incompatibility of BMP ligands for being tagged with bigger tags such as fluorescent proteins, we are still limited with small tags and use of nanobodies against these small tags. In a recent work on the BMP diffusion in the *Drosophila* wing disc (Matsuda, Schaefer et al. 2021), the Affolter group used a small, single chain variable fragment binder against HA tag or against BMP homolog *Dpp, respectively,* to block BMP dispersal by trapping it at the membrane (Figure 3.3). This method was dubbed "Morphotrap" where morphogens are prevented from binding to their receptors at the recipient cell and thereby inhibit the pathway *in vivo*. Several llama-derived nanobodies which bind specifically to BMP4, BMP2/BMP4 and BMP2/4/5/6 were reported. Some of these binders inhibit canonical BMP signaling *in vitro*. (Calpe, Wagner et al. 2015) . The small size of these nanobodies, around 15 kDa, makes them suitable for viral delivery for in vivo trapping of BMPs. Tethering HA antibodies or BMP nanobodies to the membrane or retain them in the endoplasmic reticulum of the neuronal subtypes together with BRE reporter would allow us to understand which BMPs are secreted from neurons that are responsible for the

functions of PV interneurons in the cortex. Finally, HA binders or BMP nanobodies could be employed to probe the cellular and sub-cellular sources of BMP ligands. For example, a pre-synaptically tagged binder could assess whether BMPs are exchanged via synapses.
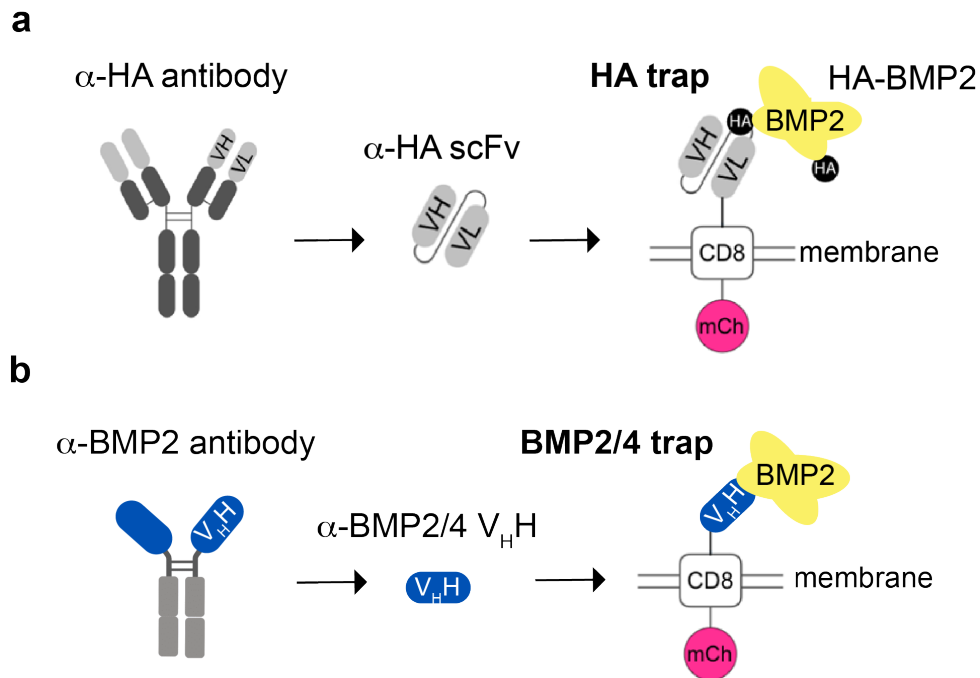
Figure 3.3: Different protein binder methods proposed to identify source of BMP2 ligands in the neocortex. a) A schematic view of HA trap (VH: antibody-derived variable heavy chain, V_HH: llama derived variable heavy domain of heavy chain, VL: variable light chain, mCh: mCherry) and b) BMP2 trap. Adapted from (Matsuda, Schaefer et al. 2021).

3.2.2 It is a SMAD world that is talking to the neurons

As it is tightly regulated upstream of transcription, an additional layer of restriction for the BMP signaling pathway arises at the level of the phosphorylation of effector proteins, pSMAD1/5/8 as they can selectively activate or silence particular sets of their targets. Activation of SMAD TFs through phosphorylation is facilitated by the activation of type 1 receptors, which is initially phosphorylated by type 2 receptors. Receptor mediated phosphorylation of SMADs occurs at the serine-X-serine motif where X is either Val or Met. Receptor-mediated SMADs, SMAD1,5 and 8, are thought to function as trimers but there are cases where they can also function as dimers (Chacko, Qin et al. 2001, Wu, Fairman et al. 2001, Inman and Hill 2002). Wired in such tight way that both the level and duration of receptor activation are correlated

with the level and persistence of activated SMAD complexes in the nucleus, which adds another layer to the combinatorial code (Schmierer et al. 2008).

It has been more than two decades that SMADs were discovered, and we learnt quite a lot about their mechanisms of action. Binding of active pSMAD1/5/8 to DNA can happen at both the promoters and enhancers of their target genes. Indeed, it is well known that cell-type specific events are mainly regulated through transcription factor interactions with enhancers rather than the promoters. SMAD TFs are weak interactors with DNA and therefore they co-operate with other site-specific factors which facilitates them to interact with both promoters and enhancers. They have been also shown to remodel the chromatin template by recruiting coactivator or corepressor chromatin modifiers (Derynck and Zhang 2003).

The main binding motif for pSMAD1/5/8 is GGCGCC which is present in promoters and the enhancers of the best-known SMAD1/5/8 targets, the ID genes (Korchynskyi and ten Dijke 2002; Blitz and Cho 2009; Nakahiro et al. 2010; Morikawa et al. 2011). In addition to recognizing this short DNA-binding motif, pSMADs interact with other TFs which likely is critical for target gene specificity. For instance, SMAD1 can interact with an enhancer-binding transcription factor C/EBP-E box element alpha (CEBPα) which has been shown to be mediated through BDNF/TrkB signaling in neurons (Calella, Nerlov et al. 2007). In our ChiP-sequencing dataset, we identified the GGCGCC motif as the top-hit. Interestingly, we found this motif only in the BMP2-responsive genes but not the constitutively SMAD1-bound genes. We found SMAD1/5 being recruited mainly around the promoters of the BMP2-responsive genes in contrast to the findings from non-neuronal cells. However, when we look closer to the binding sites, we could see that SMADs are not always necessarily at the TSS but sometimes a bit further. It is known that there are also enhancers proximal to the promoters which could explain why our analysis is more indicative for the promoters. To further understand how neurons use the BMP code, it would be interesting to identify protein binding partners of pSMADs in mature cortical neurons. Another possibility would be to perform foot-printing assay at the regulatory regions identified from ChiP-sequencing to be able to infer for the motifs of other TFs.

Interestingly, we observed that transcriptional targets of pSMADs have different temporal regulation than IEGs. IEGs are activated through calcium influx mainly from VGCCs and activation of calcium-dependent signaling pathways, whereas induction of pSMAD targets is regulated by the receptor activation. It is known that the BMP

receptors stay active at least 3-4 hours after ligand binding to maintain SMAD mediators in the nucleus where pSMADs are indeed continuously dephosphorylated and shuttled back to the cytoplasm (Inman, Nicolas et al. 2002, Xu, Kang et al. 2002). pSMADs also regulate the expression of their intracellular inhibitors which are SMAD6 and SMAD7, which we also found to be strongly upregulated in neurons. We found SMAD7 significantly expressed in cortical neurons and stayed strongly induced after 6 hours of BMP2 stimulation whereas SMAD6, which was also induced after one hour, remained less induced. Since our cortical cultures are composed of excitatory, inhibitory neurons and glia cells, it is possible that in neurons SMAD7 is the major inhibitor of the pathway while in glia it is SMAD6.

Combination of ChiP- and RNA-sequencing methods allowed us to decipher the sequence of events that occur from activated SMAD complexes appearing in the nucleus to the transcription of target genes being up- or down-regulated. We are now just beginning to get into the cell-type specific regulations of canonical BMP pathway. We identified array of genes that are identified as IEGs of neuronal activity. Amongst those, JUN is one of the best known IEG as a TF since JUN form heterodimers with FOS and function as AP1 complex in neurons. JUN/FOS dimers have been shown to be extensively bind at the cell-type specific enhancers in neurons and thereby regulate downstream targets (Yap and Greenberg 2018). It is possible that Jun is induced in PV interneurons as a response to BMP2 release and, therefore, could regulate PV interneuron-specific gene expression programs which are instructed by pSMADs.

We also identified SMAD TFs as regulators of genes which encode for the extracellular matrix components and glutamatergic synapses. Two direct targets of pSMADs in neurons were Brevican and Grin3a. Both of these proteins have cell-type specific expression patterns: Brevican (Bcan) is mainly expressed in PV interneurons and glia cells while Grin3a has been a distinguishing feature of somatostatin interneurons (SST interneurons) starting from the postnatal development (Pfeffer, Xue et al. 2013, Favuzzi, Marques-Smith et al. 2017, Favuzzi, Deogracias et al. 2019). Interestingly, both Bcan and Grin3a expression levels were shown to be regulated during critical period plasticity of sensory areas (Wong, Liu et al. 2002, Gundelfinger, Frischknecht et al. 2010).

BCAN is enriched at the perineuronal nets around PV interneurons and shown to regulate AMPA receptor compositions and thereby glutamatergic synapses and plasticity of PV interneurons. We found that SMAD1 regulates the expression levels

93

of perineuronal nets and which could be the result of downregulated mRNA levels of Bcan. Bcan transcript levels were indicated to be regulated by enriched environment or auditory fear conditioning where former induce positive memory formation while the latter one induces fear memories (Banerjee, Gutzeit et al. 2017, Favuzzi, Marques-Smith et al. 2017). Therefore, it would be interesting to test if the formation of new glutamatergic synapses onto PV interneurons during memory encoding are regulated by BMP signaling.

GRIN3A is a calcium impermeable - and thus atypical - subunit of NMDA receptors located at the extra-synaptic sites on neurons. During development, GRIN3A has been shown to regulate insertion of AMPA receptors and thereby regulate the maturation of sensory areas by eliminating synapses (Das, Sasaki et al. 1998, Roberts, Diez-Garcia et al. 2009). Even though GRIN3A is significantly downregulated in the adult brain, it is viewed as a brake for plasticity in the adult since Grin3a mutants were shown to exhibit increased performance in some learning tasks. GRIN3A has also been shown to differentially gate insertion of calcium permeable AMPA receptors after cocaine exposure and thereby redirect the brain toward addiction-related behavioral and motivational states. It is quite striking that SST interneurons have very selective GRIN3A expression levels which ramps up at postnatal day 10 in the mouse cortex and remains expressed in the adulthood. SST interneurons are very particular in the sense that they target the dendritic compartments of the principal cells and have been shown to regulate state-dependent behaviors or memory consolidation (Raven and Aton 2021). However, only limited molecular programs were identified for the plasticity of SST interneurons in such behaviors. As we found Grin3a mRNA levels being significantly upregulated after BMP2 stimulation, it would be interesting to test if BMP2-SMAD1 signaling would also be altered after cocaine exposure or during memory formation to reinstate plasticity mechanisms controlled by SST interneurons.

3.2.3 Future steps to decipher the code: Could SMADs serve as a reporter of activity in neuronal circuits?

A crucial but yet very challenging goal of neuroscientists is to understand how neuronal activity-driven transcription regulates cellular plasticity, circuit dynamics, and behavior. Several powerful methods have been developed to tag activated neurons. Such methods most commonly are based on activity-driven expression of immediate early genes (IEGs), reporters of calcium influx, and synaptic events such as transmitter release. IEG-based TRAP knock-in mice or the more recently developed viral-based activity marking tools (RAM) combine promoters and enhancers of several IEGs. Genetically encoded calcium indicators (GECIs) or light-activatable Calcium reporters (Cal-Light, FLARE, etc.) have been developed and one of the widely used methods which serves as a great instantaneous reporter of both evoked and spontaneous activity (Choi, Kim et al. 2020). To capture activated synapses, methods combining proximity-based synapse labeling techniques such as GFP Reconstitution Across Synaptic Partners, GRASP, and IEGs has been developed for accurate and static mapping of synapses in activated neuronal populations (Choi, Sim et al. 2018).

In the same line, it would be very interesting to test if the BRE reporter I generated could be used to label activated neuronal ensembles. For example, it would be very interesting to combine BRE reporters and calcium imaging or eGRASP methods to investigate if BMP2-SMAD1 signaling controls the feedforward inhibitory responses of principal cells to the sensory-evoked stimulation.

In addition to dissecting out the broader functions of BMP signaling through marking, BRE could serve as a perfect sorting marker to isolate nuclei of BMP-responsive neurons. Our initial screen for pSMAD target genes in neurons was performed from a mixed population of neurons and in a reductionist system. However, given that the BMP pathway has a significant potential to regulate cell-type specific transcriptional programs, it will be more informative to assess cell-type specific targets of SMADs by combining multiple single-cell approaches for chromatin, DNA and RNA analyses. As we found that pSMADs regulate glutamatergic drive onto PV interneurons in the adult somatosensory cortex, the next step could be to figure out what transcriptional programs are directed by SMADs specifically in PV interneurons. PV interneurons compose only about 5% of the total cells in this brain area and are a quite heterogenous populations in their cellular, electrophysiological and synaptic

properties (Huang and Paul 2019). Thus, investigating the transcriptional programs regulated by BMP signaling in these cells might reveal transcriptomic alterations in PV interneurons identified by the activated BRE reporter.

3.4 Leveraging BMP signaling for therapeutic interventions

In this study, we found crucial roles for BMP signaling in the stability of cortical circuits. Our PV specific SMAD1 knockout mouse model displayed severe epileptic seizure-like phenotypes and epileptiform brain activity. It is therefore very intriguing to further investigate potential ways to rescue these alterations.

Over-activation or under-activation of BMP pathway have been long implicated in variety of disease states such as diseases related to bone degeneration, defects in vascular system, traumatic brain injury and cancer (Kim and Choe 2011). Therefore, several potential therapeutic strategies have been tested to recover the improper BMP signaling in diseases. Developed strategies involve activating the pathway through extracellular agents such as overexpression of BMP ligands via gene transfer or overexpressing BMP receptors and stabilizing the nuclear pSMADs by inhibiting Smurf ubiquitin ligase. By contrast, for conditions that require inhibiting the BMP pathway led to the delivery of extracellular antagonists, RNA interference-mediated silencing of ligands and BMP receptors or inhibiting the receptor kinase activity through specific inhibitors (Lowery and Rosen 2018). Several FDA approved approaches like synthetic BMP2 or BMP7 peptides or drugs activating or potentiating the BMP pathway are successfully used for the treatment of defects caused by aberrant BMP functions (Lowery, Brookshire et al. 2016, Lowery and Rosen 2018).

In the case of neuronal circuit defects where under-activation of BMP signaling drives epileptiform brain activity, applications of such therapeutic agents become very challenging. First of all, delivering the drugs to activate the pathway or overexpression of recombinant BMP ligands ectopically in the human brain is not straightforward. Second, to specifically target PV interneurons it will be essential to develop BMP mimetics that preferentially activate BMP receptors on PV cells. To date, there is no direct evidence for mutations in components of the BMP pathway in epilepsy patients. However, recent surveys on the transcriptomic alterations and inflammatory signs in tissues obtained from human epilepsy patients demonstrated aberrant regulation of BMP pathway (Kumar, Lim et al. 2022). As SMADs are regulators of many genes, it is unrealistic to rescue the pathway by overexpressing many PV-specific targets of

pSMADs. In addition to this, as described in the previous section, the shuttling of SMADs between cytoplasm and nucleus is also under control of other signaling pathways. Therefore, methods leveraging PV interneuron-deficits which we found as a result of loss of BMP2-SMAD1 signaling would be necessary.

As concluding remarks, it is extremely fascinating how much specificity BMP pathway can acquire through restricting its responses at multiple levels to make it selective to the external world. This thesis provided one of the first examples of how the specificity of BMP pathway can be smartly utilized by neuronal circuits. Therefore, to provide targeted and effective therapeutic solutions for so many diseases where BMP pathway is altered, we have to understand what is its combinatorial code in different contexts.

4. Materials and methods

4.1 Materials and Methods – Okur et al., 2023

Mice

All procedures involving animals were approved by and performed in accordance with the guidelines of the Kantonales Veterinäramt Basel-Stadt. All experiments were performed in mice in C57Bl/6J background, except for some of the experiments performed in cultured wild-type neurons which used RjOrl:SWISS mice. Both males and females were used at similar numbers for the experiments.

Smad1^floxed mice (Huang, Tang et al. 2002), *Pvalb-cre* mice (Hippenmeyer, Vrieseling et al. 2005) and *Ai9* mice (Madisen, Zwingman et al. 2010) were obtained from Jackson Laboratories (Jax stock no: 008366, 017320, and 007909 respectively). Bmp2-2xHA mice were generated using a Crispr-Cas9 strategy (Richardson, Ray et al. 2016) inserting a double HA tag at the N-terminus of the mature BMP2 protein, between amino acids S292 and S293. Guide RNAs (gRNAs) employed were 5'-GTCTCTTGCAGCTGGACTTG-3' and 5'-CAAAGGGTGTCTCTTGCAGC-3', together with a 200 bp single-stranded DNA ultramer: 5'-GACTTTTGGACATGATGGAAAAGGACATCCGCTCCACAAACGAGAAAAGCGTCAAG CCAAACACAAACAGCGGAAGCGCCTCAAGTCCGCTAGC**TACCCATACGATGTTCCA GATTACGCT**GGCTATCCCTATGACGTCCCGGACTATGCAGCTAGCAGCTGCAAGAG ACACCCTTTGTATGTGGACTTCAGTGATGTGG-3' (sequencing encoding the HA tags highlighted in bold).

Recombinant DNA

The following plasmids were obtained from Addgene: pAAV-hSyn-DIO-hM4D(Gi)-mCherry (RRID:Addgene_44362, gift from Bryan Roth), p4XBRE-SBE-SV40-GL3 (RRID:Addgene_67811, gift from Ron Prywes), pGL4.10/RSV_SF3B3-miniXon_Luciferase (RRID:Addgene_174660, gift from Beverly L. Davidson), FingR-PSD-95-eGFP-CCR5TC and FingR-Gephyrin-eGFP-CCR5TC (RRID:Addgene_46295 and RRID:Addgene_46296, gift from Donald Arnold), Xph20-eGFP-CCR5TC (RRID:Addgene_135530, gift from Daniel Choquet), pAAV-CAG-mGreenLantern (RRID:Addgene_164469, gift from Gregory Petsko).

pAAV-4XBRE-SV40-DIO-X^on-GFP was generated by combining 4XBRE-SV40 promotor elements, the X^on mini-cassette, and eGFP sequences, flanked by loxP and lox2272 sites in a double floxed inverted orientation (DIO). In pAAV-hSyn-DIO-X^on-GFP the 4XBRE-SV40 sequence was replaced by the human Synapsin (hSyn) promoter.

For conditional viral expression of intrabodies in PV interneurons, FingR or Xph20 coding sequences were introduced into pAAV vectors in double-floxed inverted orientation under control of the hSyn promoter combined with the CCR5 zinc finger interaction site. For enhancement of the PSD-95 binders, eGFP was replaced by mGreenLantern coding sequence.

Viral supernatants were produced by co-transfection of HEK293T cells grown on 15cm dishes using calcium phosphate transfection of 70µg of AAV helper plasmid (Rep/Cap, Serotype 9), 200µg of AAV pHGTI-adeno1 (Plasmid factory) and 70µg of AAV vector plasmid carrying the cDNAs to be expressed. 45-60h after transfection, medium containing viral particles was harvested and purified using the Iodixanol purification method. Viral preparations were concentrated in Millipore Amicon 100K columns at 4°C. Virus samples were suspended in PBS, frozen in aliquots and stored at -80°C. Viral titers were determined by qPCR and were $>10^{13}$ particles/mL.

<u>Surgery</u>
Injections of recombinant AAVs were performed into the barrel cortex of 42-49 days old male and female mice performed under isoflurane anesthesia (Baxter AG, Vienna, Austria). Mice were placed in a stereotactic frame (Kopf, Germany) and a small incision (0.5 – 1 cm) was made over the barrel cortex at the following coordinates targeting two sites: ML ±3.0 mm and ±3.4 mm, at AP 0.6 mm and AP -1.6 mm, DV –1.5 mm from Bregma to target layer 2/3 and layer 4). For injections of FingR intrabodies, two injection sites restricted to layer 2/3 were used: ML ±3.0 mm and ±3.4 mm at AP –1.0 mm, DV –0.96 mm from Bregma. Recombinant AAVs (titer: 10^{12}-10^{13}) were injected via a glass capillary with outer diameter of 1 mm and inner diameter of 0.25 mm (Hilgenberg) for a total volume of 100 nL per injection site. The wound was closed with sutures (Braun, # C0766194) and mice were analyzed 10-25 days after surgery.

Implantations of Electroencephalograph (EEG) electrodes were performed in mice at age 12-16 weeks. EEG signals were recorded using two stainless steel screws inserted ipsilaterally into the skull. One was inserted 1.2 mm from the midline and 1.5 mm anterior to bregma, and the other was inserted 1.7 mm from midline and 2.25 mm posterior from to bregma. Seven days post surgery, mice were transferred to individual behavior cages with a 12:12 h light/dark cycle and a constant temperature of about 23°C. Animals had access *ad libitum* to food and water and were allowed to recover from surgery for 7 days.

<u>Primary neuron culture</u>
Cortical cultures were prepared from E16.5 mouse embryos or newborn (P0) mice. Neocortices were digested by addition of papain (145 units in 7 ml, Worthington Biochemical #LK003176) for 30 min at 37°C and then mechanically dissociated. Cells were maintained in neurobasal medium (Gibco #21103) containing 2% B27 supplement (Gibco #17504-044), 2mM Glutamax (Gibco #35050-038), and 1% penicillin/streptomycin (Gibco, #15140122) at 37°C / 5% CO_2. For neuronal network activity stimulation experiments, cortical cultures were treated for 6 hours at day *in vitro* 14 (DIV14) with 25 mM KCl or with 20 µM bicuculline (Tocris #0130), a GABA A receptor antagonist that blocks inhibitory synaptic transmission and, thus, results in a robust elevation of neuronal network activity. For ChiP-seq and RNA-seq experiments, DIV14 cultures were stimulated with 20 ng/ml human recombinant BMP2 (in 0.1 % BSA in 4 mM HCl, R&D systems, #355-BM-050) or vehicle for 1 or 6 hours. For neuron-specific *Smad1* loss of function experiments, cortical cultures from P0 *Smad1*$^{fl/fl}$ mice were infected at DIV9 with AAV9-hSyn-iCre virus at a multiplicity of infection of 20,000 or with a AAV9-hSyn-eGFP virus as negative control.

<u>ChiP-seq library preparation and sequencing:</u>
For ChiP-seq analysis, 24×10^6 cultured primary neurons (DIV14) were cross-linked with 1% formaldehyde for 10 min at room temperature. Crosslinking was stopped by the addition of glycine solution (Cell Signaling Technology, #7005) for 5 min at room temperature. Cells were scraped, pelleted, and lysed for 10 min on ice in 100 mM HEPES-NaOH pH 7.5, 280 mM NaCl, 2 mM EDTA, 2 mM EGTA, 0.5% Triton X-100, 1% NP-40, 20% glycerol. Nuclei were pelleted by centrifugation, washed in 10 mM Tris-HCl pH 8.0, 200 mM NaCl, and suspended in 10 mM Tris-HCl pH 8.0, 100 mM NaCl, 1 mM EDTA, 0.5 mM EGTA, 0.1% Na-Deoxycholate, 0.5% N-Lauroylsarcosine. Chromatin was sheared using a Covaris Sonicator for 20 minutes in sonication buffer (in mM:) to obtain fragments in the range of 200-500 bp. After sonication, sheared chromatin was centrifuged at 16,000 g for 20 minutes at 4 °C and dissolved in 1x ChIP buffer from SimpleChIP Plus Sonication Kit (Cell Signaling Technology, #57976). 2% input was taken and chromatin was incubated with following antibodies overnight at 4C: Smad1/Smad5 (Cell Signaling #9743 and

#12534, 2 µg for 20 µg chromatin), H3K27ac (Abcam 4729, 0.2 µg for 8 µg chromatin). Incubation with Protein G magnetic beads, decrosslinking and elution were performed as described in the SimpleChIP Plus Sonication Kit.

ChIPs were performed for 3 replicates with a given antibody from independent neuronal cultures. Libraries were generated using the KAPA Hyper Prep (Roche, KK8504) according to the manufacturer's instructions and PCR amplified. Library quality was assessed using the High Sensitivity NGS Fragment Analysis Kit (Advanced Analytical, #DNF-474) on the Fragment Analyzer (Advanced Analytical, Ames, IA, USA). Libraries were sequenced Paired-End 41 bases on NextSeq 500 (Illumina) using using 2 NextSeq 500 High Output Kit 75-cycles (Illumina, Cat# FC-404-1005) loaded at 2.5pM and including 1% PhiX. Primary data analysis was performed with the Illumina RTA version 2.4.11 and Basecalling Version bcl2fastq-2.20.0.422. Two Nextseq runs were performed to compile enough reads (on average per sample in total: 50±2 millions pass-filter reads).

RNA isolation and reverse transcription
21 days after stereotactic injections of AAV9-hSyn-DIO-hM4Di-mcherry or AAV9-hSyn-mCherry viruses in the layer 4 of barrel cortex, mice were treated with 5 mg/kg CNO or saline solutions. 5 hours post-treatment, mice were were anesthetized with isoflurane (Baxter AG, Vienna, Austria) and brain was taken out into ice-cold PBS solution. Injected area was then dissected under Binocular Stereo Microscope (Olympus #MVX10) by using red fluorescence signal from mCherry expression. Dissected tissue was harvested in Trizol reagent (Sigma, T9424). Total RNAs were isolated and DNase treated on columns (RNeasy Micro kit, Qiagen, 74004) following the manufacturer's instructions. The cDNA libraries were built using between 100 and 200ng RNA reverse transcribed with ImPromII Reverse Transcriptase (Promega, #M314A), RNasin™ Plus RNase Inhibitor (Promega, #N261B), ImPromII 5X Reaction Buffer (Promega, #M289A), dNTPs (Sigma, D7295) and oligo(dT)$_{15}$ primer (Promega, C1101). Primary cortical cultures were washed 1x with PBS and lysed using Trizol reagent (Sigma, T9424) and followed by total RNA isolation and cDNA library preparation as described above.

Real-time quantitative PCRs were performed either with FastStart Universal SYBR GreenMaster (Roche, 04-913-850-001) or FastStart Universal Probe Master (Roche, 04-913-195-7001). PCRs were carried out in a StepOnePlus qPCR system (Applied Biosystems) and were analyzed with the StepOne software. Gene expression assays were used either with FastStart Universal SYBR GreenMaster (Roche, 04-913-850-001) or TaqMan Master Mix (Applied Biosystems) and comparative C_T method. The mRNA levels were normalized to housekeeping β-actin mRNA or to Gapdh mRNA. For each assay, two to three technical replicates were performed and the mean was calculated.

Commercially available gene expression assays for Fos (Mm00487425_m1), Bdnf (Mm04230607_s1), *Id1 (Mm00775963_g1),* *Id3* (Mm01188138_g1)*,* *Smad6* (Mm00484738_m1)*,* *Smad7* (Mm00484742_m1)*,* *ActB (Mm00607939_s1)* (Mm.PT.58.13518911), *Bmp2* (Mm01340178_m1), *Bmp4* (Mm00432087_m1), *Bmp6* (Mm01332882_m1), *Bmp7* (Mm00432102_m1), *Gapdh* (Mm99999915_g1) were from ThermoFisher. Primers used for SyberGreen were custom designed and obtained from IDT DNA Technologies. Primer sequences are listed below.

Primer Name	Sequence
Brevican-Exon11-Fwd	5'-CAT CGA GGG TGA CTT CTT GT-3'
Brevican-Exon12-Rev	5'-ACC ATG ACC ACA CAG TTC TC-3'

Id3-Exon1-Fwd	5'-GCA GCG TGT CAT AGA CTA CAT C-3'
Id3-Exon2-Rev	5'-GTC CTT GGA GAT CAC AAG TTC C-3'
Grin3a-Exon7-Fwd	5'-CTG CTG CTA CCA CGA ATC AA-3'
Grin3a-Exon8-Rev	5'-TCT TGG AAC ATG GCT GCT T-3'
ActB-Exon5-Fwd	5'-AGA TTA CTG CTC TGG CTC CTA-3'
ActB-Exon6-Rev	5'-CTG CTT GCT GAT CCA CAT CT-3'

RNA library preparation and sequencing

Libraries of Bmp2-stimulated naïve cortical cultures (three biological replicates) were prepared from 200 ng total RNA by using the TruSeq Stranded mRNA Library Kit (Cat# 20020595, Illumina, San Diego, CA, USA) and the TruSeq RNA UD Indexes (Cat# 20022371, Illumina, San Diego, CA, USA). 15 cycles of PCR were performed.

Quality check was performed by using the Standard Sensitivity NGS Fragment Analysis Kit (Cat# DNF-473, Advanced Analytical) on the Fragment Analyzer (Advanced Analytical, Ames, IA, USA) and quantified (average concentration was 213±15 nmol/L and average library size was 357±8 base pairs) in order to prepare a pool of libraries with equal molarity. The pool was quantified by Fluorometry using using the QuantiFluor ONE dsDNA System (Cat# E4871, Promega, Madison, WI, USA) on Quantus instrument (Promega). Libraries were sequenced Single-reads 76 bases (in addition: 8 bases for index 1 and 8 bases for index 2) on NextSeq 500 (Illumina) using the NextSeq 500 High Output Kit 75-cycles (Illumina, Cat# FC-404-1005). Flow lanes were loaded at 1.4pM of pool and including 1% PhiX. Primary data analysis was performed with the Illumina RTA version 2.4.11 and Basecalling Version bcl2fastq-2.20.0.422. The Nextseq runs were performed to compile on average per sample: 56±3 millions pass-filter reads (illumina PF reads).

For the libraries from control and Smad1 mutant primary cortical cultures (four biological replicates), 100 ng total RNA was used and library preparation and quality check were performed as described above. Quantification yielded average concentration as 213±15 nmol/L and average library size as 357±8 base pairs. Libraries were sequenced Paired-End 51 bases (in addition: 8 bases for index 1 and 8 bases for index 2) setup using the NovaSeq 6000 instrument (Illumina). SP Flow-Cell was loaded at a final concentration in Flow-Lane loaded of 400pM and including 1% PhiX. Primary data analysis was performed as described above and 43±5 millions per sample (on average) pass-filter reads were collected on 1 SP Flow-Cell.

ChIP- and RNA-seq data analysis

ChiP-seq reads were aligned to the December 2011 (mm10) mouse genome assembly from UCSC (Rosenbloom, Armstrong et al. 2015). Alignments were performed in R using the qAlign function from the QuasR package1 (v. 1.14.0) with default settings(Gaidatzis, Lerch et al. 2015). This calls the Bowtie aligner with the parameters " -m 1 –best –strata", which reports only reads that map to a unique position in the genome2. The reference genome package ("BSgenome.Mmusculus.UCSC.mm10") was downloaded from Bioconductor (https://www.bioconductor.org). BigWig files were created using qExportWig from the QuasR package with the bin size set to 50. Peaks were called for each ChIP replicate against a matched input using the MACS2 callpeak function with the default options. Peaks were then annotated to the closest gene and to a genomic feature (promoter, 3' UTR, exon, intron, 5' UTR or distal intergenic) using the ChIPseeker R package. The promoter region was defined as -3 kb to + 3kb around the annotated TSS. Transcripts were extracted from the TxDb.Mmusculus.UCSC.mm10.ensGene annotation

R package. All analyses in R were run in RStudio v. 1.1.447 running R v. 3.5.1. Enrichment of Bmp2-induced peaks over constitutive peaks was analyzed by using default settings in voom/limma analysis software packages. Motif enrichment analysis for Bmp2-induced peaks and constitutive peaks was performed separately by screening for the enrichment of known motifs with default settings of HOMER (Heinz, Benner et al. 2010). Output motif results with the lowest p-value and highest enrichment in targets compared to the background sequences were displayed for each peak set.

RNA-seq reads were aligned to mm10 using STAR and visualized in IGV genome browser to determine strand protocol. By using QuasR's qQCReport, read quality scores, GC content, sequence length, adapter content, library complexity and mapping rate were checked and QC report was generated. Reads with quality scores less than 30, and mapping rates below 65 and having contaminations from noncoding RNAs were not considered for further analysis. If passed QC, QuasR's qCount function was used to count reads mapping to annotated exons (from Ensembl genome annotations). Each read was counted once based on its start (if reads are on the plus strand) or end (if reads are on the minus strand) position. For each gene, counts were summed for all annotated exons, without double-counting exons present in multiple transcript isoforms ("exon-union model"). Correlations between replicates and batch structure were checked by plotting correlation heatmap, PCA plot of samples, scatter plots of normalized read counts. EdgeR package from R was used to build a model and test for differentially expressed (DE) genes. For DE analysis, counts were normalized using TMM method (built-in to edgeR). Any genes with less than in total 30 reads from all samples were dropped from further analysis. Differential expression (DE) analyses were conducted with the voom/limma analysis software packages by using total number of mapped reads as a scaling factor. Results were extracted from edgeR as tables and used for generating volcano or box plots in ggplot2 in RStudio.

To generate IGV genome browser tracks for ChIP- and RNA-seq data, all aligned bam files for each replicate of a given experiment were pooled and converted to BED format with bedtools bamtobed and filtered to be coverted into coverageBED format using the bedtools. Finally, bedGraphToBigWig (UCSC-tools) was used to generate the bigWIG files displayed on IGV browser tracks in the manuscript.

Gene ontology analysis was performed by using Statistical overrepresentation test and cellular component function PANTHER (http://pantherdb.org/). All genes being detected as expressed in RNA-sequencing data was used as reference. GO terms with at least 10 genes, at least 1.5-fold enrichment with less than 0.05 false discovery rate (FDR) were considered as significantly enriched. Significant GO terms were plotted in Prism 9.

<u>Western blot</u>

Primary cortical cells were lysed in 50 mM Tris HCl pH 7.5, 150 mM NaCl, 10% Glycerol, protease inhibitor Roche Complete™ mini, 1% Triton X-100). Lysate was centrifuged for 10 minutes at 16'000 g at 4°C and solubilized proteins were analyzed by polyacrylamide gel electrophoresis on 4%-20% gradient gels (BioRad, 4561093) followed by transfered onto nitrocellulose membrane. The following antibodies were used: rabbit-anti-SMAD1 (Cell Signaling, #9743), rabbit-anti-SMAD5 (Cell Signaling, #12534), rabbit-anti-phospho-SMAD1/5/9 (Cell Signaling, #13820), mouse-anti-BMPR2 (BD Pharmingen, #612292), rabbit-anti-Calnexin (stressGen, SPA-865), rabbit-anti-HA (Cell Signaling, 3724) and rat-anti-GAPDH (Biolegend, 607902). Secondary antibodies coupled to horse radish peroxidase (HRP) were from Jackson ImmunoResearch (goat anti-rabbit #111-035-003; goat anti-rat #112-035-143 and goat-anti-mouse #115-035-149). For enhanced

chemiluminescence detection, WesternBright ECL kit (Advansta #K 12045-D20) and WesternBright Quantum (Advansta #K-12042-D20) were used. Signals were acquired using an image analyzer (Bio-Rad, ChemiDoc MP Imaging System and Li-Cor, Odyssey).

Fluorescent *in situ* hybridization

Multiplex fluorescent *in situ* hybridization (FiSH) was performed using the RNAScope Fluorescent Multiplex Kit (Advanced Cell Diagnostics) for both primary cortical cultures and tissue sections. P25 wild-type mouse brains (C57BL/6J background) were snap frozen in liquid nitrogen and 18 µm coronal sections were cut between Bregma -1.43 and -2.15 (including barrel cortex and dorsal hippocampus) on a cryostat. Sections were fixed at 4°C overnight with 4% paraformaldehyde in 100mM phosphate buffered saline, pH 7.4. The procedure followed the manufacturers' instructions. For *in vitro* FISH experiments, cortical cultures were plated on glass coverslips. At DIV12 were treated with 25 mM KCl or 25 mM NaCl (as negative control) for 6 hours and fixed with 4% PFA for 15 minutes. The procedure was then followed as manufacturers' instructions. Following probes were used: *Bmp2* (406661), *Camk2* (411851) and *Pvalb* (421931). Images were acquired with an upright LSM700 confocal microscope (Zeiss) using 40X or 63x Apochromat objectives. Cell types were identified based on the presence of the corresponding marker transcript. A region of interest (ROI) was drawn to define the area of the cell and dots in the ROI were manually counted. The number of dots in the ROI were then normalized to the cell area.

Immunocytochemistry and image analysis

For immunocytochemistry, mouse primary neocortical neurons were treated for 45 minutes with recombinant human BMP2 (R&D Systems, 355-BM-010) or recombinant mouse Noggin (R&D Systems, 1967-NG-025) or vehicle and then fixed with 4% PFA in 1X PBS for 15min. Cells were then permeabilized with ice-cold methanol for 10min at -20 °C and blocked (5% donkey serum, 0.3% Triton X-100 in PBS) for 1hr at room temperature. Primary antibody incubation was performed overnight at 4°C in a humidified chamber. Secondary antibody incubation was then performed for 1hr at room temperature. The following antibodies were used: anti-phosphoSMAD1/5/9 (Cell signaling, 13820), anti-MAP2 (Synaptic systems, 188011), anti CamKII alpha (ThermoFisher, MA1-048), anti-GAD67 (Millipore, MAB5406), Alexa 488 conjugated-donkey anti rabbit (ThermoFisher, R37118) and Cy3-conjugated donkey anti-mouse (Jackson, 715-165-151) and Cy3-conjugated donkey anti-rabbit (Jackson, 711-165-152). Imaging was performed on a widefield microscope (FEI MORE) with a 40X objective (NA 0.95, air). Image analysis was performed on Fiji (Schindelin, Arganda-Carreras et al. 2012). Briefly, neuronal somata were identified and DAPI signal was used to determine the margin of the nucleus. The mean of nuclear phospho-SMAD1/5/9 signal intensity for each neuronal cell body was then measured and background signal was subtracted.

Immunohistochemistry and image analysis

Mice at postnatal day 56 - 72 were deeply anesthetized with ketamine/xylazine (100/10 mg/kg i.p.) and transcardially perfused with fixative (4% paraformaldehyde in 0.1 M phosphate buffer, pH 7.4). After perfusion, brains were post-fixed overnight in fixative at 4°C, washed 3 times with 100 mM phosphate buffer (PB). Coronal brain slices were cut at 40 µm with a Vibratome ((VT1000S, Leica). The following reagents were used: goat anti-Parvalbumin antibody (Swant, PVG213), biotinylated WFA (B-1355-2, Vector laboratories), Cy5-conjugated donkey anti goat (Jackson, 705-175-147) and Cy2-conjugated Streptavidin (Jackson, 016-220-084). Brain sections were incubated for 30 minutes in blocking solution containing 0.3% Triton X-100 and 3% Bovine Serum Albumin

(BSA) in PBS. Sections were incubated with primary antibodies in blocking solution overnight at 4°C, washed three times (10 minutes each) with 0.05% Triton X-100 in PBS, followed by incubation for 1.5 hours at room temperature with secondary antibodies in blocking solution. Sections were washed three times with PBS, and DAPI dye was co-applied during the wash at final concentration of 1.0 µg/ml. Sections were mounted using Microscope cover glasses 24x60mm (Marienfeld Superior™ 0101242) on Menzel-Gläser microscope slides SUPERFROST® PLUS (Thermo Scientific, J1800AMNZ) with ProLongTM Diamond Antifade Mountant (InvitrogenTM, P36970). Images were acquired at room temperature on an inverted LSM700 confocal microscope (Zeiss) using 20x and 40X Apochromat objectives (numerical aperture 0.45 and 1.30, respectively). For density quantifications of PV interneurons, tilescan images from Barrel Cortex were taken by using nuclear signal in the 405 nm channel, tdTomato expressing somatic signal in the 555 nm channel and parvalbumin immunostaining signal in 639 nm channel. For the intensity quantifications, images were acquired with the same channels above but in addition with immunostaining signal for WFA in the 488 nm channel. Mean intensity analyses for parvalbumin and WFA stainings were performed in ImageJ with a custom-made script in Python. Briefly, H-Watershed was applied to segment PV interneurons based on tdTomato signal on the soma. After applying thresholding, parvalbumin and WFA mean intensity values were automatically calculated and displayed as arbitrary units. Statistical analysis was done with Prism 9 (GraphPad software) using unpaired t-test. Data presented are mean ± SEM. Images were assembled using ImageJ and Adobe Illustrator softwares.

Mice injected with AAV-encoded BRE reporters were kept for 21 days after injections. 1 hour prior to CNO delivery, 25 mg/kg LMI070 (MedChemExpress, HY-19620, suspended in 20% cyclodextrin and 10% DMSO to 5 mg/ml concentration) was administrated by oral gavage. Mice were then injected intraperitonially with 5 mg/kg Clozapine N-oxide (CNO, Sigma Aldrich, C0832) or saline (0.9% NaCl). 5 hours post treatments, mice went through transcardial perfusion and sectioned as described above. Sections containing the injection site were stained with DAPI dye and mounted. Images were acquired with an inverted LSM700 confocal microscope (Zeiss) using 40X Apochromat objectives. Images were assembled and quantified with ImageJ. Region of interest was drawn around the nuclei by using DAPI signal from mCherry-positive cells and mean intensity was measured for nuclear GFP signal. Thresholding was applied for each cell by subtracting the mean intensity of the nuclear signal averaged from two to three mCherry-negative cells in each image.

Mice at postnatal day 56 to 72 were deeply anesthetized as described above and transcardially perfused with fixative (4% paraformaldehyde + 15% picric acid in 0.1 M phosphate buffer, pH 7.4). After perfusion, brains were post-fixed overnight in fixative at 4°C, washed 3 times with 100 mM phosphate buffer (PB) and kept overnight in 30% sucrose in 100mM PB at 4°C before cryo-protection in OCT. Coronal brain slices were cut at 30 µm with a Cryostat (Microm HM560, Thermo Scientific). For immunohistochemistry, brain sections were incubated for 30 minutes in blocking solution containing 0.1% Triton X-100 and 10% normal donkey serum in PBS. Sections were incubated with primary antibodies in blocking solution at 4°C for 48 hours, washed three times with 0.05% Triton X-100 in PBS, all washes being 10 minutes each, followed by incubation for 1.5 hours at room temperature with secondary antibodies in PBS containing 0.05% Triton X-100. Sections were washed three times with PBS, and DAPI dye was co-applied during the wash at final concentration of 1.0 µg/ml. Sections were mounted using Microscope cover glasses 24x60mm (Marienfeld Superior™ 0101242) on Menzel-Gläser microscope slides SUPERFROST® PLUS (Thermo Scientific, J1800AMNZ) with ProLongTM Diamond Antifade Mountant (InvitrogenTM, P36970). The following antibodies were used in this

study: Monoclonal mouse-anti-Synaptotagmin 2 (Zebrafish International Resource Center, # ZNP-1) and rabbit-anti-vGlut1 polyclonal purified antibody (Synaptic Systems, #135303). Fluorophore-conjugated secondary antibodies were from Jackson ImmunoResearch (Cy5 donkey-anti-rabbit, #711-175-152, Cy5 donkey-anti-mouse, #715-175-511, Cy3 donkey-anti-guineapig, #706-165-148). DAPI dye was used for nuclear staining (TOCRIS bio techne®, 5748). Images were acquired with LSM700 point scanning confocal microscopy with the PlanApo 63x/1.4 oil immersion objective. All acquired images present nuclear signal in the 405 nm channel, tdTomato expressing somatic signal in the 555 nm channel, presynaptic marker (SYT2 / vGlut1) in the 639 nm channel and postsynaptic FingR GPHN / PSD-95 / Xph20 in the 488 nm channel. Images were then post-processed by conservative deconvolution with the Huygens Deconvolution software with the classic maximum likelihood estimation deconvolution algorithm. Quantitative analysis of synaptic markers was performed using Imaris 9.8 by application of spots and surface detection tool. Data collection and image analysis was done blinded to the genotype of the animal.

Electrophysiology

Cortical slice preparation from adult mice (P56-72) was adapted from previously described protocols (Jiang, Shen et al. 2015). Briefly, animals were anesthetized with isoflurane (Baxter AG, Vienna, Austria). Parasaggital slices of 300 µm were cut with a vibratome (VT1200S, Leica) in ice-cold oxygenated (95% O_2/5% CO_2) NMDG solution (93 mM NMDG, 93 mM HCl, 2.5 mM KCl, 1.2 mM NaH_2PO_4, 30 mM $NaHCO_3$, 20 mM HEPES, 25 mM glucose, 5 mM sodium ascorbate, 2 mM Thiourea, 3 mM sodium pyruvate, 12 mM N-acetyl L-cysteine, 10mM $MgSO_4$ and 0.5 mM $CaCl_2$, pH 7.35). Slices were kept at 33.0 ± 1 °C in oxygenated NMDG solution for 12 minutes and then transferred to artificial cerebrospinal fluid (aCSF; 125 mM NaCl, 2.5 mM KCl, 1.25 mM NaH_2PO_4, 24 mM $NaHCO_3$, Na-Ascorbate (5 mM), 12.5 mM glucose, 1 mM $MgCl_2$ and 2 mM $CaCl_2$, pH 7.4) and kept at room temperature for at least 1 h before starting the recordings. During the recording sessions the slices were held in a custom chamber heated to 33.0 ± 1 °C with oxygenated aCSF perfusion.

Whole-cell patch-clamp recordings from layer2/3 PV interneurons of the barrel cortex were performed in voltage or current clamp mode using a Multiclamp 700B amplifier (Molecular Devices, Sunnyvale, CA) and under visualization in an upright microscope (Olympus) equipped with gradient contrast infrared visualization (Luigs and Neumann) using a 60× objective. For all experiments, data was digitized by Digidata 1440a (Molecular Devices) at 10 kHz and filtered at 1 kHz. For mEPSC and mIPSC recordings, patch pipettes (3–6 MΩ) were pulled with Sutter P-1000 micropipette puller (Sutter Instruments) and were filled with the following intracellular solution: 130 mM $CsMeSO_3$, 8 mM NaCl, 4 mM Mg-ATP, 0.3 mM Na-GTP, 0.5 mM EGTA, 10 mM HEPES, 5 mM QX314. For excitability measurements, intracellular solution composition is 142 mM K-gluconate, 10 mM HEPES, 1 mM EGTA, 2.5 mM $MgCl_2$, 4 mM Mg-ATP, 0.3 mM Na-GTP, 10 mM Na-phosphocreatine. mEPSCs and mIPSCs were recorded in the presence of 1 µM tetrodotoxin (TTX). To isolate both mEPSCs and mIPSCs from the same cell, mEPSCs were recorded at -70 mV holding potential and mIPSCs at 0 mV holding potential. Cells with >20% change in the series resistance were excluded from the analysis. mEPSCs and mIPSCs were analyzed using a template-matching algorithm implemented in Clampfit 10 (Molecular Devices). Automatically detected events were visually controlled and false positive events were deleted. Amplitude and frequencies were then manually analyzed. Input resistance, membrane time constant and capacitance were calculated also calculated in Clampfit 10. Action potentials of PV interneurons were automatically detected with Neuromatic (Rothman and Silver 2018) and analyzed using a custom-made script written for this project in Igor Pro 8 software (WaveMetrics).

Cortical slice preparations and excitability measurements from layer 2/3 PV interneurons of P26-P30 mice were performed as described above with the following modifications: Slices were cut in sucrose-based solution: 75 mM sucrose, 87 mM NaCl, 25 mM NaHCO$_3$, 2.5 mM KCl, 1.25 mM NaH$_2$PO$_4$, 0.5 mM CaCl$_2$, 7 mM MgCl$_2$ and 10 mM glucose. Slices were immediately transferred to a storage chamber containing artificial cerebral spinal fluid (aCSF) containing: 125 mM NaCl, 25 mM NaHCO$_3$, 2.5 mM KCl, 1.25 mM NaH$_2$PO$_4$, 2 mM MgCl$_2$, 2.5 mM CaCl$_2$ and 11mM glucose, pH 7.4, constantly bubbled with 95% O2 and 5% CO2; 315-320 mOsm. Slices were maintained at 35°C in aCSF for 60 min and then kept at room temperature before their transfer to the recording chamber. During the recordings, the slices were continuously perfused with aCSF at 35.0 ± 2.0°C throughout the experiments. Neuronal activity of layer 2/3 PV interneurons was recorded with borosilicate glass pipettes (4-6 MΩ) filled with an intracellular solution containing: 125 mM K-gluconate, 20 mM KCl, 10 mM HEPES, 10 mM EGTA, 2 mM MgCl$_2$, 2 mM Na$_2$ATP, 1 mM Na$_2$-phosphocreatine, 0.3 mM Na$_3$GTP and 0.2% biocytin. Passive membrane properties and detection of action potentials were measured by using a custom-made script in Igor Pro 8 software (WaveMetrics).

EEG recordings and behavioral monitoring
EEG recordings and behavioral monitoring were performed in individual cages equipped with overhead cameras (FLIR). Animals were connected to an amplifier (A-M Systems 1600) via a commutator. EEG signals were amplified and analog filtered (Gain 500, Low pass filter: 0.3 Hz, High pass filter: 100 Hz) and then digitized at 200Hz using Spike2 (CED Micro1401). Spontaneous sleep/wake behavior was monitored longitudinally via EEG recordings and video tracking. Epileptic episodes were scored manually by inspecting both the EEG signals and simultaneous video recordings.

Open field test
Behavioral testing was done with males and females which were aged between 10 and 16 weeks. Mice were handled for at least 3 days before the test and acclimatized to the testing room for at least an hour before starting the experimentation. Mice were placed in the center of a rectangular OFT box (30 cm in width and 45 cm in length, with 30-cm-tall walls) for 15 minutes. Videos were recorded with a downward-facing camera from above with ANY-maze at a rate of up to 30 Hz. Distance (as cm) was extracted from ANY-MAZE and velocity (cm/min) was calculated.

Quantification and statistical analysis
Statistical analysis was conducted with GraphPad Prism 9. Sample sizes were chosen based on previous experiments and literature surveys. No statistical methods were used to pre-determine sample sizes. Exclusion criteria used throughout this manuscript were pre-defined. There are detailed descriptions in the respective sections of the methods. Group assignment was defined by genotype; thus, no randomization was necessary. Appropriate statistical tests were chosen based on sample size and are indicated in individual experiments.

Other Supplementary Materials:

Supplementary Movie 1. FingR-PSD-95 intrabody expression in PV^{Cre} mice.
Representative video generated from optical sections of FingR-PSD-95-mGreenLantern expressing layer2/3 PV interneuron showing the labelling of glutamatergic synapses forming on its dendrites and the soma. Images were taken from cleared 120-micron thick sections.

Supplementary Movie 2. *Smad1ᴬᴾⱽ* **mice have altered cortical network activity.**
Representative EEG recording from *Smad1ᴬᴾⱽ* mice showing the brain activity of the mouse before, during and after a seizure event that occurred during a cage change.

Supplementary Table 1. Summary of ChiP-seq datasets collected from BMP2-stimulated primary cortical cultures.

Supplementary Table 2. Summary of RNA-seq datasets collected from BMP2-stimulated primary cortical cultures.

Supplementary Table 3. Summary of RNA-seq datasets collected from control and Smad1 mutant and BMP2 stimulated primary cortical cultures.

4.2 Materials and Methods – Vickers et al., 2020

Materials and Methods

Ethics statement

All experiments with laboratory mice followed the guidelines and regulations

of the Swiss Federal law on the protection of animals ("Loi fédérale sur la protection des

animaux"). The specific experimental procedures with laboratory mice were approved by

the SCAV (Service of Consumption and Veterinary Affairs, Canton of Vaud, Switzerland;

authorizations VD2063.3, VD2063.4).

Mouse pups were kept in the homecage with their mother; weaning was done at P25. One

mouse at a time, at age P19 to P24, was carefully removed from the cage, and killed by

decapitation either without prior anesthesia, or after a brief isoflurane anesthesia in later

experiments (protocols approved by the SCAV).

Mouse lines

We wished to inactivate BMP-signaling in PV-INs, by genetically deleting two essential

BMP type-1 receptors, BMPR1a and -1b. For this purpose, we generated a

conditional/conventional double KO (DKO) mouse model of BMP-receptor (BMPR) 1a and

1b, based on an interbreeding of four mouse lines. 1) A conditional knock-out (KO) mouse

line of the Alk3 gene which codes for BMPR1a (BMPR1a$^{lox/lox}$; ref. (Mishina, Hanks et al.

2002)). 2) A conventional KO mouse of the Alk6 gene which codes for BMPR1b (BMPR1b$^{-/-}$; ref. (Yi, Daluiski et al. 2000)). 3) A PV^{Cre} mouse line to drive Cre-expression in PV-INs

(PV$^{Cre/+}$; ref. (Hippenmeyer, Vrieseling et al. 2005)). 4) A reporter mouse line driving the

expression of tdTomato in Cre-expressing cells (Ai9; ref. (Madisen, Zwingman et al. 2010);

called here "tdT"), which was used to target recordings to PV-INs and to guide cellular

gene expression analyses. In breeding pairs that gave rise to mice used here, both males

and females were heterozygous for the BMPR1a locus (BMPR1a$^{+/lox}$) and for the BMPR1b

locus (BMPR1b$^{+/-}$), and homozygous in the PV locus (PV$^{mut/mut}$) and for the tdT transgene (tdT$^{mut/mut}$). The offspring of these breedings therefore showed the following genotypes: 1) Homozygous (c)DKO mice with genotype of BMPR1a$^{lox/lox}$, BMPR1b$^{-/-}$; this genotype is expected to occur at a fraction of 1/16. 2) Homozygous wild-type mice with genotype of 1a$^{+/+}$ [for BMPR1a$^{+/+}$], 1b$^{+/+}$ [for BMPR1b$^{+/+}$]; expected at a rate of 1/16). 3) Heterozygous animals with at least one functional allele of each BMP-type 1 receptor (i.e. genotypes 1a$^{+/+}$, 1b$^{+/-}$ at 1/8; 1a$^{+/lox}$, 1b$^{+/-}$ at 1/4; 1a$^{lox/+}$, 1b$^{+/+}$ at 1/8). Because homozygous wild-type mice were difficult to obtain in this breeding scheme, we used mice with at least one functional allele of each BMP type 1 receptor as "wild-type" controls (all genotypes listed in group 3) above). 4) Single KO (sKO) mice for the BMPR1b (genotypes, 1a$^{+/+}$, 1b$^{-/-}$ at 1/16; 1a$^{+/lox}$, 1b$^{-/-}$ at 1/8); these mice were used to control for compensatory networks effects that might result from the constitutive inactivation of the BMPR1b allele (see Results). 5) Single conditional KO mice of the BMPR1a allele (genotypes, 1a$^{lox/lox}$, 1b$^{+/-}$ at 1/8; 1a$^{lox/lox}$, 1b$^{+/+}$ at 1/16) - these mice were not used for experiments. We observed that the genotype fractions roughly conformed with the expected Mendelian ratios, although in some cases fewer (c)DKO mice than expected seemed to be present by ~P6. For this reason, in early breedings, at least one parent was homozygous for BMPR1a^{lox}. Although (c)DKO mice could only be obtained at low numbers, the above breeding scheme had the advantage that all three mouse genotype groups were obtained from the same breedings ("wild-type" control mice, (c)DKO mice, and BMPR1b sKO mice).

Slice preparation and patch-clamp electrophysiology

We made patch-clamp recordings of PV-INs identified by their tdTomato fluorescence, either alone or together with a recording of a connected principal neuron. Recordings were made in slices of auditory cortex of young mice (P19 - P24), at a depth of 30 - 50% from the cortical surface, which we regard as layer 4 (ref. [Vickers, Clark et al. 2018]). By targeting tdTomato-positive neurons using PV^{Cre} mice, we assume that we target fast-firing, PV-positive basket cells, which are an abundant interneuron population in layer 4 of mouse

auditory cortex (Levy and Reyes 2012). However, because chandelier cells also express PV (ref. (DeFelipe and Gonzalez-Albo 1998)), and have similar AP firing properties as basket cells (Taniguchi, Lu et al. 2013), it remains possible that a minority of the sampled cells represent chandelier cells. We note, however, that in primary auditory cortex and other sensory cortices of mice, only few of the more complex nerve endings of chandelier cells were detected (Inda, DeFelipe et al. 2009), and that in many cortical areas, the density of chandelier cells is low in layer 4.

Parahorizontal thalamocortical auditory slices (300 µm) of mouse brain were made with a vibratome (Leica VT 1200). Whole-cell patch-clamp recordings were performed at room temperature (21 - 23°C), in set-ups with an upright microscope (either Olympus BX51WI, or ZEISS Axioskop 2), equipped with 60x, 0.9 numerical aperture objectives (Olympus). The tdTomato fluorescence of genetically labeled PV-INs (tdT reporter mice; see above) was excited with a Polychrome V (or Polychrome IV; TILL Photonics) monochromator at 550 nm (using a 570-613 nm emission filter). Images were detected with a CCD camera (either Retiga 2000RV or PCO Sensicam).

The patch-pipette (intracellular) solution for recording PV-INs contained (in mM): 135 K-gluconate, 10 KCl, 0.5 HEPES, 5 Na_2-Phosphocreatine, 4 Mg-ATP, 0.3 Na_2-GTP, 0.5 EGTA. The pH was set to 7.2 by adding KOH, the osmolarity was ~ 305 mOsm. The patch pipette solution for recording postsynaptic principal neurons was similar to the above solution, but contained 160 mM KCl and no K-gluconate. Because of the high intracellular [Cl^-], IPSCs were recorded as inward currents at a holding potential of -70 mV. The extracellular solution was a standard bicarbonate-buffered solution containing 2 mM $CaCl_2$ and 1 mM $MgCl_2$. For the measurement of spike-timing- dependent plasticity of IPSCs, the series resistance (R_S) of the postsynaptic recording was minimized, and R_S was verified regularly throughout the recording. A change in the R_S by more than ± 50%, and above a value of 20 MOhm led to the exclusion of a recording from the final dataset.

For measurements of the AP-firing behavior and passive membrane properties in recordings of PV-INs alone (Fig. 1), 1 s current steps between -200 and +500 pA (increments of +100 pA) were applied in current-clamp experiments in single recordings. During paired recordings, unitary IPSCs between the PV-IN and a L4 principal neuron were first measured under baseline conditions, by applying short (3 ms) current steps in the PV-INs under current clamp to evoke single APs repeated every 10s; the resulting postsynaptic IPSC was measured with a second patch-clamp amplifier under voltage-clamp at a holding potential of -70 mV. Following this baseline period, a spike-timing dependent plasticity protocol was applied, in which a postsynaptic AP was followed by a presynaptic AP (post - pre induction; see ref. (Vickers, Clark et al. 2018)). Specifically, post- and presynaptic current injections (1 nA of 3 ms duration in both recordings) were applied with a time offset of 5 ms, 50 times every 5s.

Fluorescent *in situ* hybridization

Fluorescence *in situ* hybridization (FISH) was performed using the RNAscope® Fluorescent Multiplex Kit (ACD) protocol. Briefly, brains were dissected from P25 male and female mice and snap frozen in liquid nitrogen. Coronal sections (18 µm thick) were cut with a cryostat between Bregma -2 and -3.6 mm to include auditory cortex, adhered to Superfrost ultra plus slides (Thermo Scientific) and stored at -80ºC. Sections were fixed for 30 min in 4% PFA and treated with Protease IV. Hybridization was for 2 hours at 40°C. The following probes (50x dilution), coupled to specific fluorophores, were used in the same hybridization reaction: *Ntrk2* (C1 # 423611; coupled to Atto 550), *Cacna1A* (C2 # 493141; Alexa 488) and *tdTomato* (C3, # 317041; Atto 647). DAPI was used to identify the nuclei. Images were acquired with an upright LSM700 confocal microscope (Zeiss) using a 40x Apochromat objective in z-stacks (19-22 images, 0.4 µm intervals), using laser lines of 405 nm (for exciting DAPI), of 488 nm (for Alexa 488), of 555 nm (for Atto 550), and of 639 nm (for Atto 647). PV-INs were identified based on the presence of the tdTomato

probe signal, and the expression of TrkB and Cacna1a was analyzed in PV-INs contained in a depth of 20 - 50% of auditory cortex. A region of interest (ROI) was drawn to define the area of the cell soma. Thresholding for detection of the signal throughout the stacks and the number of pixels were first set through the TrackMate plugin of the FiJi software. The number of puncta for each probe set were then counted with the automated TrackMate plugin in the ROI. The number of puncta in the ROI, normalized to the area, were used as a proxy for expression strength of a given probe. The density of tdTomato positive cells spanning from 20% to 50% depth of auditory cortex was quantified from images acquired on a Widefield Axio Scan Z1 slide scanner. Images were assembled using Fiji and Illustrator Software.

Analysis and Statistics

The membrane time-constant (τ_m) was measured by fitting a single exponential function to the relaxation of the membrane potential (V_m) trace in response to a 1 s, -100 pA current step. The instantaneous AP frequency was measured from the inter-AP intervals for all pairs of subsequent APs in response to 1s current injections. The maximal adaption was calculated as the last interspike interval (ISI) in the train divided by the second ISI in the train.

Statistical tests for the analysis of electrophysiological data were performed in GraphPad Prism 5.01. For repeated experiments, the number of recorded cells or cell pairs is reported as "n", and the number of investigated mice as "N". For experiments in which the control group and the BMPR1a/1b (c)DKO group were compared, we first performed a Shapiro-Wilk normality test to determine whether the data was normally distributed. For datasets which passed the normality test we performed an unpaired Student's test to determine the statistical significance of the difference between the two groups. If one of the groups failed the normality test, we performed a non-parametric Mann-Whitney test for unpaired comparisons instead, as indicated in the Results. For the comparison of paired-

pulse ratios (PPR) before- and after LTP induction in a given recording, we used paired Student's t-test.

For experiments in which three groups of mice were compared, we used one-way ANOVA if all datasets passed the Shapiro-Wilk normality test. If one or more of the datasets failed the normality test, a non-parametric Kruskal-Wallis test was used, as indicated in the Results. In both cases, if the p value of the ANOVA / Kruskal-Wallis test was below 0.05, we performed post hoc tests, corrected for multiple comparisons. For parametric one-way ANOVA, we used the Tukey's multiple comparisons test. In case of the non-parametric Kruskal-Wallis test, we used Dunn's multiple comparisons test. In either case, alpha was set to 0.05.

Statistical tests for the quantifications of PV-IN cell density, TrkB and Cacna1A mRNA levels were performed in GraphPad Prism 8. The number of dots per cell were averaged to yield an average expression level in a given control- and (c)DKO mouse for both the TrkB- and Cacna1a probe. This analysis was repeated in a total of N = 3 control mice and N = 4 (c)DKO mice, and the statistical difference was tested with a non-parametric Mann-Whitney test for unpaired comparisons.

Data availability

The raw data leading to the conclusions of this paper can be found at Zenodo (10.5281/zenodo.3827171).

5. Appendix

Index of figures

Index of abbreviations

(c)DKO= conditional double knock-out

A1= primary auditory cortex

AAV= adenovirus

AMPA= α-amino-3-hydroxy-5-methyl-4-isoxazolepropionate-type

AP= action potential

Bcan= Brevican

BDN= brain-derived neurotrophic factor

BMP= Bone Morphogenetic Proteins

BRE= BMP-responsive element

Bmpr1a= BMP receptor-1a

Bmpr1b= BMP receptor-1b

Bmpr2= BMP receptor-2

CA= Cornu Ammonis

Ca^{2+}= calcium

CamK2= Ca^{2+}/calmodulin-dependent protein kinase 2

ChiP-seq= Chromatin immunoprecipitation-sequencing

CRE= cis-regulatory elements

CRISPR-CAS9= Clustered Regularly Interspaced Short Palindromic Repeats-CRISPR associated protein 9

DIV= days in vitro

DNA= deoxyribonucleic acid

Dpp= Decapentaplegic

E-I= excitation-inhibition

E16.5= embryonic stage 16.5

EEG= electroencephalogram

eGFP= enhanced green fluorescent protein

FC= fold change

FingR= Fibronectin intrabodies generated by mRNA display

FISH= Fluorescence in situ hybridization

fl= floxed

FPKM= Fragments Per Kilobase of transcript per Million

GABA= γ-aminobutyric acid

Gbb= glass bottom boat

GDF= growth differentiation factor

GFP= green fluorescent protein

GO= Gene Ontology

GPHN= Gephryin

Grik4= Glutamate Ionotropic Receptor Kainate Type Subunit 4

H3K27ac= histone 3 acetylated at lysine 27

HA= Human influenza hemagglutinin

hSyn= human synapsin promoter

HZ= Hertz

IEG= immediate early gene

IGF1= insulin growth factor 1

iLTD= inhibitory Long-Term Depression

iLTP= inhibitory Long-Term Potentiation

IN= interneuron

kDa= kilo Dalton

KO= knock-out

L-VGCC= L-type voltage-sensitive calcium channels

L2/3= layer 2/3

L4= layer 4

LRG= late response gene

MAPK= mitogen-activated protein kinases

mEPSC= miniature excitatory post-synaptic current

mIPSC= miniature inhibitory post-synaptic current

miRNA= microRNA

mRNA= messenger Ribonucleic acid

ms= milli-second

mV= milli-volt

NMDA= N-methyl-D-aspartate

NMJ= neuromuscular junction

p-val= p-value

pA= pico amper

PC= principal cell

PNN= perineuronal net

PPR= paired pulse ratio

PSD-95= post-synaptic density protein 95

PV= Parvalbumin

qPCR= quantitative PCR

RAM= Robust Activity Marking

RiboTRAP= tagged-ribosomal affinity purification

RNA-seq=RNA-sequencing

RNA= ribonucleic acid

ROI= region of interest

rPRG= rapid primary response gene

RT-PCR= Reverse transcription PCR

S1= primary somatosensory cortex

S2= secondary somatosensory cortex

Sax= saxophone

SBE= SMAD binding element

SRG= secondary response gene

SST= somatostatin

STDP= Spike timing dependent plasticity

TF= transcription factor

TGF= Transforming growth factor

Tkv= thickveins

TRAP= Targeted Recombination in Active Populations

V1= primary visual cortex

Vgf: VGF Nerve Growth Factor Inducible

VIP= Vasoactive Intestinal Protein

WB= western blot

ZnF= zinc finger motif

6. References

References

Abbott, L. F. and S. B. Nelson (2000). "Synaptic plasticity: taming the beast." Nature Neuroscience **3**(11): 1178-1183.

Aberle, H., A. P. Haghighi, R. D. Fetter, B. D. McCabe, T. R. Magalhaes and C. S. Goodman (2002). "wishful thinking encodes a BMP type II receptor that regulates synaptic growth in Drosophila." Neuron **33**(4): 545-558.

Abidin, I., T. Kohler, E. Weiler, G. Zoidl, U. T. Eysel, V. Lessmann and T. Mittmann (2006). "Reduced presynaptic efficiency of excitatory synaptic transmission impairs LTP in the visual cortex of BDNF-heterozygous mice." European Journal of Neuroscience **24**(12): 3519-3531.

Adesnik, H. and M. Scanziani (2010). "Lateral competition for cortical space by layer-specific horizontal circuits." Nature **464**(7292): 1155-U1171.

Aid, T., A. Kazantseva, M. Piirsoo, K. Palm and T. Timmusk (2007). "Mouse and rat BDNF gene structure and expression revisited." J Neurosci Res **85**(3): 525-535.

Aihara, S., S. Fujimoto, R. Sakaguchi and T. Imai (2021). "BMPR-2 gates activity-dependent stabilization of primary dendrites during mitral cell remodeling." Cell Rep **35**(12): 109276.

Akin, O., B. T. Bajar, M. F. Keles, M. A. Frye and S. L. Zipursky (2019). "Cell-type-Specific Patterned Stimulus-Independent Neuronal Activity in the Drosophila Visual System during Synapse Formation." Neuron **101**(5): 894-904 e895.

Ascoli, G. A., L. Alonso-Nanclares, S. A. Anderson, G. Barrionuevo, R. Benavides-Piccione, A. Burkhalter, G. Buzsaki, B. Cauli, J. DeFelipe, A. Fairen, D. Feldmeyer, G. Fishell, Y. Fregnac, T. F. Freund, D. Gardner, E. P. Gardner, J. H. Goldberg, M. Helmstaedter, S. Hestrin, F. Karube, Z. F. Kisvarday, B. Lambolez, D. A. Lewis, O. Marin, H. Markram, A. Munoz, A. Packer, C. C. H. Petersen, K. S. Rockland, J. Rossier, B. Rudy, P. Somogyi, J. F. Staiger, G. Tamas, A. M. Thomson, M. Toledo-Rodriguez, Y. Wang, D. C. West, R. Yuste and P. I. N. G (2008). "Petilla terminology: nomenclature of features of GABAergic interneurons of the cerebral cortex." Nature Reviews Neuroscience **9**(7): 557-568.

Ataman, B., G. L. Boulting, D. A. Harmin, M. G. Yang, M. Baker-Salisbury, E. L. Yap, A. N. Malik, K. Mei, A. A. Rubin, I. Spiegel, E. Durresi, N. Sharma, L. D. S. Hu, M. Pletikos, E. C. Griffith, J. N. Partlow, C. R. Stevens, M. Adli, M. Chahrour, N. Sestan, C. A. Walsh, V. K. Berezovskii, M. S. Livingstone and M. E. Greenberg (2016). "Evolution of Osteocrin as an activity-regulated factor in the primate brain." Nature **539**(7628): 242-+.

Augsburger, A., A. Schuchardt, S. Hoskins, J. Dodd and S. Butler (1999). "BMPs as mediators of roof plate repulsion of commissural neurons." Neuron **24**(1): 127-141.

Avermann, M., C. Tomm, C. Mateo, W. Gerstner and C. C. H. Petersen (2012). "Microcircuits of excitatory and inhibitory neurons in layer 2/3 of mouse barrel cortex." Journal of Neurophysiology **107**(11): 3116-3134.

Axelrod, J. D., J. R. Miller, J. M. Shulman, R. T. Moon and N. Perrimon (1998). "Differential recruitment of Dishevelled provides signaling specificity in the planar cell polarity and Wingless signaling pathways." Genes & Development **12**(16): 2610-2622.

Ball, R. W., M. Warren-Paquin, K. Tsurudome, E. H. Liao, F. Elazzouzi, C. Cavanagh, B. S. An, T. T. Wang, J. H. White and A. P. Haghighi (2010). "Retrograde BMP signaling controls synaptic growth at the NMJ by regulating trio expression in motor neurons." Neuron **66**(4): 536-549.

Banerjee, S. B., V. A. Gutzeit, J. Baman, H. S. Aoued, N. K. Doshi, R. C. Liu and K. J. Ressler (2017). "Perineuronal Nets in the Adult Sensory Cortex Are Necessary for Fear Learning." Neuron **95**(1): 169-+.

Barkat, T. R., D. B. Polley and T. K. Hensch (2011). "A critical period for auditory thalamocortical connectivity." Nature Neuroscience **14**(9): 1189-1194.

Bauer, M., G. Aguilar, K. A. Wharton, S. Matsuda and M. Affolter (2023). "Heterodimerization-dependent secretion of bone morphogenetic proteins in Drosophila." Dev Cell **58**(8): 645-659 e644.

Ben-Ari, Y., E. Cherubini, R. Corradetti and J. L. Gaiarsa (1989). "Giant synaptic potentials in immature rat CA3 hippocampal neurones." J Physiol **416**: 303-325.

Bibel, M., E. Hoppe and Y. A. Barde (1999). "Biochemical and functional interactions between the neurotrophin receptors trk and p75(NTR)." Embo Journal **18**(3): 616-622.

Bier, E. and E. M. De Robertis (2015). "BMP gradients: A paradigm for morphogen-mediated developmental patterning." Science **348**(6242).

Bito, H., K. Deisseroth and R. W. Tsien (1996). "CREB phosphorylation and dephosphorylation: a Ca(2+)- and stimulus duration-dependent switch for hippocampal gene expression." Cell **87**(7): 1203-1214.

Blankenship, A. G. and M. B. Feller (2010). "Mechanisms underlying spontaneous patterned activity in developing neural circuits." Nat Rev Neurosci **11**(1): 18-29.

Bloodgood, B. L., N. Sharma, H. A. Browne, A. Z. Trepman and M. E. Greenberg (2013). "The activity-dependent transcription factor NPAS4 regulates domain-specific inhibition." Nature **503**(7474): 121-+.

Bond, A. M., O. G. Bhalala and J. A. Kessler (2012). "The dynamic role of bone morphogenetic proteins in neural stem cell fate and maturation." Developmental Neurobiology **72**(7): 1068-1084.

Borodinsky, L. N., C. M. Root, J. A. Cronin, S. B. Sann, X. N. Gu and N. C. Spitzer (2004). "Activity-dependent homeostatic specification of transmitter expression in embryonic neurons." Nature **429**(6991): 523-530.

Bruckner, G., K. Brauer, W. Hartig, J. R. Wolff, M. J. Rickmann, A. Derouiche, B. Delpech, N. Girard, W. H. Oertel and A. Reichenbach (1993). "Perineuronal Nets Provide a Polyanionic, Glia-Associated Form of Microenvironment around Certain Neurons in Many Parts of the Rat-Brain." Glia **8**(3): 183-200.

Butler, S. J. and J. Dodd (2003). "A role for BMP heterodimers in roof plate-mediated repulsion of commissural axons." Neuron **38**(3): 389-401.

Calella, A. M., C. Nerlov, R. G. Lopez, C. Sciarretta, O. von Bohlen und Halbach, O. Bereshchenko and L. Minichiello (2007). "Neurotrophin/Trk receptor signaling mediates C/EBPalpha, -beta and NeuroD recruitment to immediate-early gene promoters in neuronal cells and requires C/EBPs to induce immediate-early gene transcription." Neural Dev **2**: 4.

Calpe, S., K. Wagner, M. El Khattabi, L. Rutten, C. Zimberlin, E. Dolk, C. T. Verrips, J. P. Medema, H. Spits and K. K. Krishnadath (2015). "Effective Inhibition of Bone Morphogenetic Protein Function by Highly Specific Llama-Derived Antibodies." Molecular Cancer Therapeutics **14**(11): 2527-2540.

Campanac, E., C. Gasselin, A. Baude, S. Rama, N. Ankri and D. Debanne (2013). "Enhanced Intrinsic Excitability in Basket Cells Maintains Excitatory-Inhibitory Balance in Hippocampal Circuits." Neuron **77**(4): 712-722.

Campbell, B. C., E. M. Nabel, M. H. Murdock, C. Lao-Peregrin, P. Tsoulfas, M. G. Blackmore, F. S. Lee, C. Liston, H. Morishita and G. A. Petsko (2020). "mGreenLantern: a bright monomeric fluorescent protein with rapid expression and cell filling properties for neuronal imaging." Proc Natl Acad Sci U S A **117**(48): 30710-30721.

Cardozo, M. J., M. Almuedo-Castillo and P. Bovolenta (2019). "Patterning the Vertebrate Retina with Morphogenetic Signaling Pathways." Neuroscientist: 1073858419874016.

Carlson, W. D., P. C. Keck, D. Bosukonda and F. R. Carlson, Jr. (2022). "A Process for the Design and Development of Novel Bone Morphogenetic Protein-7 (BMP-7) Mimetics With an Example: THR-184." Front Pharmacol **13**: 864509.

Carter, A. R., C. Chen, P. M. Schwartz and R. A. Segal (2002). "Brain-derived neurotrophic factor modulates cerebellar plasticity and synaptic ultrastructure." J Neurosci **22**(4): 1316-1327.

Carulli, D., T. Pizzorusso, J. C. F. Kwok, E. Putignano, A. Poli, S. Forostyak, M. R. Andrews, S. S. Deepa, T. T. Glant and J. W. Fawcett (2010). "Animals lacking link protein have attenuated perineuronal nets and persistent plasticity." Brain **133**: 2331-2347.

Carulli, D., K. E. Rhodes, D. J. Brown, T. P. Bonnert, S. J. Pollack, K. Oliver, P. Strata and J. W. Fawcett (2006). "Composition of perineuronal nets in the adult rat cerebellum and the cellular origin of their components." Journal of Comparative Neurology **494**(4): 559-577.

Cellot, G. and E. Cherubini (2014). "GABAergic signaling as therapeutic target for autism spectrum disorders." Front Pediatr **2**: 70.

Chacko, B. M., B. Qin, J. J. Correia, S. S. Lam, M. P. de Caestecker and K. Lin (2001). "The L3 loop and C-terminal phosphorylation jointly define Smad protein trimerization." Nat Struct Biol **8**(3): 248-253.

Chang, M. C., J. M. Park, K. A. Pelkey, H. L. Grabenstatter, D. Xu, D. J. Linden, T. P. Sutula, C. J. McBain and P. F. Worley (2010). "Narp regulates homeostatic scaling of excitatory synapses on parvalbumin-expressing interneurons." Nat Neurosci **13**(9): 1090-1097.

Chen, L., X. Li, M. Tjia and S. Thapliyal (2022). "Homeostatic plasticity and excitation-inhibition balance: The good, the bad, and the ugly." Curr Opin Neurobiol **75**: 102553.

Cheng, S., S. Butrus, L. Tan, R. Xu, S. Sagireddy, J. T. Trachtenberg, K. Shekhar and S. L. Zipursky (2022). "Vision-dependent specification of cell types and function in the developing cortex." Cell **185**(2): 311-327 e324.

Choi, J. E., J. Kim and J. Kim (2020). "Capturing activated neurons and synapses." Neurosci Res **152**: 25-34.

Choi, J. H., S. E. Sim, J. I. Kim, D. I. Choi, J. Oh, S. Ye, J. Lee, T. Kim, H. G. Ko, C. S. Lim and B. K. Kaang (2018). "Interregional synaptic maps among engram cells underlie memory formation." Science **360**(6387): 430-435.

Chowdhury, S., J. D. Shepherd, H. Okuno, G. Lyford, R. S. Petralia, N. Plath, D. Kuhl, R. L. Huganir and P. F. Worley (2006). "Arc/Arg3.1 interacts with the endocytic machinery to regulate AMPA receptor trafficking." Neuron **52**(3): 445-459.

Clements, J. D. and R. A. Silver (2000). "Unveiling synaptic plasticity: a new graphical and analytical approach." TINS **23**: 105-113.

Close, J., H. Xu, N. D. Garcia, R. Batista-Brito, E. Rossignol, B. Rudy and G. Fishell (2012). "Satb1 Is an Activity-Modulated Transcription Factor Required for the Terminal Differentiation and Connectivity of Medial Ganglionic Eminence-Derived Cortical Interneurons." Journal of Neuroscience **32**(49): 17690-17705.

Cruikshank, S. J., H. Urabe, A. V. Nurmikko and B. W. Connors (2010). "Pathway-specific feedforward circuits between thalamus and neocortex revealed by selective optical stimulation of axons." Neuron **65**(2): 230-245.

D'Amour, J. A. and R. C. Froemke (2015). "Inhibitory and excitatory spike-timing-dependent plasticity in the auditory cortex." Neuron **86**(2): 514-528.

Dalessandro, J. S. and E. A. Wang (1994). "Bone Morphogenetic Proteins Inhibit Proliferation, Induce Reversible Differentiation and Prevent Cell-Death in Astrocyte Lineage Cells." Growth Factors **11**(1): 45-52.

Das, S., Y. F. Sasaki, T. Rothe, L. S. Premkumar, M. Takasu, J. E. Crandall, P. Dikkes, D. A. Conner, P. V. Rayudu, W. Cheung, H. S. Chen, S. A. Lipton and N. Nakanishi (1998). "Increased NMDA current and spine density in mice lacking the NMDA receptor subunit NR3A." Nature **393**(6683): 377-381.

Daswani, R., C. Gilardi, M. Soutschek, P. Nanda, K. Weiss, S. Bicker, R. Fiore, C. Dieterich, P. L. Germain, J. Winterer and G. Schratt (2022). "MicroRNA-138 controls hippocampal interneuron function and short-term memory in mice." Elife **11**.

Davis, B. N., A. C. Hilyard, G. Lagna and A. Hata (2008). "SMAD proteins control DROSHA-mediated microRNA maturation." Nature **454**(7200): 56-U52.

Davis, B. N., A. C. Hilyard, P. H. Nguyen, G. Lagna and A. Hata (2010). "Smad Proteins Bind a Conserved RNA Sequence to Promote MicroRNA Maturation by Drosha." Molecular Cell **39**(3): 373-384.

De Marco Garcia, N. V., T. Karayannis and G. Fishell (2011). "Neuronal activity is required for the development of specific cortical interneuron subtypes." Nature **472**(7343): 351-355.

De Robertis, E. M. and H. Kuroda (2004). "Dorsal-ventral patterning and neural induction in Xenopus embryos." Annu Rev Cell Dev Biol **20**: 285-308.

de Villers-Sidani, E., E. F. Chang, S. Bao and M. M. Merzenich (2007). "Critical period window for spectral tuning defined in the primary auditory cortex (A1) in the rat." J. Neuroscience **27**(1): 180-189.

DeFelipe, J. and M. C. Gonzalez-Albo (1998). "Chandelier cell axons are immunoreactive for GAT-1 in the human neocortex." Neuroreport **9**(3): 467-470.

Dehorter, N., G. Ciceri, G. Bartolini, L. Lim, I. del Pino and O. Marin (2015). "Tuning of fast-spiking interneuron properties by an activity-dependent transcriptional switch." Science **349**(6253): 1216-1220.

Dehorter, N., N. Marichal, O. Marin and B. Berninger (2017). "Tuning neural circuits by turning the interneuron knob." Curr Opin Neurobiol **42**: 144-151.

Deisseroth, K., E. K. Heist and R. W. Tsien (1998). "Translocation of calmodulin to the nucleus supports CREB phosphorylation in hippocampal neurons." Nature **392**(6672): 198-202.

DeNardo, L. and L. Q. Luo (2017). "Genetic strategies to access activated neurons." Current Opinion in Neurobiology **45**: 121-129.

DeNardo, L. A., C. D. Liu, W. E. Allen, E. L. Adams, D. Friedmann, L. S. Fu, C. J. Guenthner, M. Tessier-Lavigne and L. Q. Luo (2019). "Temporal evolution of cortical ensembles promoting remote memory retrieval." Nature Neuroscience **22**(3): 460-+.

Derynck, R. and Y. E. Zhang (2003). "Smad-dependent and Smad-independent pathways in TGF-beta family signalling." Nature **425**(6958): 577-584.

Devienne, G., S. Picaud, I. Cohen, J. Piquet, L. Tricoire, D. Testa, A. A. Di Nardo, J. Rossier, B. Cauli and B. Lambolez (2021). "Regulation of perineuronal nets in the adult cortex by the activity of the cortical network." J Neurosci **41**(27): 5779-5790.

Doischer, D., J. A. Hosp, Y. Yanagawa, K. Obata, P. Jonas, I. Vida and M. Bartos (2008). "Postnatal differentiation of basket cells from slow to fast signaling devices." J Neuroscience **28**(48): 12956-12968.

Dolmetsch, R. E., U. Pajvani, K. Fife, J. M. Spotts and M. E. Greenberg (2001). "Signaling to the nucleus by an L-type calcium channel - Calmodulin complex through the MAP kinase pathway." Science **294**(5541): 333-339.

Duchamp-Viret, P., M. A. Chaput and A. Duchamp (1999). "Odor response properties of rat olfactory receptor neurons." Science **284**(5423): 2171-2174.

Dutko, J. A. and M. C. Mullins (2011). "SnapShot: BMP signaling in development." Cell **145**(4): 636, 636 e631-632.

Eaton, B. A. and G. W. Davis (2005). "LIM Kinase1 Controls Synaptic Stability Downstream of the Type II BMP Receptor." Neuron **47**(5): 695-708.

Ebert, D. H., H. W. Gabel, N. D. Robinson, N. R. Kastan, L. S. Hu, S. Cohen, A. J. Navarro, M. J. Lyst, R. Ekiert, A. P. Bird and M. E. Greenberg (2013). "Activity-dependent phosphorylation of MeCP2 threonine 308 regulates interaction with NCoR." Nature **499**(7458): 341-U116.

Ernfors, P., K. F. Lee and R. Jaenisch (1994). "Mice Lacking Brain-Derived Neurotrophic Factor Develop with Sensory Deficits." Nature **368**(6467): 147-150.

Exposito-Alonso, D. and B. Rico (2022). "Mechanisms Underlying Circuit Dysfunction in Neurodevelopmental Disorders." Annu Rev Genet **56**: 391-422.

Favuzzi, E., R. Deogracias, A. Marques-Smith, P. Maeso, J. Jezequel, D. Exposito-Alonso, M. Balia, T. Kroon, A. J. Hinojosa, F. M. E and B. Rico (2019). "Distinct molecular programs regulate synapse specificity in cortical inhibitory circuits." Science **363**(6425): 413-417.

Favuzzi, E., A. Marques-Smith, R. Deogracias, C. M. Winterflood, A. Sanchez-Aguilera, L. Mantoan, P. Maeso, C. Fernandes, H. Ewers and B. Rico (2017). "Activity-Dependent Gating of Parvalbumin Interneuron Function by the Perineuronal Net Protein Brevican." Neuron **95**(3): 639-655 e610.

Finelli, M. J., K. J. Murphy, L. Chen and H. Y. Zou (2013). "Differential Phosphorylation of Smad1 Integrates BMP and Neurotrophin Pathways through Erk/Dusp in Axon Development." Cell Reports **3**(5): 1592-1606.

Fischer, A., F. Sananbenesi, X. Y. Wang, M. Dobbin and L. H. Tsai (2007). "Recovery of learning and memory is associated with chromatin remodelling." Nature **447**(7141): 178-U172.

Friedman, W. J. (2010). "Proneurotrophins, seizures, and neuronal apoptosis." Neuroscientist **16**(3): 244-252.

Froemke, R. C. (2015). "Plasticity of cortical excitatory-inhibitory balance." Annu Rev Neurosci **38**: 195-219.

Furlanis, E., L. Traunmuller, G. Fucile and P. Scheiffele (2019). "Landscape of ribosome-engaged transcript isoforms reveals extensive neuronal-cell-class-specific alternative splicing programs." Nat Neurosci **22**(10): 1709-1717.

Furlanis, E., L. Traunmuller, G. Fucile and P. Scheiffele (2019). "Landscape of ribosome-engaged transcript isoforms reveals extensive neuronal-cell-class-specific alternative splicing programs." Nature Neuroscience **22**(10): 1709-+.

Gabernet, L., S. P. Jadhav, D. E. Feldman, M. Carandini and M. Scanziani (2005). "Somatosensory integration controlled by dynamic thalamocortical feed-forward inhibition." Neuron **48**(2): 315-327.

Gaidatzis, D., A. Lerch, F. Hahne and M. B. Stadler (2015). "QuasR: quantification and annotation of short reads in R." Bioinformatics **31**(7): 1130-1132.

Gaiddon, C., J. P. Loeffler and Y. Larmet (1996). "Brain-derived neurotrophic factor stimulates AP-1 and cyclic AMP-responsive element dependent transcriptional activity in central nervous system neurons." J Neurochem **66**(6): 2279-2286.

Gil-Sanz, C., A. Espinosa, S. P. Fregoso, K. K. Bluske, C. L. Cunningham, I. Martinez-Garay, H. K. Zeng, S. J. Franco and U. Muller (2015). "Lineage Tracing Using Cux2-Cre and Cux2-CreERT2 Mice." Neuron **86**(4): 1091-1099.

Gogolla, N., P. Caroni, A. Luthi and C. Herry (2009). "Perineuronal Nets Protect Fear Memories from Erasure." Science **325**(5945): 1258-1261.

Goldenberg, A. M., S. Schmidt, R. Mitelman, D. R. Levy, M. Prigge, Y. Katz, O. Yizhar, H. Beck and I. Lampl (2022). "Localized chemogenetic silencing of inhibitory neurons: a novel mouse model of focal cortical epileptic activity." Cereb Cortex.

Goldman, A. L., W. V. van Naters, D. Lessing, C. G. Warr and J. R. Carlson (2005). "Coexpression of two functional odor receptors in one neuron." Neuron **45**(5): 661-666.

Golgi, C. (1989). "On the Structure of Nerve-Cells." Journal of Microscopy-Oxford **155**: 3-7.

Gratacos, E., N. Checa, E. Perez-Navarro and J. Alberch (2001). "Brain-derived neurotrophic factor (BDNF) mediates bone morphogenetic protein-2 (BMP-2) effects on cultured striatal neurones." J Neurochem **79**(4): 747-755.

Greenberg, M. E. and E. B. Ziff (1984). "Stimulation of 3t3 Cells Induces Transcription of the C-Fos Proto-Oncogene." Nature **311**(5985): 433-438.

Gross, G. G., J. A. Junge, R. J. Mora, H. B. Kwon, C. A. Olson, T. T. Takahashi, E. R. Liman, G. C. Ellis-Davies, A. W. McGee, B. L. Sabatini, R. W. Roberts and D. B. Arnold (2013). "Recombinant probes for visualizing endogenous synaptic proteins in living neurons." Neuron **78**(6): 971-985.

Guillamon-Vivancos, T., M. Anibal-Martinez, L. Puche-Aroca, J. A. Moreno-Bravo, M. Valdeolmillos, F. J. Martini and G. Lopez-Bendito (2022). "Input-dependent segregation of visual and somatosensory circuits in the mouse superior colliculus." Science **377**(6608): 845-850.

Gundelfinger, E. D., R. Frischknecht, D. Choquet and M. Heine (2010). "Converting juvenile into adult plasticity: a role for the brain's extracellular matrix." European Journal of Neuroscience **31**(12): 2156-2165.

Haapasalo, A., I. Sipola, K. Larsson, K. E. Akerman, P. Stoilov, S. Stamm, G. Wong and E. Castren (2002). "Regulation of TRKB surface expression by brain-derived neurotrophic factor and truncated TRKB isoforms." J Biol Chem **277**(45): 43160-43167.

Hagenston, A. M. and H. Bading (2011). "Calcium Signaling in Synapse-to-Nucleus Communication." Cold Spring Harbor Perspectives in Biology **3**(11).

Hagihara, K., R. Miura, R. Kosaki, E. Berglund, B. Ranscht and Y. Yamaguchi (1999). "Immunohistochemical evidence for the brevican-tenascin-R interaction: Colocalization in perineuronal nets suggests a physiological role for the interaction in the adult rat brain." Journal of Comparative Neurology **410**(2): 256-264.

Hallem, E. A. and J. R. Carlson (2006). "Coding of odors by a receptor repertoire." Cell **125**(1): 143-160.

Hanover, J. L., Z. J. Huang, S. Tonegawa and M. P. Stryker (1999). "Brain-derived neurotrophic factor overexpression induces precocious critical period in mouse visual cortex." Journal of Neuroscience **19**(22): art. no.-RC40.

Harris, J. A., K. E. Hirokawa, S. A. Sorensen, H. Gu, M. Mills, L. L. Ng, P. Bohn, M. Mortrud, B. Ouellette, J. Kidney, K. A. Smith, C. Dang, S. Sunkin, A. Bernard, S. W. Oh, L. Madisen and H. K. Zeng (2014). "Anatomical characterization of Cre driver mice for neural circuit mapping and manipulation." Frontiers in Neural Circuits **8**.

Hazama, M., A. Aono, N. Ueno and Y. Fujisawa (1995). "Efficient Expression of a Heterodimer of Bone Morphogenetic Protein Subunits Using a Baculovirus Expression System." Biochemical and Biophysical Research Communications **209**(3): 859-866.

He, M., Y. Liu, X. Wang, M. Q. Zhang, G. J. Hannon and Z. J. Huang (2012). "Cell-type-based analysis of microRNA profiles in the mouse brain." Neuron **73**(1): 35-48.

Hefft, S. and P. Jonas (2005). "Asynchronous GABA release generates long-lasting inhibition at a hippocampal interneuron-principal neuron synapse." Nat Neurosci **8**(10): 1319-1328.

Heinz, S., C. Benner, N. Spann, E. Bertolino, Y. C. Lin, P. Laslo, J. X. Cheng, C. Murre, H. Singh and C. K. Glass (2010). "Simple combinations of lineage-determining transcription factors prime cis-regulatory elements required for macrophage and B cell identities." Mol Cell **38**(4): 576-589.

Hensch, T. K. (2005). "Critical period plasticity in local cortical circuits." Nat Rev Neurosci **6**(11): 877-888.

Higashi, T., S. Tanaka, T. Iida and S. Okabe (2018). "Synapse Elimination Triggered by BMP4 Exocytosis and Presynaptic BMP Receptor Activation." Cell Rep **22**(4): 919-929.

Hippenmeyer, S., E. Vrieseling, M. Sigrist, T. Portmann, C. Laengle, D. R. Ladle and S. Arber (2005). "A developmental switch in the response of DRG neurons to ETS transcription factor signaling." PLoS Biol **3**(5): e159.

Hogan, B. L. (1996). "Bone morphogenetic proteins in development." Curr Opin Genet Dev **6**(4): 432-438.

House, D. R. C., J. Elstrott, E. Koh, J. Chung and D. E. Feldman (2011). "Parallel Regulation of Feedforward Inhibition and Excitation during Whisker Map Plasticity." Neuron **72**(5): 819-831.

Hrvatin, S., D. R. Hochbaum, M. A. Nagy, M. Cicconet, K. Robertson, L. Cheadle, R. Zilionis, A. Ratner, R. Borges-Monroy, A. M. Klein, B. L. Sabatini and M. E. Greenberg (2018). "Single-cell analysis of experience-dependent transcriptomic states in the mouse visual cortex." Nat Neurosci **21**(1): 120-129.

Hrvatin, S., D. R. Hochbaum, M. A. Nagy, M. Cicconet, K. Robertson, L. Cheadle, R. Zilionis, A. Ratner, R. Borges-Monroy, A. M. Klein, B. L. Sabatini and M. E. Greenberg (2018). "Single-cell analysis of experience-dependent transcriptomic states in the mouse visual cortex (vol 21, pg 120, 2018)." Nature Neuroscience **21**(7): 1017-1017.

Hu, H., J. Gan and P. Jonas (2014). "Interneurons. Fast-spiking, parvalbumin(+) GABAergic interneurons: from cellular design to microcircuit function." <u>Science</u> **345**(6196): 1255263.

Huang, S., B. Tang, D. Usoskin, R. J. Lechleider, S. P. Jamin, C. Li, M. A. Anzano, T. Ebendal, C. Deng and A. B. Roberts (2002). "Conditional knockout of the Smad1 gene." <u>Genesis</u> **32**(2): 76-79.

Huang, Z. J., A. Kirkwood, T. Pizzorusso, V. Porciatti, B. Morales, M. F. Bear, L. Maffei and S. Tonegawa (1999). "BDNF regulates the maturation of inhibition and the critical period of plasticity in mouse visual cortex." <u>Cell</u> **98**(6): 739-755.

Huang, Z. J. and A. Paul (2019). "The diversity of GABAergic neurons and neural communication elements." <u>Nature Reviews Neuroscience</u> **20**(9): 563-572.

Iascone, D. M., Y. Li, U. Sumbul, M. Doron, H. Chen, V. Andreu, F. Goudy, H. Blockus, L. F. Abbott, I. Segev, H. Peng and F. Polleux (2020). "Whole-Neuron Synaptic Mapping Reveals Spatially Precise Excitatory/Inhibitory Balance Limiting Dendritic and Somatic Spiking." <u>Neuron</u> **106**(4): 566-578 e568.

Inagaki, T., T. Begum, F. Reza, S. Horibe, M. Inaba, Y. Yoshimura and Y. Komatsu (2008). "Brain-derived neurotrophic factor-mediated retrograde signaling required for the induction of long-term potentiation at inhibitory synapses of visual cortical pyramidal neurons." <u>Neuroscience Research</u> **61**(2): 192-200.

Inda, M. C., J. DeFelipe and A. Munoz (2009). "Morphology and distribution of chandelier cell axon terminals in the mouse cerebral cortex and claustroamygdaloid complex." <u>Cereb Cortex</u> **19**(1): 41-54.

Inman, G. J. and C. S. Hill (2002). "Stoichiometry of active smad-transcription factor complexes on DNA." <u>J Biol Chem</u> **277**(52): 51008-51016.

Inman, G. J., F. J. Nicolas and C. S. Hill (2002). "Nucleocytoplasmic shuttling of Smads 2, 3, and 4 permits sensing of TGF-beta receptor activity." <u>Molecular Cell</u> **10**(2): 283-294.

Iozzo, R. V. (1998). "Matrix proteoglycans: From molecular design to cellular function." <u>Annual Review of Biochemistry</u> **67**: 609-652.

Isaacson, J. S. and M. Scanziani (2011). "How Inhibition Shapes Cortical Activity." <u>Neuron</u> **72**(2): 231-243.

Israel, D. I., J. Nove, K. M. Kerns, R. J. Kaufman, V. Rosen, K. A. Cox and J. M. Wozney (1996). "Heterodimeric bone morphogenetic proteins show enhanced activity in vitro and in vivo." <u>Growth Factors</u> **13**(3-4): 291-300.

Iwasaki, S., A. Momiyama, O. D. Uchitel and T. Takahashi (2000). "Developmental changes in calcium channel types mediating central synaptic transmission." <u>J. Neurosci.</u> **20**: 59-65.

Jabaudon, D. (2017). "Fate and freedom in developing neocortical circuits." <u>Nature Communications</u> **8**.

Jiang, X., S. Shen, C. R. Cadwell, P. Berens, F. Sinz, A. S. Ecker, S. Patel and A. S. Tolias (2015). "Principles of connectivity among morphologically defined cell types in adult neocortex." <u>Science</u> **350**(6264): aac9462.

Jones, K. R., I. Farinas, C. Backus and L. F. Reichardt (1994). "Targeted disruption of the BDNF gene perturbs brain and sensory neuron development but not motor neuron development." <u>Cell</u> **76**(6): 989-999.

Joseph, D. J., M. Von Deimling, Y. Hasegawa, A. G. Cristancho, R. C. Ahrens-Nicklas, S. L. Rogers, R. Risbud, A. J. McCoy and E. D. Marsh (2021). "Postnatal Arx transcriptional activity regulates functional properties of PV interneurons." <u>iScience</u> **24**(1): 101999.

Kalinovsky, A., F. Boukhtouche, R. Blazeski, C. Bornmann, N. Suzuki, C. A. Mason and P. Scheiffele (2011). "Development of axon-target specificity of ponto-cerebellar afferents." <u>Plos Biology</u> **9**(2).

Kalinovsky, A., F. Boukhtouche, R. Blazeski, C. Bornmann, N. Suzuki, C. A. Mason and P. Scheiffele (2011). "Regulation of axon-target specificity of ponto-cerebellar afferents by BMP signaling." <u>PLoS Biol</u> **9**(2): e1001013.

Kang, H. and A. Hata (2012). "Control of Drosha-Mediated MicroRNA Maturation by Smad Proteins." Enzymes, Vol 32: Eukaryotic Rnases and Their Partners in Rna Degradation and Biogenesis, Pt B **32**: 123-136.

Karaca, K. G., J. Kupke, D. V. C. Brito, B. Zeuch, C. Thome, D. Weichenhan, P. Lutsik, C. Plass and A. M. M. Oliveira (2020). "Neuronal ensemble-specific DNA methylation strengthens engram stability." Nature Communications **11**(1).

Kashima, R., S. Roy, M. Ascano, V. Martinez-Cerdeno, J. Ariza-Torres, S. Kim, J. Louie, Y. Lu, P. Leyton, K. D. Bloch, T. B. Kornberg, P. J. Hagerman, R. Hagerman, G. Lagna and A. Hata (2016). "Augmented noncanonical BMP type II receptor signaling mediates the synaptic abnormality of fragile X syndrome." Science Signaling **9**(431).

Keck, T., G. B. Keller, R. I. Jacobsen, U. T. Eysel, T. Bonhoeffer and M. Hubener (2013). "Synaptic scaling and homeostatic plasticity in the mouse visual cortex in vivo." Neuron **80**(2): 327-334.

Kernie, S. G., D. J. Liebl and L. F. Parada (2000). "BDNF regulates eating behavior and locomotor activity in mice." EMBO J **19**(6): 1290-1300.

Keshishian, H. and Y. S. Kim (2004). "Orchestrating development and function: retrograde BMP signaling in the Drosophila nervous system." Trends Neurosci **27**(3): 143-147.

Khazipov, R. and H. J. Luhmann (2006). "Early patterns of electrical activity in the developing cerebral cortex of humans and rodents." Trends Neurosci **29**(7): 414-418.

Kim, M. and S. Choe (2011). "BMPs and their clinical potentials." Bmb Reports **44**(10): 619-634.

Kim, T. K., M. Hemberg, J. M. Gray, A. M. Costa, D. M. Bear, J. Wu, D. A. Harmin, M. Laptewicz, K. Barbara-Haley, S. Kuersten, E. Markenscoff-Papadimitriou, D. Kuhl, H. Bito, P. F. Worley, G. Kreiman and M. E. Greenberg (2010). "Widespread transcription at neuronal activity-regulated enhancers." Nature **465**(7295): 182-U165.

Klumpe, H. E., M. A. Langley, J. M. Linton, C. J. Su, Y. E. Antebi and M. B. Elowitz (2022). "The context-dependent, combinatorial logic of BMP signaling." Cell Syst **13**(5): 388-407 e310.

Kobayashi, M., M. Fujii, K. Kurihara and I. Matsuoka (1998). "Bone morphogenetic protein-2 and retinoic acid induce neurotrophin-3 responsiveness in developing rat sympathetic neurons." Brain Res Mol Brain Res **53**(1-2): 206-217.

Korte, M., P. Carroll, E. Wolf, G. Brem, H. Thoenen and T. Bonhoeffer (1995). "Hippocampal Long-Term Potentiation Is Impaired in Mice Lacking Brain-Derived Neurotrophic Factor." Proceedings of the National Academy of Sciences of the United States of America **92**(19): 8856-8860.

Kronander, E., C. Clark and R. Schneggenburger (2019). "Role of BMP Signaling for the Formation of Auditory Brainstem Nuclei and Large Auditory Relay Synapses." Dev Neurobiol **79**(2): 155-174.

Kubota, Y., S. Kondo, M. Nomura, S. Hatada, N. Yamaguchi, A. A. Mohamed, F. Karube, J. Lübke and Y. Kawaguchi (2015). "Functional effects of distinct innervation styles of pyramidal cells by fast spiking cortical interneurons." Elife **4**.

Kuhlman, S. J., N. D. Olivas, E. Tring, T. Ikrar, X. Xu and J. T. Trachtenberg (2013). "A disinhibitory microcircuit initiates critical-period plasticity in the visual cortex." Nature **501**(7468): 543-546.

Kumar, P., A. Lim, S. N. Hazirah, C. J. H. Chua, A. Ngoh, S. L. Poh, T. H. Yeo, J. Lim, S. M. Ling, N. B. Sutamam, E. Petretto, D. C. Y. Low, L. Zeng, E. K. Tan, T. Arkachaisri, J. G. Yeo, F. Ginhoux, D. Chan and S. Albani (2022). "Single-cell transcriptomics and surface epitope detection in human brain epileptic lesions identifies pro-inflammatory signaling." Nature Neuroscience **25**(7): 956-+.

Lee, F. S. and M. V. Chao (2001). "Activation of Trk neurotrophin receptors in the absence of neurotrophins." Proc Natl Acad Sci U S A **98**(6): 3555-3560.

Lessmann, V., K. Gottmann and M. Malcangio (2003). "Neurotrophin secretion: current facts and future prospects." Prog Neurobiol **69**(5): 341-374.

Levenson, J. M., K. J. O'Riordan, K. D. Brown, M. A. Trinh, D. L. Molfese and J. D. Sweatt (2004). "Regulation of histone acetylation during memory formation in the hippocampus." Journal of Biological Chemistry **279**(39): 40545-40559.

Levy, R. B. and A. D. Reyes (2012). "Spatial profile of excitatory and inhibitory synaptic connectivity in mouse primary auditory cortex." J. Neuroscience **32**(16): 5609-5619.

Lewis, T. C. and R. Prywes (2013). "Serum regulation of Id1 expression by a BMP pathway and BMP responsive element." Biochim Biophys Acta **1829**(10): 1147-1159.

Li, K. X., Y. M. Lu, Z. H. Xu, J. Zhang, J. M. Zhu, J. M. Zhang, S. X. Cao, X. J. Chen, Z. Chen, J. H. Luo, S. Duan and X. M. Li (2011). "Neuregulin 1 regulates excitability of fast-spiking neurons through Kv1.1 and acts in epilepsy." Nat Neurosci **15**(2): 267-273.

Li, L., M. A. Gainey, J. E. Goldbeck and D. E. Feldman (2014). "Rapid homeostasis by disinhibition during whisker map plasticity." Proc Natl Acad Sci U S A **111**(4): 1616-1621.

Liem, K. F., Jr., G. Tremml and T. M. Jessell (1997). "A role for the roof plate and its resident TGFbeta-related proteins in neuronal patterning in the dorsal spinal cord." Cell **91**(1): 127-138.

Liguz-Lecznar, M., J. Urban-Ciecko and M. Kossut (2016). "Somatostatin and Somatostatin-Containing Neurons in Shaping Neuronal Activity and Plasticity." Frontiers in Neural Circuits **10**.

Lim-Tio, S. S. and P. J. Fuller (1998). "Intracellular signaling pathways confer specificity of transactivation by mineralocorticoid and glucocorticoid receptors." Endocrinology **139**(4): 1653-1661.

Lin, Y. X., B. L. Bloodgood, J. L. Hauser, A. D. Lapan, A. C. Koon, T. K. Kim, L. S. Hu, A. N. Malik and M. E. Greenberg (2008). "Activity-dependent regulation of inhibitory synapse development by Npas4." Nature **455**(7217): 1198-U1123.

Little, S. C. and M. C. Mullins (2009). "Bone morphogenetic protein heterodimers assemble heteromeric type I receptor complexes to pattern the dorsoventral axis." Nature Cell Biology **11**(5): 637-U439.

Liu, A. and L. A. Niswander (2005). "Bone morphogenetic protein signalling and vertebrate nervous system development." Nat Rev Neurosci **6**(12): 945-954.

Liu, H. Q., J. T. Zhou, W. Tian, C. Y. Luo, A. Bartlett, A. Aldridge, J. Lucero, J. K. Osteen, J. R. Nery, H. M. Chen, A. Rivkin, R. G. Castanon, B. Clock, Y. E. Li, X. M. Hou, O. B. Poirion, S. Preissl, A. Pinto-Duarte, C. O'Connor, L. Boggeman, C. Fitzpatrick, M. Nunn, E. A. Mukamel, Z. Z. Zhang, E. M. Callaway, B. Ren, J. R. Dixon, M. M. Behrens and J. R. Ecker (2021). "DNA methylation atlas of the mouse brain at single-cell resolution." Nature **598**(7879): 120-+.

Lourenco, J., S. Pacioni, N. Rebola, G. M. van Woerden, S. Marinelli, D. DiGregorio and A. Bacci (2014). "Non-associative potentiation of perisomatic inhibition alters the temporal coding of neocortical layer 5 pyramidal neurons." PLoS biology **12**(7): e1001903.

Lowery, J. W., B. Brookshire and V. Rosen (2016). "A Survey of Strategies to Modulate the Bone Morphogenetic Protein Signaling Pathway: Current and Future Perspectives." Stem Cells International **2016**.

Lowery, J. W. and V. Rosen (2018). "Bone Morphogenetic Protein-Based Therapeutic Approaches." Cold Spring Harbor Perspectives in Biology **10**(4).

Lyons, W. E., L. A. Mamounas, G. A. Ricaurte, V. Coppola, S. W. Reid, S. H. Bora, C. Wihler, V. E. Koliatsos and L. Tessarollo (1999). "Brain-derived neurotrophic factor-deficient mice develop aggressiveness and hyperphagia in conjunction with brain serotonergic abnormalities." Proceedings of the National Academy of Sciences of the United States of America **96**(26): 15239-15244.

Lyst, M. J., R. Ekiert, D. H. Ebert, C. Merusi, J. Nowak, J. Selfridge, J. Guy, N. R. Kastan, N. D. Robinson, F. D. Alves, J. Rappsilber, M. E. Greenberg and A. Bird (2013). "Rett syndrome mutations abolish the interaction of MeCP2 with the NCoR/SMRT co-repressor." Nature Neuroscience **16**(7): 898-U268.

Ma, H., R. D. Groth, S. M. Cohen, J. F. Emery, B. Li, E. Hoedt, G. Zhang, T. A. Neubert and R. W. Tsien (2014). "gammaCaMKII shuttles Ca(2)(+)/CaM to the nucleus to trigger CREB phosphorylation and gene expression." Cell **159**(2): 281-294.

Madisen, L., T. A. Zwingman, S. M. Sunkin, S. W. Oh, H. A. Zariwala, H. Gu, L. L. Ng, R. D. Palmiter, M. J. Hawrylycz, A. R. Jones, E. S. Lein and H. Zeng (2010). "A robust and high-throughput Cre reporting and characterization system for the whole mouse brain." Nat Neurosci **13**(1): 133-140.

Madisen, L., T. A. Zwingman, S. M. Sunkin, S. W. Oh, H. A. Zariwala, H. Gu, L. L. Ng, R. D. Palmiter, M. J. Hawrylycz, A. R. Jones, E. S. Lein and H. Zeng (2010). "A robust and high-throughput Cre reporting and characterization system for the whole mouse brain." Nat Neuroscience **13**(1): 133-140.

Maffei, A., K. Nataraj, S. B. Nelson and G. G. Turrigiano (2006). "Potentiation of cortical inhibition by visual deprivation." Nature **443**(7107): 81-84.

Malnic, B., J. Hirono, T. Sato and L. B. Buck (1999). "Combinatorial receptor codes for odors." Cell **96**(5): 713-723.

Marder, E. and J. M. Goaillard (2006). "Variability, compensation and homeostasis in neuron and network function." Nat Rev Neurosci **7**(7): 563-574.

Mardinly, A. R., I. Spiegel, A. Patrizi, E. Centofante, J. E. Bazinet, C. P. Tzeng, C. Mandel-Brehm, D. A. Harmin, H. Adesnik, M. Fagiolini and M. E. Greenberg (2016). "Sensory experience regulates cortical inhibition by inducing IGF1 in VIP neurons." Nature **531**(7594): 371-+.

Mardinly, A. R., I. Spiegel, A. Patrizi, E. Centofante, J. E. Bazinet, C. P. Tzeng, C. Mandel-Brehm, D. A. Harmin, H. Adesnik, M. Fagiolini and M. E. Greenberg (2016). "Sensory experience regulates cortical inhibition by inducing IGF1 in VIP neurons." Nature **531**(7594): 371-375.

Markram, H., E. Muller, S. Ramaswamy, M. W. Reimann, M. Abdellah, C. A. Sanchez, A. Ailamaki, L. Alonso-Nanclares, N. Antille, S. Arsever, G. A. Kahou, T. K. Berger, A. Bilgili, N. Buncic, A. Chalimourda, G. Chindemi, J. D. Courcol, F. Delalondre, V. Delattre, S. Druckmann, R. Dumusc, J. Dynes, S. Eilemann, E. Gal, M. E. Gevaert, J. P. Ghobril, A. Gidon, J. W. Graham, A. Gupta, V. Haenel, E. Hay, T. Heinis, J. B. Hernando, M. Hines, L. Kanari, D. Keller, J. Kenyon, G. Khazen, Y. Kim, J. G. King, Z. Kisvarday, P. Kumbhar, S. Lasserre, J. V. Le Be, B. R. Magalhaes, A. Merchan-Perez, J. Meystre, B. R. Morrice, J. Muller, A. Munoz-Cespedes, S. Muralidhar, K. Muthurasa, D. Nachbaur, T. H. Newton, M. Nolte, A. Ovcharenko, J. Palacios, L. Pastor, R. Perin, R. Ranjan, I. Riachi, J. R. Rodriguez, J. L. Riquelme, C. Rossert, K. Sfyrakis, Y. Shi, J. C. Shillcock, G. Silberberg, R. Silva, F. Tauheed, M. Telefont, M. Toledo-Rodriguez, T. Trankler, W. Van Geit, J. V. Diaz, R. Walker, Y. Wang, S. M. Zaninetta, J. DeFelipe, S. L. Hill, I. Segev and F. Schurmann (2015). "Reconstruction and Simulation of Neocortical Microcircuitry." Cell **163**(2): 456-492.

Marques, G., H. Bao, T. E. Haerry, M. J. Shimell, P. Duchek, B. Zhang and M. B. O'Connor (2002). "The Drosophila BMP type II receptor Wishful Thinking regulates neuromuscular synapse morphology and function." Neuron **33**(4): 529-543.

Marques, G., H. Bao, T. E. Haerry, M. J. Shimell, P. Duchek, B. Zhang and M. B. O'Connor (2002). "The Drosophila BMP type II receptor Wishful Thinking regulates neuromuscular synapse morphology and function." Neuron **33**(4): 529-543.

Marques, G., T. E. Haerry, M. L. Crotty, M. Xue, B. Zhang and M. B. O'Connor (2003). "Retrograde Gbb signaling through the Bmp type 2 receptor wishful thinking regulates systemic FMRFa expression in Drosophila." Development **130**(22): 5457-5470.

Massague, J. (2000). "How cells read TGF-beta signals." Nat Rev Mol Cell Biol **1**(3): 169-178.

Massague, J., J. Seoane and D. Wotton (2005). "Smad transcription factors." Genes Dev **19**(23): 2783-2810.

Matsuda, S., J. V. Schaefer, Y. Mii, Y. Hori, D. Bieli, M. Taira, A. Pluckthun and M. Affolter (2021). "Asymmetric requirement of Dpp/BMP morphogen dispersal in the Drosophila wing disc." Nature Communications **12**(1).

Matsui, F., M. Nishizuka, Y. Yasuda, S. Aono, E. Watanabe and A. Oohira (1998). "Occurrence of a N-terminal proteolytic fragment of neurocan, not a C-terminal half, in a perineuronal net in the adult rat cerebrum." Brain Research **790**(1-2): 45-51.

Matsumoto, T., S. Rauskolb, M. Polack, J. Klose, R. Kolbeck, M. Korte and Y. A. Barde (2008). "Biosynthesis and processing of endogenous BDNF: CNS neurons store and secrete BDNF, not pro-BDNF." Nat Neurosci **11**(2): 131-133.

Mauger, O., F. Lemoine and P. Scheiffele (2016). "Targeted Intron Retention and Excision for Rapid Gene Regulation in Response to Neuronal Activity." Neuron **92**(6): 1266-1278.

Mazille, M., K. Buczak, P. Scheiffele and O. Mauger (2022). "Stimulus-specific remodeling of the neuronal transcriptome through nuclear intron-retaining transcripts." Embo Journal **41**(21).

McBrayer, Z. L., J. Dimova, M. T. Pisansky, M. Sun, H. Beppu, J. C. Gewirtz and M. B. O'Connor (2015). "Forebrain-Specific Loss of BMPRII in Mice Reduces Anxiety and Increases Object Exploration." Plos One **10**(10).

McCabe, B. D., G. Marques, A. P. Haghighi, R. D. Fetter, M. L. Crotty, T. E. Haerry, C. S. Goodman and M. B. O'Connor (2003). "The BMP homolog Gbb provides a retrograde signal that regulates synaptic growth at the Drosophila neuromuscular junction." Neuron **39**(2): 241-254.

McCabe, B. D., G. Marques, A. P. Haghighi, R. D. Fetter, M. L. Crotty, T. E. Haerry, C. S. Goodman and M. B. O'Connor (2003). "The BMP homolog Gbb provides a retrograde signal that regulates synaptic growth at the Drosophila neuromuscular junction." Neuron **39**(2): 241-254.

Meyer, A. C., E. Neher and R. Schneggenburger (2001). "Estimation of quantal size and number of functional active zones at the calyx of Held synapse by nonstationary EPSC variance analysis." J Neurosci **21**(20): 7889-7900.

Miller, C. A., S. L. Campbell and J. D. Sweatt (2008). "DNA methylation and histone acetylation work in concert to regulate memory formation and synaptic plasticity." Neurobiology of Learning and Memory **89**(4): 599-603.

Mishina, Y., M. C. Hanks, S. Miura, M. D. Tallquist and R. R. Behringer (2002). "Generation of Bmpr/Alk3 conditional knockout mice." Genesis **32**(2): 69-72.

Miyagi, M., S. Mikawa, T. Hasegawa, S. Kobayashi, Y. Matsuyama and K. Sato (2011). "Bone morphogenetic protein receptor expressions in the adult rat brain." Neuroscience **176**: 93-109.

Miyazono, K., Y. Kamiya and M. Morikawa (2010). "Bone morphogenetic protein receptors and signal transduction." J Biochem **147**(1): 35-51.

Modol, L., Y. Bollmann, T. Tressard, A. Baude, A. Che, Z. R. S. Duan, R. Babij, N. V. D. Garcia and R. Cossart (2020). "Assemblies of Perisomatic GABAergic Neurons in the Developing Barrel Cortex." Neuron **105**(1): 93-+.

Monteys, A. M., A. A. Hundley, P. T. Ranum, L. Tecedor, A. Muehlmatt, E. Lim, D. Lukashev, R. Sivasankaran and B. L. Davidson (2021). "Regulated control of gene therapies by drug-induced splicing." Nature **596**(7871): 291-295.

Moore, A. K. and M. Wehr (2013). "Parvalbumin-expressing inhibitory interneurons in auditory cortex are well-tuned for frequency." J. Neuroscience **33**(34): 13713-13723.

Morris, G., C. R. Reschke and D. C. Henshall (2019). "Targeting microRNA-134 for seizure control and disease modification in epilepsy." EBioMedicine **45**: 646-654.

Mottis, A., L. Mouchiroud and J. Auwerx (2013). "Emerging roles of the corepressors NCoR1 and SMRT in homeostasis." Genes & Development **27**(8): 819-835.

Mukhopadhyay, A., T. McGuire, C. Y. Peng and J. A. Kessler (2009). "Differential effects of BMP signaling on parvalbumin and somatostatin interneuron differentiation." Development **136**(15): 2633-2642.

Mukhopadhyay, A., T. McGuire, C. Y. Peng and J. A. Kessler (2009). "Differential effects of BMP signaling on parvalbumin and somatostatin interneuron differentiation." Development **136**(15): 2633-2642.

Nakagawa, F., B. A. Schulte and S. S. Spicer (1986). "Selective Cytochemical Demonstration of Glycoconjugate-Containing Terminal N-Acetylgalactosamine on Some Brain Neurons." Journal of Comparative Neurology **243**(2): 280-290.

Nelson, S. B. and V. Valakh (2015). "Excitatory/Inhibitory Balance and Circuit Homeostasis in Autism Spectrum Disorders." Neuron **87**(4): 684-698.

Niekisch, H., J. Steinhardt, J. Berghauser, S. Bertazzoni, E. Kaschinski, J. Kasper, M. Kisse, J. Mitloehner, J. B. Singh, J. Weber, R. Frischknecht and M. F. K. Happel (2019). "Learning Induces Transient Upregulation of Brevican in the Auditory Cortex during Consolidation of Long-Term Memories." Journal of Neuroscience **39**(36): 7049-7060.

Okaty, B. W., M. N. Miller, K. Sugino, C. M. Hempel and S. B. Nelson (2009). "Transcriptional and electrophysiological maturation of neocortical fast-spiking GABAergic interneurons." The Journal of neuroscience : the official journal of the Society for Neuroscience **29**(21): 7040-7052.

Okun, M. and I. Lampl (2008). "Instantaneous correlation of excitation and inhibition during ongoing and sensory-evoked activities." Nat Neurosci **11**(5): 535-537.

Okur, Z. and P. Scheiffele (2019). "The Yin and Yang of Arnt2 in Activity-Dependent Transcription." Neuron **102**(2): 270-272.

Oohashi, T., M. Edamatsu, Y. Bekku and D. Carulli (2015). "The hyaluronan and proteoglycan link proteins: Organizers of the brain extracellular matrix and key molecules for neuronal function and plasticity." Experimental Neurology **274**: 134-144.

Palay, S. L. and G. E. Palade (1955). "The fine structure of neurons." J Biophys Biochem Cytol **1**(1): 69-88.

Pang, P. T. and B. Lu (2004). "Regulation of late-phase LTP and long-term memory in normal and aging hippocampus: role of secreted proteins tPA and BDNF." Ageing Res Rev **3**(4): 407-430.

Patterson, S. L., T. Abel, T. A. S. Deuel, K. C. MArtin, J. C. Rose and E. R. Kandel (1996). "Recombinant BDNF rescues deficits in basal synaptic transmission and hippocampal LTP in BDNF knockout mice." Neuron **16**(6): 1137-1145.

Pelkey, K. A., E. Barksdale, M. T. Craig, X. Q. Yuan, M. Sukumaran, G. A. Vargish, R. M. Mitchell, M. S. Wyeth, R. S. Petralia, R. Chittajallu, R. M. Karlsson, H. A. Cameron, Y. Murata, M. T. Colonnese, P. F. Worley and C. J. McBain (2016). "Pentraxins Coordinate Excitatory Synapse Maturation and Circuit Integration of Parvalbumin Interneurons (vol 85, pg 1257, 2015)." Neuron **90**(3): 661-661.

Pettit, N. L., E. L. Yap, M. E. Greenberg and C. D. Harvey (2022). "Fos ensembles encode and shape stable spatial maps in the hippocampus." Nature **609**(7926): 327-+.

Pfeffer, C. K., M. S. Xue, M. He, Z. J. Huang and M. Scanziani (2013). "Inhibition of inhibition in visual cortex: the logic of connections between molecularly distinct interneurons." Nature Neuroscience **16**(8): 1068-U1130.

Poo, M. M. (2001). "Neurotrophins as synaptic modulators." Nature Reviews Neuroscience **2**(1): 24-32.

Pouchelon, G., F. Gambino, C. Bellone, L. Telley, I. Vitali, C. Luscher, A. Holtmaat and D. Jabaudon (2014). "Modality-specific thalamocortical inputs instruct the identity of postsynaptic L4 neurons." Nature **511**(7510): 471-474.

Preissl, S., K. J. Gaulton and B. Ren (2022). "Characterizing cis-regulatory elements using single-cell epigenomics." Nature Reviews Genetics.

Pruunsild, P., C. P. Bengtson and H. Bading (2017). "Networks of Cultured iPSC-Derived Neurons Reveal the Human Synaptic Activity-Regulated Adaptive Gene Program." Cell Reports **18**(1): 122-135.

Qiu, J., J. McQueen, B. Bilican, O. Dando, D. Magnani, K. Punovuori, B. T. Selvaraj, M. Livesey, G. Haghi, S. Heron, K. Burr, R. Patani, R. Rajan, O. Sheppard, P. C. Kind, T. I. Simpson, V. L. J. Tybulewicz, D. J. A. Wyllie, E. M. C. Fisher, S. Lowell, S. Chandran and G. E. Hardingham (2016). "Evidence for evolutionary divergence of activity-dependent gene expression in developing neurons." Elife **5**.

Ramsaran, A. I., Y. Wang, A. Golbabaei, S. Aleshin, M. L. de Snoo, B. A. Yeung, A. J. Rashid, A. Awasthi, J. Lau, L. M. Tran, S. Y. Ko, A. Abegg, L. C. Duan, C. McKenzie, J. Gallucci, M. Ahmed, R. Kaushik, A. Dityatev, S. A. Josselyn and P. W. Frankland (2023). "A shift in the mechanisms controlling hippocampal engram formation during brain maturation." Science **380**(6644): 543-551.

Raven, F. and S. J. Aton (2021). "The Engram's Dark Horse: How Interneurons Regulate State-Dependent Memory Processing and Plasticity." Frontiers in Neural Circuits **15**.

Richardson, C. D., G. J. Ray, M. A. DeWitt, G. L. Curie and J. E. Corn (2016). "Enhancing homology-directed genome editing by catalytically active and inactive CRISPR-Cas9 using asymmetric donor DNA." Nat Biotechnol **34**(3): 339-344.

Rimbault, C., C. Breillat, B. Compans, E. Toulmé, F. N. Vicente, M. Fernandez-Monreal, P. Mascalchi, C. Genuer, V. Puente-Muñoz, I. Gauthereau, E. Hosy, G. Giannone, I. Chamma, C. D. Mackereth, C. Poujol, D. Choquet and M. Sainlos (2021). "Engineering paralog-specific PSD-95 synthetic binders as potent and minimally invasive imaging probes." bioRxiv: 2021.2004.2007.438431.

Roberts, A. C., J. Diez-Garcia, R. M. Rodriguiz, I. P. Lopez, R. Lujan, R. Martinez-Turrillas, E. Pico, M. A. Henson, D. R. Bernardo, T. M. Jarrett, D. J. Clendeninn, L. Lopez-Mascaraque, G. P. Feng, D. C. Lo, J. F. Wesseling, W. C. Wetsel, B. D. Philpot and I. Perez-Otano (2009). "Downregulation of NR3A-Containing NMDARs Is Required for Synapse Maturation and Memory Consolidation." Neuron **63**(3): 342-356.

Rogers, K. W. and A. F. Schier (2011). "Morphogen Gradients: From Generation to Interpretation." Annual Review of Cell and Developmental Biology, Vol 27 **27**: 377-407.

Rogers, S. L., E. Rankin-Gee, R. M. Risbud, B. E. Porter and E. D. Marsh (2018). "Normal Development of the Perineuronal Net in Humans; In Patients with and without Epilepsy." Neuroscience **384**: 350-360.

Rosenbloom, K. R., J. Armstrong, G. P. Barber, J. Casper, H. Clawson, M. Diekhans, T. R. Dreszer, P. A. Fujita, L. Guruvadoo, M. Haeussler, R. A. Harte, S. Heitner, G. Hickey, A. S. Hinrichs, R. Hubley, D. Karolchik, K. Learned, B. T. Lee, C. H. Li, K. H. Miga, N. Nguyen, B. Paten, B. J. Raney, A. F. Smit, M. L. Speir, A. S. Zweig, D. Haussler, R. M. Kuhn and W. J. Kent (2015). "The UCSC Genome Browser database: 2015 update." Nucleic Acids Res **43**(Database issue): D670-681.

Rossignol, E., I. Kruglikov, A. M. van den Maagdenberg, B. Rudy and G. Fishell (2013). "CaV 2.1 ablation in cortical interneurons selectively impairs fast-spiking basket cells and causes generalized seizures." Ann Neurol **74**(2): 209-222.

Rothman, J. S. and R. A. Silver (2018). "NeuroMatic: An Integrated Open-Source Software Toolkit for Acquisition, Analysis and Simulation of Electrophysiological Data." Front Neuroinform **12**: 14.

Rowitch, D. H. and A. R. Kriegstein (2010). "Developmental genetics of vertebrate glial-cell specification." Nature **468**(7321): 214-222.

Rubenstein, J. L. and M. M. Merzenich (2003). "Model of autism: increased ratio of excitation/inhibition in key neural systems." Genes Brain Behav **2**(5): 255-267.

Rudy, B., G. Fishell, S. Lee and J. Hjerling-Leffler (2011). "Three groups of interneurons account for nearly 100% of neocortical GABAergic neurons." Dev Neurobiol **71**(1): 45-61.

Ruoslahti, E. (1996). "Brain extracellular matrix." Glycobiology **6**(5): 489-492.

Salinas, P. C. (2003). "Synaptogenesis: Wnt and TGF-beta take centre stage." Current Biology **13**(2): R60-R62.

Samanta, J., G. M. Burke, T. McGuire, A. J. Pisarek, A. Mukhopadhyay, Y. Mishina and J. A. Kessler (2007). "BMPR1a signaling determines numbers of oligodendrocytes and calbindin-expressing interneurons in the cortex." J Neurosci **27**(28): 7397-7407.

Sando, R., N. Gounko, S. Pieraut, L. J. Liao, J. Yates and A. Maximov (2012). "HDAC4 Governs a Transcriptional Program Essential for Synaptic Plasticity and Memory." Cell **151**(4): 821-834.

Sapkota, G., C. Alarcon, F. M. Spagnoli, A. H. Brivanlou and J. Massague (2007). "Balancing BMP signaling through integrated inputs into the Smad1 linker." Molecular Cell **25**(3): 441-454.

Sato, T., S. Mikawa and K. Sato (2010). "BMP2 expression in the adult rat brain." J Comp Neurol **518**(22): 4513-4530.

Scheyltjens, I. and L. Arckens (2016). "The Current Status of Somatostatin-Interneurons in Inhibitory Control of Brain Function and Plasticity." Neural Plasticity **2016**.

Schindelin, J., I. Arganda-Carreras, E. Frise, V. Kaynig, M. Longair, T. Pietzsch, S. Preibisch, C. Rueden, S. Saalfeld, B. Schmid, J. Y. Tinevez, D. J. White, V. Hartenstein, K. Eliceiri, P. Tomancak and A. Cardona (2012). "Fiji: an open-source platform for biological-image analysis." Nat Methods **9**(7): 676-682.

Schnitzler, A. C., T. J. Mellott, I. Lopez-Coviella, Y. N. Tallini, M. I. Kotlikoff, M. T. Follettie and J. K. Blusztajn (2010). "BMP9 (bone morphogenetic protein 9) induces NGF as an autocrine/paracrine cholinergic trophic factor in developing basal forebrain neurons." The Journal of Neuroscience **30**(24): 8221-8228.

Schratt, G. M., F. Tuebing, E. A. Nigh, C. G. Kane, M. E. Sabatini, M. Kiebler and M. E. Greenberg (2006). "A brain-specific microRNA regulates dendritic spine development (vol 439, pg 283, 2006)." Nature **441**(7095): 902-902.

Schwartz, P. M., P. R. Borghesani, R. L. Levy, S. L. Pomeroy and R. A. Segal (1997). "Abnormal cerebellar development and foliation in BDNF-/- mice reveals a role for neurotrophins in CNS patterning." Neuron **19**(2): 269-281.

Selten, M., C. Bernard, F. Hamid, A. Hanusz-Godoy, F. Oozeer, C. Zimmer and O. Marín (2023). "Regulation of parvalbumin interneuron plasticity by neuropeptide-encoding genes." bioRxiv: 2023.2002.2003.527010.

Sharma, N., E. A. Pollina, M. A. Nagy, E. L. Yap, F. A. DiBiase, S. Hrvatin, L. D. Hu, C. Lin and M. E. Greenberg (2019). "ARNT2 Tunes Activity-Dependent Gene Expression through NCoR2-Mediated Repression and NPAS4-Mediated Activation." Neuron **102**(2): 390-+.

Shaul, Y. D. and R. Seger (2007). "The MEK/ERK cascade: From signaling specificity to diverse functions." Biochimica Et Biophysica Acta-Molecular Cell Research **1773**(8): 1213-1226.

Shi, Y. and J. Massague (2003). "Mechanisms of TGF-beta signaling from cell membrane to the nucleus." Cell **113**(6): 685-700.

Silberberg, G., S. Grillner, F. E. LeBeau, R. Maex and H. Markram (2005). "Synaptic pathways in neural microcircuits." Trends Neurosci **28**(10): 541-551.

Simms, B. A. and G. W. Zamponi (2014). "Neuronal Voltage-Gated Calcium Channels: Structure, Function, and Dysfunction." Neuron **82**(1): 24-45.

Sorensen, A. T., Y. A. Cooper, M. V. Baratta, F. J. Weng, Y. Zhang, K. Ramamoorthi, R. Fropf, E. LaVerriere, J. Xue, A. Young, C. Schneider, C. R. Gotzsche, M. Hemberg, J. C. Yin, S. F. Maier and Y. Lin (2016). "A robust activity marking system for exploring active neuronal ensembles." Elife **5**.

Sorg, B. A., S. Berretta, J. M. Blacktop, J. W. Fawcett, H. Kitagawa, J. C. F. Kwok and M. Miquel (2016). "Casting a Wide Net: Role of Perineuronal Nets in Neural Plasticity." Journal of Neuroscience **36**(45): 11459-11468.

Spiegel, I., A. R. Mardinly, H. W. Gabel, J. E. Bazinet, C. H. Couch, C. P. Tzeng, D. A. Harmin and M. E. Greenberg (2014). "Npas4 Regulates Excitatory-Inhibitory Balance within Neural Circuits through Cell-Type-Specific Gene Programs." Cell **157**(5): 1216-1229.

Spiegel, I., A. R. Mardinly, H. W. Gabel, J. E. Bazinet, C. H. Couch, C. P. Tzeng, D. A. Harmin and M. E. Greenberg (2014). "Npas4 regulates excitatory-inhibitory balance within neural circuits through cell-type-specific gene programs." Cell **157**(5): 1216-1229.

Stroud, H., S. C. Su, S. Hrvatin, A. W. Greben, W. Renthal, L. D. Boxer, M. A. Nagy, D. R. Hochbaum, B. Kinde, H. W. Gabel and M. E. Greenberg (2017). "Early-Life Gene Expression in Neurons Modulates Lasting Epigenetic States." Cell **171**(5): 1151-+.

Su, C. J., A. Murugan, J. M. Linton, A. Yeluri, J. Bois, H. Klumpe, M. A. Langley, Y. E. Antebi and M. B. Elowitz (2022). "Ligand-receptor promiscuity enables cellular addressing." Cell Syst **13**(5): 408-425 e412.

Su, C. J., A. Murugan, J. M. Linton, A. Yeluri, J. Bois, H. Klumpe, M. A. Langley, Y. E. Antebi and M. B. Elowitz (2022). "Ligand-receptor promiscuity enables cellular addressing." Cell Systems **13**(5): 408-+.

Sun, M., J. C. Gewirtz, L. Bofenkamp, R. J. Wickham, H. Ge and M. B. O'Connor (2010). "Canonical TGF-beta Signaling Is Required for the Balance of Excitatory/Inhibitory Transmission within the Hippocampus and Prepulse Inhibition of Acoustic Startle." Journal of Neuroscience 30(17): 6025-6035.

Sun, M., M. J. Thomas, R. Herder, M. L. Bofenkamp, S. B. Selleck and M. B. O'Connor (2007). "Presynaptic contributions of chordin to hippocampal plasticity and spatial learning." Journal of Neuroscience 27(29): 7740-7750.

Sun, Y., T. Ikrar, M. F. Davis, N. Gong, X. Zheng, Z. D. Luo, C. Lai, L. Mei, T. C. Holmes, S. P. Gandhi and X. Xu (2016). "Neuregulin-1/ErbB4 Signaling Regulates Visual Cortical Plasticity." Neuron 92(1): 160-173.

Sun, Y. J., T. Ikrar, M. F. Davis, N. Gong, X. T. Zheng, Z. D. Luo, C. Lai, L. Mei, T. C. Holmes, S. P. Gandhi and X. M. Xu (2016). "Neuregulin-1/ErbB4 Signaling Regulates Visual Cortical Plasticity." Neuron 92(1): 160-173.

Takesian, A. E. and T. K. Hensch (2013). "Balancing plasticity/stability across brain development." Prog Brain Res 207: 3-34.

Taniguchi, H., J. Lu and Z. J. Huang (2013). "The spatial and temporal origin of chandelier cells in mouse neocortex." Science 339(6115): 70-74.

Tao, X., S. Finkbeiner, D. B. Arnold, A. J. Shaywitz and M. E. Greenberg (1998). "Ca2+ influx regulates BDNF transcription by a CREB family transcription factor-dependent mechanism." Neuron 20(4): 709-726.

Tasic, B., Z. Yao, L. T. Graybuck, K. A. Smith, T. N. Nguyen, D. Bertagnolli, J. Goldy, E. Garren, M. N. Economo, S. Viswanathan, O. Penn, T. Bakken, V. Menon, J. Miller, O. Fong, K. E. Hirokawa, K. Lathia, C. Rimorin, M. Tieu, R. Larsen, T. Casper, E. Barkan, M. Kroll, S. Parry, N. V. Shapovalova, D. Hirschstein, J. Pendergraft, H. A. Sullivan, T. K. Kim, A. Szafer, N. Dee, P. Groblewski, I. Wickersham, A. Cetin, J. A. Harris, B. P. Levi, S. M. Sunkin, L. Madisen, T. L. Daigle, L. Looger, A. Bernard, J. Phillips, E. Lein, M. Hawrylycz, K. Svoboda, A. R. Jones, C. Koch and H. Zeng (2018). "Shared and distinct transcriptomic cell types across neocortical areas." Nature 563(7729): 72-78.

Timmusk, T., N. Belluardo, H. Persson and M. Metsis (1994). "Developmental regulation of brain-derived neurotrophic factor messenger RNAs transcribed from different promoters in the rat brain." Neuroscience 60(2): 287-291.

Timmusk, T., K. Palm, M. Metsis, T. Reintam, V. Paalme, M. Saarma and H. Persson (1993). "Multiple promoters direct tissue-specific expression of the rat BDNF gene." Neuron 10(3): 475-489.

Ting, C. Y., T. Herman, S. Yonekura, S. Gao, J. Wang, M. Serpe, M. B. O'Connor, S. L. Zipursky and C. H. Lee (2007). "Tiling of r7 axons in the Drosophila visual system is mediated both by transduction of an activin signal to the nucleus and by mutual repulsion." Neuron 56(5): 793-806.

Tolonen, M., J. M. Palva, S. Andersson and S. Vanhatalo (2007). "Development of the spontaneous activity transients and ongoing cortical activity in human preterm babies." Neuroscience 145(3): 997-1006.

Turrigiano, G. G. and S. B. Nelson (2004). "Homeostatic plasticity in the developing nervous system." Nat Rev Neurosci 5(2): 97-107.

Tyssowski, K. M., N. R. DeStefino, J. H. Cho, C. J. Dunn, R. G. Poston, C. E. Carty, R. D. Jones, S. M. Chang, P. Romeo, M. K. Wurzelmann, J. M. Ward, M. L. Andermann, R. N. Saha, S. M. Dudek and J. M. Gray (2018). "Different Neuronal Activity Patterns Induce Different Gene Expression Programs." Neuron 98(3): 530-546 e511.

Vecchia, D., A. Tottene, A. M. van den Maagdenberg and D. Pietrobon (2014). "Mechanism underlying unaltered cortical inhibitory synaptic transmission in contrast with enhanced excitatory transmission in CaV2.1 knockin migraine mice." Neurobiol Dis 69: 225-234.

Vicidomini, R. and M. Serpe (2022). "Local BMP signaling: A sensor for synaptic activity that balances synapse growth and function." Curr Top Dev Biol 150: 211-254.

Vickers, E., D. Osypenko, C. Clark, Z. Okur, P. Scheiffele and R. Schneggenburger (2020). "LTP of inhibition at PV interneuron output synapses requires developmental BMP signaling." Sci Rep 10(1): 10047.

Vickers, E. D., C. Clark, D. Osypenko, A. Fratzl, O. Kochubey, B. Bettler and R. Schneggenburger (2018). "Parvalbumin-Interneuron Output Synapses Show Spike-Timing-Dependent Plasticity that Contributes to Auditory Map Remodeling." Neuron **99**(4): 720-735 e726.

Vierbuchen, T., E. Ling, C. J. Cowley, C. H. Couch, X. F. Wang, D. A. Harmin, C. W. M. Roberts and M. E. Greenberg (2017). "AP-1 Transcription Factors and the BAF Complex Mediate Signal-Dependent Enhancer Selection." Molecular Cell **68**(6): 1067-+.

Vogels, T. P., H. Sprekeler, F. Zenke, C. Clopath and W. Gerstner (2011). "Inhibitory plasticity balances excitation and inhibition in sensory pathways and memory networks." Science **334**(6062): 1569-1573.

Volosin, M., W. Song, R. D. Almeida, D. R. Kaplan, B. L. Hempstead and W. J. Friedman (2006). "Interaction of survival and death signaling in basal forebrain neurons: roles of neurotrophins and proneurotrophins." J Neurosci **26**(29): 7756-7766.

Vormstein-Schneider, D., J. D. Lin, K. A. Pelkey, R. Chittajallu, B. Guo, M. A. Arias-Garcia, K. Allaway, S. Sakopoulos, G. Schneider, O. Stevenson, J. Vergara, J. Sharma, Q. Zhang, T. P. Franken, J. Smith, L. A. Ibrahim, K. J. Mastro, E. Sabri, S. Huang, E. Favuzzi, T. Burbridge, Q. Xu, L. Guo, I. Vogel, V. Sanchez, G. A. Saldi, B. L. Gorissen, X. Yuan, K. A. Zaghloul, O. Devinsky, B. L. Sabatini, R. Batista-Brito, J. Reynolds, G. Feng, Z. Fu, C. J. McBain, G. Fishell and J. Dimidschstein (2022). "Publisher Correction: Viral manipulation of functionally distinct interneurons in mice, non-human primates and humans." Nat Neurosci **25**(9): 1247.

Wang, D. F. and J. Fawcett (2012). "The perineuronal net and the control of CNS plasticity." Cell and Tissue Research **349**(1): 147-160.

Wehr, M. and A. M. Zador (2003). "Balanced inhibition underlies tuning and sharpens spike timing in auditory cortex." Nature **426**(6965): 442-446.

West, A. E., W. G. Chen, M. B. Dalva, R. E. Dolmetsch, J. M. Kornhauser, A. J. Shaywitz, M. A. Takasu, X. Tao and M. E. Greenberg (2001). "Calcium regulation of neuronal gene expression." Proceedings of the National Academy of Sciences of the United States of America **98**(20): 11024-11031.

Westenbroek, R. E., M. K. Ahlijanian and W. A. Catterall (1990). "Clustering of L-Type Ca-2+ Channels at the Base of Major Dendrites in Hippocampal Pyramidal Neurons." Nature **347**(6290): 281-284.

Wheeler, D. G., R. D. Groth, H. Ma, C. F. Barrett, S. F. Owen, P. Safa and R. W. Tsien (2012). "Ca(v)1 and Ca(v)2 Channels Engage Distinct Modes of Ca2+ Signaling to Control CREB-Dependent Gene Expression." Cell **149**(5): 1112-1124.

Wong, H. K., X. B. Liu, M. F. Matos, S. F. Chan, I. Perez-Otano, M. Boysen, J. Cui, N. Nakanishi, J. S. Trimmer, E. G. Jones, S. A. Lipton and N. J. Sucher (2002). "Temporal and regional expression of NMDA receptor subunit NR3A in the mammalian brain." J Comp Neurol **450**(4): 303-317.

Wu, J. W., R. Fairman, J. Penry and Y. G. Shi (2001). "Formation of a stable heterodimer between Smad2 and Smad4." Journal of Biological Chemistry **276**(23): 20688-20694.

Xiao, L., N. Michalski, E. Kronander, E. Gjoni, C. Genoud, G. Knott and R. Schneggenburger (2013). "BMP signaling specifies the development of a large and fast CNS synapse." Nat Neurosci **16**(7): 856-864.

Xiao, L., N. Michalski, E. Kronander, E. Gjoni, C. Genoud, G. Knott and R. Schneggenburger (2013). "BMP signaling specifies the development of a large and fast CNS synapse." Nat Neurosci **16**(7): 856-864.

Xu, L., Y. Kang, S. Col and J. Massague (2002). "Smad2 nucleocytoplasmic shuttling by nucleoporins CAN/Nup214 and Nup153 feeds TGFbeta signaling complexes in the cytoplasm and nucleus." Mol Cell **10**(2): 271-282.

Xue, M., B. V. Atallah and M. Scanziani (2014). "Equalizing excitation-inhibition ratios across visual cortical neurons." Nature **511**(7511): 596-600.

Yang, Y., T. Yamada, K. K. Hill, M. Hemberg, N. C. Reddy, H. Y. Cho, A. N. Guthrie, A. Oldenborg, S. A. Heiney, S. Ohmae, J. F. Medina, T. E. Holy and A. Bonni (2016). "Chromatin remodeling inactivates activity genes and regulates neural coding." Science **353**(6296): 300-305.

Yap, E. L. and M. E. Greenberg (2018). "Activity-Regulated Transcription: Bridging the Gap between Neural Activity and Behavior." <u>Neuron</u> **100**(2): 330-348.

Yap, E. L., N. L. Pettit, C. P. Davis, M. A. Nagy, D. A. Harmin, E. Golden, O. Dagliyan, C. Lin, S. Rudolph, N. Sharma, E. C. Griffith, C. D. Harvey and M. E. Greenberg (2021). "Bidirectional perisomatic inhibitory plasticity of a Fos neuronal network." <u>Nature</u> **590**(7844): 115-121.

Yi, S. E., A. Daluiski, R. Pederson, V. Rosen and K. M. Lyons (2000). "The type I BMP receptor BMPRIB is required for chondrogenesis in the mouse limb." <u>Development</u> **127**(3): 621-630.

Yu, X., G. C. Zhao, D. Wang, S. Wang, R. Li, A. Li, H. Wang, M. Nollet, Y. Y. Chun, T. Y. Zhao, R. Yustos, H. M. Li, J. S. Zhao, J. N. Li, M. Cai, A. L. Vyssotski, Y. L. Li, H. L. Dong, N. P. Franks and W. Wisden (2022). "A specific circuit in the midbrain detects stress and induces restorative sleep." <u>Science</u> **377**(6601): 63-+.

Zagrebelsky, M., A. Holz, G. Dechant, Y. A. Barde, T. Bonhoeffer and M. Korte (2005). "The p75 neurotrophin receptor negatively modulates dendrite complexity and spine density in hippocampal neurons." <u>Journal of Neuroscience</u> **25**(43): 9989-9999.

Zaitsev, A. V., N. V. Povysheva, D. A. Lewis and L. S. Krimer (2007). "P/Q-type, but not N-type, calcium channels mediate GABA release from fast-spiking interneurons to pyramidal cells in rat prefrontal cortex." <u>J Neurophysiol</u> **97**(5): 3567-3573.

Zeisel, A., A. B. Munoz-Manchado, S. Codeluppi, P. Lonnerberg, G. La Manno, A. Jureus, S. Marques, H. Munguba, L. He, C. Betsholtz, C. Rolny, G. Castelo-Branco, J. Hjerling-Leffler and S. Linnarsson (2015). "Brain structure. Cell types in the mouse cortex and hippocampus revealed by single-cell RNA-seq." <u>Science</u> **347**(6226): 1138-1142.

Zhang, D., M. F. Mehler, Q. Song and J. A. Kessler (1998). "Development of bone morphogenetic protein receptors in the nervous system and possible roles in regulating trkC expression." <u>J Neurosci</u> **18**(9): 3314-3326.

Zhang, Y., K. Chen, S. A. Sloan, M. L. Bennett, A. R. Scholze, S. O'Keeffe, H. P. Phatnani, P. Guarnieri, C. Caneda, N. Ruderisch, S. Deng, S. A. Liddelow, C. Zhang, R. Daneman, T. Maniatis, B. A. Barres and J. Q. Wu (2014). "An RNA-sequencing transcriptome and splicing database of glia, neurons, and vascular cells of the cerebral cortex." <u>J Neurosci</u> **34**(36): 11929-11947.

Zhao, G. Q. (2003). "Consequences of knocking out BMP signaling in the mouse." <u>Genesis</u> **35**(1): 43-56.

Zhou, M., F. Liang, X. R. Xiong, L. Li, H. Li, Z. Xiao, H. W. Tao and L. I. Zhang (2014). "Scaling down of balanced excitation and inhibition by active behavioral states in auditory cortex." <u>Nat Neurosci</u> **17**(6): 841-850.

Zhou, Y., L. Mesik, Y. J. Sun, F. Liang, Z. Xiao, H. W. Tao and L. I. Zhang (2012). "Generation of spike latency tuning by thalamocortical circuits in auditory cortex." <u>J Neuroscience</u> **32**(29): 9969-9980.

Zhu, W., J. Kim, C. Cheng, B. A. Rawlins, O. Boachie-Adjei, R. G. Crystal and C. Hidaka (2006). "Noggin regulation of bone morphogenetic protein (BMP) 2/7 heterodimer activity in vitro." <u>Bone</u> **39**(1): 61-71.

Acknowledgements

"To the families we were born into and the ones we have acquired over time."

First and topmost, I would like to thank my PhD supervisor, Peter Scheiffele, for being such an amazing supervisor to me. From the first day I came into his lab, he has been my mentor not only for science, but also how to see my capacity, how to not just accept the facts but challenge them, and be confident about myself. You lifted me up when I hit the ground, nurtured me to strengthen my roots and helped me to find my balance. Thank you so much for being a true "Doktorvater" to me. I feel so lucky to be trained by you who became my sole role model, and will keep sharing the same passion for science I could find in you.

I am extremely grateful to my committee members, Markus Affolter and Filippo Rijli for their great support and help in shaping the project and helping me to find my direction both throughout my PhD and also for my further steps.

I especially would like to thank Michael Greenberg for accepting to be my external advisor and making one of my biggest dreams come true. His discoveries about how "Nature and Nurture" works together have been my biggest inspiration throughout my PhD, and will for sure continue to be for my future projects.

Every member of the Scheiffele lab I met, both current and past, thank you all so much. What I know, I learnt them from each one of you. I feel extremely grateful for getting to know Lisa and Elisabetta, for setting the best examples of how to be colleagues and at the same time being great friends. I learnt so much from both of you, thank you for being always there for me from the beginning. I especially would like to thank Nadia, for being an amazing collaborator. Thank you so much for making everything so much easier, but most importantly, for being such a good friend to me. You know, I will come back for you ;). Also, very special thanks to Shirley, for always being there for me, and being the sister to me I have always been missing.

I am also extremely grateful to Dietmar for fruitful discussions, for his great help with my project and also for his support, and making our lab life easier and fun. You are our (not so) secret power:). I am very grateful to Le and Özgür, for teaching me how to patch, for the discussions about my project and especially for being so patient with me especially while I could not. I also would like to thank Myrto for our great collaboration and support, for being very understanding and making our desk very joyful, lively and green :). I am also very grateful to Giulia, Oriane, Caroline, Elieke, Anja, Raul, Julia and Sabrina for their support and friendship. I learnt a lot from you, both scientifically and also for enjoying what I am doing despite all the obstacles.

Biozentrum was not only a work place to me, but my second home in Basel. I am very gratefully for the opportunity of the fellowship I was given, and people I met in Biozentrum. First of all, I am very grateful to Vassilis, for our amazing collaboration, and his companionship. Despite how busy you were, thank you for being so available, for our endless discussions about different cuisines, history, and eventually being a trustworthy member of our game nights and my co-chief. I also would like to thank Wuzhou, Staci, Corina and Clare for making my Basel life so much more fun with the game nights, and for being very good friends. I am also very grateful to Gustavo, my favorite fellow, for always being by my side. Your enthusiasm and knowledge about science was and will be very inspirational to me.

Special thanks to Nesibe and Remzi, for their friendship, for cheering with me and making their house a third home in Basel to me. I also want to thank Ersin for his friendship and support besides making his döner kebab my main nutrition supply :) I would like to also express my gratitude to all my friends from home; but especially Merve, Nurcan, Idil and Kivanç for always cheering for me. I always felt and will feel our life-long friendship with me where ever I am.

Without the support I got from my family, I wouldn't be able to follow my passion and dreams. I therefore would like to especially thank my mother, for believing in me and being so generous for me. I am also grateful to my father, for making every effort so that I could have what I need to be successful, even in the times it was very challenging. I feel blessed to be a daughter to both of you and your support made it possible for who I became. I am also very thankful to my grandparents, uncle, aunts, rest of my family, and family-in-law for their belief and support in me.

Last, but huge thanks to my best friend, my foundation, the best-partner I could never imagined that I would have ever met. I am immensely grateful to Faruk for being such an understanding and compassionate partner. Thank you for teaching me how to be the best even at my worst, making it through all the rest with and being the one I will always laugh with. Your endless support and love are making me very strong and encouraging me to be successful both in science and life.

Curriculum Vitae

Zeynep Okur (former Orhan)

Date of birth: 18.09.1990   *Place of birth: Denizli, Turkey*   *Contact:* zeynep.orhan@unibas.ch

Address: Biozentrum, University of Basel, Switzerland

OrcID: 0000-0003-4165-3414

Education

Jan 2017-Sep 2023	International PhD Program of Biozentrum, University of Basel, Switzerland
Sep 2014-Nov 2016	Master of Science degree in Neuroscience, Bilkent University, Turkey (3.76/4)
2009- 2014	Bachelor of Science degree in Molecular Biology and Genetics, Izmir Institute of Technology, Turkey (100% English in education) (3.34/4-honor student)

Academic trainings

PhD in Neurobiology, Biozentrum, University of Basel, Switzerland

Jan 2017-Sep 2023   PhD student, Professor Peter Scheiffele's laboratory

PhD thesis: Bone Morphogenetic Proteins as regulators of cortical excitation and inhibition

Master in Neuroscience, National Nanotechnology Research Center, Bilkent University, Turkey

Sep 2014-Nov 2016   Nanobiotechnology laboratory, Dr. Ayse Begum Tekinay's laboratory

MSc thesis: Promotion of neurite outgrowth by rationally designed peptide nanofibers

Short-term internship in NIPS, Okazaki, Japan

Jan, 2014   National Institute for Physiological Sciences, Okazaki, JAPAN

Biophysics and Neurobiology Laboratory, Professor Yoshihiro Kubo's laboratory

Internship project: Two Electrode Voltage Clamping by using Xenopus oocyte as a model organism

Summer Internship in IMPRS, Goettingen, Germany

Jun 10 - Sep 15, 2013   Max-Planck-Institute for Biophysical Chemistry, Genes and Behavior Department, Professor Gregor Eichele's laboratory

Internship project: Clock and Cycle genes in control of circadian rhythm

Research methods

In my research, I have applied a wide range of methodologies in cellular/molecular neuroscience in the mouse brain. A major part of my

research used advanced transcriptomic methods (Cut & Run, Chromatin immunoprecipitation, translating ribosome affinity purification) on neuronal populations from the mouse brain. I adopted novel methods for Crispr-Cas9-based genome-editing to generate a series of knock-in mouse lines for my studies on the BMP-SMAD signaling system. I further developed novel, chemically-gated transcriptional reporter systems to monitor BMP-signaling in the mouse brain with cell-type-specific resolution, and advanced genetically-encoded binders as an efficient tool for sparse in vivo synapse marking in genetically-defined cell populations. I used patch-clamp recordings from acute slice preparations to directly relate morphological synapse phenotypes to synapse function and to interrogate the intrinsic properties of parvalbumin interneurons. Finally, I used long-term EEG recordings, auditory fear conditioning, and other behavioral tests to relate molecular and cellular alterations to behavioral read-outs in mice.

Besides these bench-science efforts, I gained substantial experience in the computational analysis of RNA sequencing, ChIP-Seq and Cut & Run datasets and developed scripts for quantitative image analysis.

Teaching

August 2023-present	Supervision of Sarah Brait (Master student): *Investigating the role of RNA binding protein RBMS3 in control of TGF-beta/BMP signaling in cortical interneurons*
March 2021-July 2022	Supervision of Nadia Schlauri (Master student): *Modification of FingR intrabodies for static and dynamic synapse analysis in the mouse cortex*
October 2020-January 2021	Supervision of Shirley Dixit (rotation student for PhD program): *Investigating Bmp2 localization in dense core vesicles and synaptosomes in the mouse cortex*
February 2020	Supervision of Reto Tschannen: internship student
May 2017-present	Teaching assistant and mentoring of Bachelor students during Block course (yearly, 1-2 weeks in April or May)

Scholarships and Awards

June 2021	3rd Best Talk Award, PhD Retreat, University of Basel, Switzerland
Jan 2017-April 2020	Fellowship for Excellence PhD Scholarship, Biozentrum, University of Basel
Sep 2014-Nov 2016	Graduate school scholarship from Bilkent University
Mar 2015-Mar 2016	Graduate school scholarship in priority research areas from Scientific and Technological Research Council of Turkey, **TUBITAK**
Jan 20-Jan 31, 2014	Scholarship from National Institute for Physiological Sciences (NIPS), Okazaki, Japan, for short-term internship (196.500 JPY covering travel, accommodation and other expenses)
Jun-Sep 2013	Summer Erasmus Lifelong Learning Scholarship for a summer internship at Max Planck Institute for Biophysical Chemistry, Genes and Behavior Department (1500 Euro covering travel and accommodation for 3 months)

Oral and Poster Presentations

Invited/Selected Speaker

2023	Cellular and Molecular Neurobiology of Mental Disease Meeting- Grand Hôtel des Rasses, Switzerland, 30.08.2023
	Basel Neuroscience Workshop Series: "Neuronal Functions in Health and Disease"- Basel, Switzerland, 05.05.2023
	Seminar at the Broad Institute and Harvard Medical School, Boston, USA- invited by Professor Gordon Fishell, "Keeping the Balance: How Bone Morphogenetic Proteins control cortical excitation and inhibition", 05.04.2023
	Seminar at the Max-Planck-Institute for Biological Intelligence, Munich, Germany- invited by Dr. Christian Mayer, "Keeping the Balance: How Bone Morphogenetic Proteins control cortical excitation and inhibition", 21.03.2023
	Seminar at Karolinska Institute, Sweden- invited by Associate Professor Jens Hjerling-Leffler, "A morphogen controls cortical excitation-inhibition balance in the adult cortex", 16.03.2023
	Seminar at King's College London, Centre for Developmental Neurobiology, UK- invited by Professor Oscar Marin, "A morphogen controls cortical excitation-inhibition balance", 08.03.2023
	Seminar at Weizmann Institute, Department of Molecular Neuroscience, invited by Dr. Ivo Spiegel' "A role for Bone Morphogenetic Proteins in controlling excitation-inhibition ratio in the adult cortex", 10.01.2023
2022	Seminar at the Brain Mind Institute, EPFL, Lausanne, invited by Professor Johannes Gräff, "Keeping the Balance: A role for Bone Morphogenetic Proteins in controlling neuronal networks", 16.11.2022
	Biozentrum Discovery Seminar- Basel, Switzerland, 30.09.2022
	RNA Club Seminar- Basel, Switzerland, 04.04.2022
	Neurophysiology Seminar- Basel, Switzerland, 14.01.2022

2021	*Biozentrum & Pharmazentrum PhD Retreat- Basel, Switzerland, 18.06.2021*
2020	*Virtual Synapse Biology Meeting-online, "Talking to the nucleus: Role of Bone Morphogenetic Protein signaling in cortical neurons", 17.12.2020*
2018	Bonn Brain Meeting, Bonn Center of Neurosciences- Bonn, Germany, 28.03.2018

Poster presentations

July 2023	Gordon Research Conference and Seminar "Inhibition in the CNS"- Les Diableres, Switzerland
July 2022	13th FENS Forum of Neuroscience, Paris, France
June 2022	Biozentrum Retreat, Campus Sursee, Switzerland
March 2022	NCCR RNA and Disease annual retreat, Engelberg, Switzerland
October 2020	Virtual Neuroepigenetics Workshop from European Molecular Biology Laboratories (EMBL), Germany
September 2020	Virtual Molecular Mechanisms of Neuronal Connectivity Meeting, Cold Spring Harbour Laboratories, USA
August 2019	Mechanisms of Eukaryotic Transcription Meeting, Cold Spring Harbour Laboratories, USA
Mar 2018	Bonn Brain Meeting, Bonn Center of Neurosciences, Germany
May 2015-2016	Nanoday, National Nanotechnology Research Center, Bilkent University, Ankara, Turkey
Mar 2016	COST MP1301 NEWGEN conference in University of Aveiro, Portugal
Nov 2012-2013	International Molecular Biology Society Congress, Istanbul, Turkey

Publications

1. Control of neuronal excitation-inhibition balance by BMP-SMAD1 signaling.
Zeynep Okur, Nadia Schlauri, Vassilis Bitsikas, Myrto Panopoulou, Kajari Karmakar, Dietmar Schreiner, Peter Scheiffele
BioRxiv, 2023, DOI: https://www.biorxiv.org/content/10.1101/2023.03.11.532164v2

2. Cell type-specific control of TGF-beta/BMP signaling by mRNA transport and local translation
Furlanis E.*, **Okur Z**.*, Brait S.*, Schreiner D., Scheiffele P. *(in preparation)*
*equal contribution

3. LTP of inhibition at PV interneuron output synapses requires developmental BMP signaling.
Vickers E., Osypenko D., Clark C., **Okur Z.**, Scheiffele P., Schneggenburger R.
Sci Rep, 2020, DOI: 10.1038/s41598-020-66862-5

4. The Yin and Yang of Arnt2 in Activity-Dependent Transcription.
Okur Z., Scheiffele P.
Neuron, 2019, DOI: 10.1016/j.neuron.2019.04.006 *(Preview Article)*

5. Promotion of neurite outgrowth by rationally designed NGF-β binding peptide nanofibers.
Zeynep Okur, Oya I. Senturk, Canelif Yilmaz, Gulcihan Gulseren, Busra Mammadov, Mustafa O. Guler, Ayse B. Tekinay
Biomater. Sci., 2018, DOI: 10.1039/c8bm00311d

6. Sciatic Nerve Regeneration Induced by Glycosaminoglycan and Laminin Mimetic Peptide Nanofiber Gels.
Busra Mammadov, Melike Sever, Mevhibe Gecer, Fatih Zor, Sinan Ozturk, Hakan Akgun, Umit H. Ulas, **Zeynep Orhan**, Mustafa O. Guler, Ayse B. Tekinay
RSC Adv., 2016,**6**, 110535-110547.

Extracurricular trainings

November-December 2022	Cajal Advanced Neuroscience Training, "Neuroepigenetics: Writing, Reading and Erasing the epigenome", Bordeaux Neuroscience Campus, France
March 2021	Python Crash Course, University of Basel, Switzerland
June 2020	GALAXY introduction for life scientists, Swiss Institute of Bioinformatics, streamed
April 2018	Chromatin Immunoprecipitation sequencing data analysis: From quality check to motif discovery and more, Swiss Institute of Bioinformatics, Lausanne, Switzerland
Mar 2018	First steps in R: Programming language, Swiss Institute of Bioinformatics, Basel, Switzerland

Further qualifications

Linux: beginner   R: intermediate   Python: beginner

IGOR for patch clamp data analysis

IMARIS, Hyugens, OMERO and ImageJ for image analysis

Adobe Illustrator and Photoshop for graphical illustrations

Languages

Turkish (native)   English (fluent)   German (A2)

Referees

Prof. Dr. Peter Scheiffele	PhD thesis supervisor
	Biozentrum, University of Basel - peter.scheiffele@unibas.ch
Prof. Dr. Filippo Rijli	PhD thesis committee member
	Friedrich Miescher Institute for Biomedical Research, Basel- Filippo.Rijli@fmi.ch
Prof. Dr. Markus Affolter	PhD thesis committee member
	Biozentrum, University of Basel – markus.affolter@unibas.ch